NATIONAL ADVISORY COMMITTEE FOR AERONAUTICS

TECHNICAL NOTE

No. 1743

FLIGHT MEASUREMENTS OF THE STABILITY, CONTROL, AND STALLING CHARACTERISTICS OF AN AIRPLANE HAVING A 35° SWEPTBACK WING WITHOUT SLOTS AND WITH 80-PERCENT-SPAN SLOTS AND A COMPARISON WITH WIND-TUNNEL DATA

By S. A. Sjoberg and J. P. Reeder

Langley Aeronautical Laboratory
Langley Field, Va.

Washington
November 1948

NATIONAL ADVISORY COMMITTEE FOR AERONAUTICS

TECHNICAL NOTE NO. 1743

FLIGHT MEASUREMENTS OF THE STABILITY, CONTROL, AND STALLING CHARACTERISTICS OF AN AIRPLANE HAVING A 35° SWEPTBACK WING WITHOUT SLOTS AND WITH 80-PERCENT-SPAN SLOTS AND A COMPARISON WITH WIND-TUNNEL DATA

By S. A. Sjoberg and J. P. Reeder

SUMMARY

Flight measurements have been made to determine the low-speed flying qualities of an airplane having a wing swept back 35° at the quarter-chord line. The lateral and directional stability and control characteristics of the airplane without slots and with 80-percent-span slots on the wing are presented. Also included are measurements of the longitudinal stability, stalling, and lift characteristics with 80-percent-span slots. Tests were made both with and without a ventral-fin extension on the airplane.

The directional stability of the airplane as measured in steady sideslips by the variation of rudder angle with sideslip angle was positive with or without slots and with the flaps up or down at all test speeds. A decrease in directional stability occurred with decrease in speed. A part of the decrease in stability with speed was due to the unstable yawing moments caused by the large aileron deflections required for trim in steady sideslips at low speed. Removing the ventral-fin extension reduced the directional stability with the greatest reduction occurring at high normal-force coefficients or low speed. The pilot considered the airplane more difficult to fly with the reduced directional stability because in maneuvers inadvertent sideslipping occurred more easily and the sideslip angles reached were higher. At low speed where the dihedral effect was high, large lateral trim changes accompanied the changes in sideslip.

A large increase in dihedral effect occurred with increase in normal-force coefficient. With the 80-percent-span slots on the wing and the flaps up, slight negative stick-fixed dihedral effect was present below normal-force coefficients of approximately 0.30 and negative stick-free dihedral was present below normal-force coefficients of approximately 0.56. The pilot considered the negative dihedral more objectionable than the high positive dihedral present at high normal-force coefficients. The negative dihedral was objectionable because in rough air or in maneuvers involving changes in sideslip the response of the airplane was illogical.

The combination of high positive dihedral present at low speeds and negative dihedral present at high speeds was particularly objectionable to the pilot because he could not become accustomed to either condition. The agreement between the flight and wind-tunnel measurements of dihedral effect was good for the wing with the slots and fair for the wing without the slots. The wind-tunnel data showed a large increase in dihedral effect with increase in Reynolds number for the wing without slots.

Lateral and directional oscillations of the airplane were satisfactorily damped even with the low directional stability present when the ventral-fin extension was off.

The maximum values of wing-tip helix angle reached in rudder-fixed aileron rolls were low. For a given aileron deflection a marked decrease in maximum wing-tip helix angle occurred with decrease in speed because of the increase in dihedral effect and the higher sideslip angles reached in rolls at low speed. At 110 miles per hour with the flaps down, the high dihedral effect caused reversal of rolling velocity in left rolls.

The longitudinal stability with the 80-percent-span slots on the wing and the flaps up was high throughout the speed range. With the flaps down the longitudinal stability was high at moderate speeds, but near the stall the stability became neutral or slightly negative.

The stalling characteristics of the airplane were good with the flaps up or down when the 80-percent-span slots were on the wing. At the stall the airplane oscillated about all three axes. The attitude changes of the airplane were small during these oscillations and recovery from the stall could be made easily. With the ventral-fin extension removed, the amplitude of the oscillations at the stall increased rapidly.

INTRODUCTION

In order to study the effects of sweepback on the low-speed flying qualities of an airplane, a flight investigation has been made at the Langley Laboratory with an airplane having a wing swept back 35° at the quarter-chord line. Measurements were made of the lateral, directional, and longitudinal stability and control characteristics and the stalling characteristics without slots on the wing and with slots along 40 percent and 80 percent of the span of the sweptback wing panels. The results of an investigation of the lateral and directional stability and control characteristics with the 40-percent-span slots on the wing have been reported in reference 1. Reference 2 reports the results of an investigation of the longitudinal stability and stalling characteristics without slots and also with 40-percent-span slots.

This paper presents the lateral and directional stability and control characteristics without slots and with 80-percent-span slots and the longitudinal stability, stalling, and lift characteristics with the 80-percent-span slots on the wing. A $\frac{1}{4.5}$-scale model of the airplane was tested in the Langley 300 MPH 7- by 10-foot tunnel and wherever possible a comparison of the flight and wind-tunnel measurements is included. The results of the wind-tunnel tests are reported in reference 3.

SYMBOLS

C_l	rolling-moment coefficient
C_N	normal-force coefficient
C_n	yawing-moment coefficient
C_{n_β}	rate of change of yawing-moment coefficient with sideslip angle $(dC_n/d\beta)$
F_e	elevator stick force, pounds
$pb/2V$	wing-tip helix angle, radians
q_c	impact pressure, inches of water
R	Reynolds number
R_{eff}	effective Reynolds number
V_c	calibrated airspeed, miles per hour
α	angle of attack of thrust axis, degrees
δ_a	total aileron angle, degrees
δ_r	rudder angle, degrees
β	sideslip angle, degrees
ψ	angle of yaw, degrees

Subscript:

max	maximum

AIRPLANE

The airplane tested had a wing with a straight center panel and outer wing panels which were swept back 35° at the quarter-chord line (38.7° at the leading edge). A three-view drawing of the airplane is shown in figure 1 and general dimensions are listed in table I. Figures 2 and 3 are photographs of the test airplane.

The 80-percent-span slots which were on the airplane for some tests extended from 20 percent of the semispan of the sweptback wing panels to the wing tips. A cross section of the slot and the forward part of the wing in a plane normal to the wing leading edge is shown in figure 4. Some flights were made with the large ventral-fin extension shown in figure 3 removed from the airplane. Figure 5 is a photograph showing the test airplane without the large ventral-fin extension. The main landing gear of the airplane could not be retracted but the nose gear was retractable. The variations of elevator angle and aileron angle with stick-grip position are shown in figures 6 and 7, respectively. Figure 8 shows the variation of rudder angle with right-rudder-pedal position.

INSTRUMENTATION

The following instruments were installed in the airplane:

NACA instrument	Measured quantity
Timer	Time (for synchronizing all records)
Airspeed recorder	Airspeed
Control-position recorders	Aileron, rudder, and elevator positions
Control-force recorders	Stick and pedal forces
Sideslip-angle recorder and indicator	Sideslip angle
Recording accelerometer	Normal, longitudinal, and transverse accelerations
Angular-velocity recorders	Pitching, rolling, and yawing velocities
Angle-of-attack recorder	Angle of attack
16-millimeter cameras	Tuft studies

The installations for measuring airspeed, sideslip, and angle of attack are described in references 1 and 2. Airspeed as used in this paper is calibrated airspeed, which corresponds to the reading of a standard Army-Navy airspeed meter connected to a pitot-static system free from position error. Elevator, aileron, and rudder positions were measured at the control surfaces.

TESTS, RESULTS, AND DISCUSSION

The tests reported herein include measurements of the lateral and directional stability and control characteristics without slots and with 80-percent-span slots and measurements of the longitudinal stability, stalling, and lift characteristics with 80-percent-span slots on the wing. For the airplane with 80-percent-span slots on the wing, flights were also made without the ventral-fin extension on the airplane.

All tests were made with the engine idling. The main landing gear was fixed. The nose gear was extended for the flaps-down tests and retracted for the flaps-up tests. Difficulty was experienced in determining the amount of fuel consumed in flight and therefore the center-of-gravity locations given are believed accurate to only ±0.7 percent mean aerodynamic chord.

Static Lateral and Directional Stability

The static lateral and directional stability characteristics were measured in steady sideslips at various speeds with the flaps up and down. The data for the test airplane without slots on the wing are shown in figure 9 for the flaps-up condition and in figure 10 for the flaps-down condition. The data for the airplane with 80-percent-span slots are shown in figure 11 for the flaps-up condition and in figure 12 for the flaps-down condition.

The directional stability of the airplane was positive with the flaps up or down at all test speeds. As expected, the addition of slots had no appreciable effect on the directional stability. In figure 13 the slopes of the curves of rudder angle against sideslip angle $d\delta_r/d\beta$ from figures 9 to 12 are plotted as a function of normal-force coefficient. The values of $d\delta_r/d\beta$ were measured at zero sideslip. Figure 13 shows that the directional stability of the airplane as measured by $d\delta_r/d\beta$ is lowest at high normal-force coefficients or low speeds. A part of the decrease in $d\delta_r/d\beta$ which occurred at high normal-force coefficients is due to the unstable yawing moments caused by the large aileron deflections required for trim in steady sideslips.

The curves of aileron angle against sideslip angle in figures 9 to 12 show that a large increase in dihedral effect occurred with increase in normal-force coefficient. This effect can be seen more readily in figures 14 and 15, where the variation of aileron angle with sideslip angle $d\delta_a/d\beta$ is plotted against normal-force coefficient C_N. Figure 14 is for the flaps-up condition and figure 15 is for the flaps-down condition. The values of $d\delta_a/d\beta$ were measured at zero sideslip. At a given normal-force coefficient, the addition of slots to the wing caused a reduction in dihedral effect except at high normal-force coefficients. The reduction in dihedral effect resulting from the slots may be attributed to the increase in angle for zero lift over that part of the wing spanned by the slot. Since the inboard part of the wing is unslotted, the wing is effectively washed out when the outboard part of the wing is slotted. With the 80-percent-span slots on the wing and the flaps up, figure 14 shows that the stick-fixed dihedral effect was slightly negative below normal-force coefficients of approximately 0.30 and figure 11 shows that the stick-free dihedral effect was negative below normal-force coefficients of approximately 0.56. The pilot considered the negative dihedral present at low normal-force coefficients more objectionable than the high positive dihedral present at high normal-force coefficients. The negative dihedral was objectionable because in rough air or in maneuvers involving changes in sideslip the response of the airplane was illogical. The pilot considered the combination of high positive dihedral at low speed and negative dihedral at high speed particularly objectionable when occurring in the same airplane because he could not become accustomed to either condition.

In order to obtain flight measurements of dihedral effect which would be directly comparable with the results obtained in the wind-tunnel tests, flights were made with the airplane asymmetrically loaded. By making sideslips with the airplane asymmetrically loaded, the sideslip angle required to balance the known rolling moment caused by the asymmetric load could be determined. These flights were made by using gasoline from the nose tank with one wing tank full and the other wing tank empty. This arrangement gave rolling moments about the center line of the airplane of approximately 3200 foot-pounds. This rolling moment is believed accurate to ±300 foot-pounds. Sideslips were made at various speeds and at each speed sideslips were made with the known rolling moment acting both to the right and to the left. Data, typical of those obtained, are shown in figure 16.

At the sideslip angles at which the aileron angle is 0° in figure 16, the rolling moment due to the asymmetric load is balanced by the rolling moment due to sideslip. The variation of rolling-moment coefficient with sideslip angle was thus obtained at various normal-force coefficients and these data are shown in figure 17 for the airplane without slots and with the flaps up, in figure 18 for the airplane with 80-percent-span slots and with the flaps up, and in figure 19 for the airplane with the 80-percent-span slots and with the flaps down. Figures 17 to 19 also

include the wind-tunnel results for comparison. The wind-tunnel data presented include a correction for the rolling moment resulting from the rudder deflection required for trim in sideslip and therefore are directly comparable to the flight data. Yaw angle ψ is used rather than sideslip angle β in figures 17 to 19 for convenience in making the comparison with the wind-tunnel results. The yaw angle is numerically equal to the sideslip angle but is of the opposite sign.

For the wing without slots and with the flaps up (fig. 17), wind-tunnel data are presented for effective Reynolds numbers of 1.95×10^6 and 4.59×10^6. Increasing the Reynolds number greatly increased the dihedral effect as measured in the wind tunnel, particularly at the higher normal-force coefficients. The wind-tunnel data for an effective Reynolds number of 4.59×10^6 and the flight data are in fair agreement. The flight Reynolds number varied from approximately 7×10^6 to 11×10^6. With the 80-percent-span slots on the wing (figs. 18 and 19), the flight and wind-tunnel measurements are in good agreement with the flaps either up or down, even though the wind-tunnel data were obtained at a Reynolds number of only 2×10^6.

A measure of the aileron effectiveness could be obtained from the sideslips made with the airplane asymmetrically loaded. In figure 16, at a sideslip angle of 0°, the rolling moment due to the asymmetric load is balanced by the aileron deflections given. The change in rolling-moment coefficient with change in total aileron angle, therefore, could be obtained. See figure 20. Figure 20 also includes data obtained in the wind-tunnel tests with the 80-percent-span slots on the airplane model. The agreement between the directly comparable flight and wind-tunnel data for the 80-percent-span-slot configuration is excellent. For the wing without slots, the flight data show an apparent increase in aileron effectiveness of approximately 20 percent. As has previously been mentioned the rolling moments are believed accurate to only ± 10 percent and, therefore, a part of the apparent increase in aileron effectiveness may be caused by an error in the rolling moment.

As has previously been noted, the directional stability characteristics of the test airplane were good. The wind-tunnel tests showed C_{n_β} to be about 0.002 per degree with the flaps up. Several proposed sweptback-wing-airplane designs have considerably less directional stability than the test airplane. In order to find out what effects lower directional stability would have on the handling qualities of the test airplane, flights were made without the large ventral-fin extension on the airplane. Figures 21 and 22 show the steady sideslip characteristics of the airplane without the ventral-fin extension for the flaps-up and flaps-down conditions, respectively.

Removing the ventral-fin extension reduced the directional stability throughout the speed range but the largest reduction occurred at low speeds or high normal-force coefficients. This reduction is shown in figure 23 where the slopes of the curves of rudder angle against sideslip angle $d\delta_r/d\beta$ from figures 11, 12, 21, and 22 are plotted as a function of normal-force coefficient. The values of $d\delta_r/d\beta$ were again measured at zero sideslip. At small angles of left sideslip at low speeds, the directional stability was lower than at zero sideslip. At 100 miles per hour with the flaps down (fig. 22(a)), slight directional instability was present at small angles of left sideslip. A part of the decrease in $d\delta_r/d\beta$ which occurred with increase in normal-force coefficient as shown in figure 23 is again due to the unstable yawing moments caused by the large aileron deflections required for trim in steady sideslips at low speed.

The pilot considered the airplane more difficult to fly with the reduced directional stability because in maneuvers inadvertent sideslipping occurred more easily and the sideslip angles reached were larger. At low speed where the dihedral effect was high, large lateral trim changes accompanied the changes in sideslip.

Dynamic Lateral and Directional Stability

Reference 1 shows the oscillatory characteristics of the airplane with the ventral-fin extension on to be satisfactory with the 40-percent-span slots on the wing. The oscillatory characteristics of the airplane with the ventral-fin extension on were not investigated for the wing without slots or with 80-percent-span slots since the effects of the slots would probably be negligible.

The dynamic lateral and directional stability characteristics were investigated for the airplane with the ventral-fin extension removed and with the 80-percent-span slots on the wing by abruptly deflecting and releasing the rudder and recording the resulting oscillation. Time histories of these maneuvers are presented in figure 24(a) for the flaps-up condition at approximately 160 miles per hour and in figure 25(a) for the flaps-down condition at approximately 110 miles per hour. The oscillation at approximately 160 miles per hour (fig. 24(a)) was made with the stick free. In the oscillation at approximately 110 miles per hour (fig. 25(a)) the pilot attempted to hold the stick fixed because sufficient elevator trim tab was not available to trim the elevator stick force to zero. The oscillations of the airplane were satisfactorily damped at all speeds tested. The period of the oscillation was relatively long, approximately 5 seconds. Figures 24(b) and 25(b) are time histories of oscillations in which the pilot applied coordinated rudder and aileron to damp the oscillations. The pilot could damp the oscillations easily and had no objections to the oscillatory characteristics of the airplane. For the airplane with the ventral-fin extension off the period of the oscillation was greater than for the airplane with the ventral-fin

extension on, but the damping of the oscillation in terms of the number of cycles to damp to one-half amplitude was not changed appreciably.

Figure 26 shows time histories of left and right rudder kicks at approximately 225 miles per hour. These maneuvers were made by abruptly deflecting and holding the rudder fixed in the deflected position while the stick was free. Figure 26 shows the effect of the negative dihedral, previously discussed: When the rudder is deflected to the right the airplane rolls to the left and when the rudder is deflected to the left the airplane rolls to the right.

Lateral Control

The lateral control characteristics of the airplane were measured by performing rudder-fixed aileron rolls at various speeds with the flaps up and down. The data were evaluated in terms of the variation of maximum wing-tip helix angle $pb/2V$ with change in total aileron angle $\Delta\delta_a$. Figure 27 presents the data for the airplane with 80-percent-span slots on the wing. A few tests without slots on the wing showed the slots to have a negligible effect on the rolling characteristics of the airplane.

At 148 miles per hour with the flaps up, an aileron deflection of 30° produced a maximum wing-tip helix angle $pb/2V$ of 0.045 radian in a left roll and 0.048 radian in a right roll. For a given aileron deflection, a marked decrease in maximum $pb/2V$ occurred as the speed was decreased because of the increase in dihedral effect and the higher sideslip angles reached in the rolls at low speed. Figure 28 shows time histories of left and right aileron rolls at 110 miles per hour with the flaps down. Because of the high dihedral effect present at 110 miles per hour, the rolling characteristics of the airplane were oscillatory and in the left roll the rolling moment due to the high dihedral was sufficient to cause a reversal in rolling velocity.

By using the dihedral-effect data of figure 19, the reduction in $pb/2V$ due to the dihedral effect could be calculated. Figure 29 shows the calculated variation of maximum $pb/2V$ with change in total aileron angle for zero dihedral effect $\left(\frac{dC_l}{d\psi} = 0\right)$ for the airplane at 110 miles per hour with the flaps down and with 80-percent-span slots. The flight data are also included for comparison. The reduction in $pb/2V$ due to the dihedral effect in rudder-fixed aileron rolls was approximately 40 percent at 110 miles per hour with the flaps down (fig. 29).

Static Longitudinal Stability

Longitudinal-stability measurements with the 80-percent-span slots on the wing were made with the flaps up and down and a center-of-gravity location of approximately 27 percent mean aerodynamic chord. Figures 30 and 31 show the variation of elevator angle, elevator stick force, angle of attack of the thrust axis, and sideslip angle with calibrated airspeed for the flaps-up and flaps-down conditions, respectively. Figure 32 shows the variation of elevator angle required for trim with normal-force coefficient and figure 33 shows the variation of elevator stick force divided by impact pressure with normal-force coefficient.

With the flaps up the longitudinal stability was high throughout the speed range. With the flaps down the stability was high at moderate speeds but a large decrease in stability occurred a few miles per hour above the stall and the stability was neutral down to the stall. After the stall, stable pitching tendencies were again present as up elevator was required to keep the airplane from pitching down. Tuft surveys showed that with the flaps up, stalling occurred first at the wing root, whereas with the flaps down, the initial stall was farther out on the wing. The increased stability near the stall with flaps up was probably caused by the decrease in downwash at the tail resulting from the wing-root stall. The results obtained for the airplane with 80-percent-span slots on the wing are substantially the same as those reported in reference 2 for the airplane without slots and with 40-percent-span slots. The wind-tunnel measurements of longitudinal stability showed the same trends as the flight data with the flaps up or down.

Stalling Characteristics

Time histories of stalls with the 80-percent-span slots on the wing are shown in figure 34(a) for the flaps-up condition and in figure 35(a) for the flaps-down condition. Photographs of tufts on the wing at various times during the stall are shown in figures 34(b) and 35(b). These tuft pictures were taken with cameras mounted above the canopy and show the outboard 80 percent of the sweptback wing panels. The white lines on the wing are located at intervals of 20 percent of the semispan of the sweptback wing panels and are parallel to the airplane center line. Cameras were also mounted on the tail to photgraph tufts on the inboard part of the wing. These pictures are not shown, but the results obtained will be discussed.

Angle-of-attack measurements are not shown on the time histories when appreciable rolling, yawing, or pitching motions are present because the angle of attack does not define the flow for such unsteady conditions.

The pilot considered the stalling characteristics of the airplane with 80-percent-span slots good with flaps up or down. With the flaps up the airplane oscillated about all three axes at the stall. The rolling

and yawing motions were mild but the pitching increased in amplitude leading to successive stalls under increasing accelerations. In the flaps-down condition, the stick-fixed stability became neutral about 5 miles per hour above the stall and the airplane exhibited a tendency to pitch into the stall. The airplane became laterally unsteady about 3 miles per hour above the stall and at the stall an oscillation in roll, pitch, and yaw developed. The oscillation in roll was more pronounced with the flaps down than with the flaps up and, again, the pitch oscillation built up in amplitude. Attitude changes following the stall were not large or abrupt and recovery could be made easily.

The tuft pictures of figure 34(b) and the pictures of the tufts at the wing root showed that with the flaps up stalling first occurred over the rear part of the wing root. Some of the tufts behind the juncture of the inboard end of the slot and the wing also showed some unsteadiness. As the angle of attack was increased, that part of the wing not spanned by the slot became completely stalled, but the slotted part of the wing remained almost completely unstalled at all times. The stall patterns with the flaps deflected (fig. 35(b)) were very similar to those with the flaps up except that the wing first stalled over the rear part of the wing behind the juncture of the inboard end of the slot with the wing instead of at the wing root.

Stalls were also made when the ventral-fin extension was off the airplane. Time histories of stalls with the ventral-fin extension off and the flaps up and down are shown in figures 36 and 37, respectively. The stalling characteristics with the reduced directional stability resulting from removal of the ventral-fin extension were still good but somewhat less desirable than with the ventral-fin extension on because the oscillations which occurred at the stall increased in amplitude much more rapidly.

Lift Characteristics

The variation of normal-force coefficient with angle of attack of the thrust axis as measured in flight with the 80-percent-span slots on the wing is shown in figure 38. Wind-tunnel data are also included in figure 38 for comparison with the flight results. These wind-tunnel data are for trimmed conditions. The flight maximum normal-force coefficients presented are those attained before any appreciable uncontrolled-for motions due to stalling occurred. In the flaps-up condition, higher normal-force coefficients were reached after uncontrolled-for motions had occurred (see fig. 34(a)) but these normal-force coefficients were not considered usable. The flight and wind-tunnel results for the flaps-down condition are not directly comparable because in the wind-tunnel tests the flap deflection was 45° and in flight the flap deflection was approximately 40°.

In the flaps-up condition at moderate and low angles of attack of the thrust axis, the agreement between the flight and tunnel measurements

is excellent. At angles of attack greater than 10°, the slope of the flight curve is somewhat smaller than the slope of the tunnel curve. The maximum normal-force coefficients are approximately the same but in flight the maximum normal-force coefficient occurred at an angle of attack approximately 2° higher than in the wind tunnel.

In the flaps-down condition, the slopes of the flight and tunnel curves are approximately the same but the curves are displaced. A part of the displacement of the curves can be attributed to the greater flap deflection used in the tunnel tests. The maximum normal-force coefficients are again practically the same but the flight value occurred at an angle of attack of the thrust axis approximately 4° higher than the wind-tunnel value.

The flight values of maximum normal-force coefficient $C_{N_{max}}$ for the flaps-up and flaps-down conditions without slots and with 40-percent-span slots (obtained from reference 2) and with 80-percent-span slots are as follows:

Slots (percent span)	Flaps	$C_{N_{max}}$
0	Up	1.20
40	Up	1.11
80	Up	1.19
0	Down	1.51
40	Down	1.29
80	Down	1.42

With the flaps up the maximum normal-force coefficient for the airplane without slots and with 80-percent-span slots have about the same value, 1.20. With the flaps down and without slots the maximum normal-force coefficient of 1.51 is 0.09 higher than for the 80-percent-span slots. As previously mentioned the juncture of the inboard end of the slot with the wing caused premature separation which probably accounts for the decrease in $C_{N_{max}}$ which occurred with the slots on the wing. An increase in $C_{N_{max}}$ of 0.13 occurred when the slot span was increased from 40 to 80 percent of the wing span with the flaps down.

CONCLUSIONS

The results of the investigation to determine the low-speed stability, control, and stalling characteristics of an airplane having a 35° sweptback wing without slots and with slots along 80 percent of the span of the sweptback wing panels may be summarized as follows:

1. The directional stability of the airplane as measured in steady sideslips by the variation of rudder angle with sideslip angle was positive with or without slots and with the flaps up or down at all test speeds. A decrease in directional stability occurred with decrease in speed. A part of the decrease in directional stability with speed was due to the unstable yawing moments caused by the large aileron deflections required for trim in steady sideslips at low speed.

2. Removing the ventral-fin extension reduced the directional stability of the airplane with the largest reduction occurring at high normal-force coefficients or low speed. The pilot considered the airplane more difficult to fly with the reduced directional stability because in maneuvers inadvertent sideslipping occurred more easily and the sideslip angles reached were higher. At low speed where the dihedral effect was high, large lateral trim changes accompanied the changes in sideslip.

3. A large increase in dihedral effect occurred with increase in normal-force coefficient. With the 80-percent-span slots on the wing and the flaps up, slight negative stick-fixed dihedral effect was present below normal-force coefficients of approximately 0.30 and negative stick-free dihedral effect was present below normal-force coefficients of approximately 0.56. The pilot considered the negative dihedral more objectionable than the high positive dihedral present at high normal-force coefficients. The negative dihedral was objectionable because in rough air or in maneuvers involving changes in sideslip the response of the airplane was illogical. The combination of high positive dihedral present at low speed and negative dihedral present at high speed was particularly objectionable to the pilot because he could not become accustomed to either condition.

4. The agreement between the flight and wind-tunnel measurements of dihedral effect was good for the wing with the slots and fair for the wing without the slots. The wind-tunnel data showed a large increase in dihedral effect with increase in Reynolds number for the wing without slots.

5. Lateral and directional oscillations of the airplane were satisfactorily damped even with the low directional stability present when the ventral-fin extension was off. The pilot could damp the oscillations easily by applying coordinated rudder and aileron.

6. The maximum values of wing-tip helix angle reached in rudder-fixed aileron rolls were low. At 148 miles per hour with the flaps up, an aileron deflection of 30° produced a maximum wing-tip helix angle of 0.045 radian in a left roll and 0.048 radian in a right roll. For a given aileron deflection a marked decrease in maximum wing-tip helix angle occurred with decrease in speed because of the increase in dihedral effect and the higher sideslip angles reached in rolls at low speed. At 110 miles per hour with the flaps down, the high dihedral effect caused reversal of rolling velocity in left rolls.

7. The longitudinal stability with the 80-percent-span slots on the wing and the flaps up was high throughout the speed range. With the flaps down the longitudinal stability was high at moderate speeds, but a few miles per hour above the stall the stability decreased and was neutral down to the stall.

8. The stalling characteristics of the airplane were good with the flaps up or down when the 80-percent-span slots were on the wing. The airplane oscillated about all three axes at the stall. The attitude changes of the airplane were small during these oscillations and recovery from the stall could be made easily. With the ventral-fin extension removed, the amplitude of the oscillations at the stall increased rapidly.

Langley Memorial Aeronautical Laboratory
National Advisory Committee for Aeronautics
Langley Field, Va., May 19, 1948

REFERENCES

1. Sjoberg, S. A., and Reeder, J. P.: Flight Measurements of the Lateral and Directional Stability and Control Characteristics of an Airplane Having a 35° Sweptback Wing with 40-Percent-Span Slots and a Comparison with Wind-Tunnel Data. NACA TN No. 1511, 1948.

2. Sjoberg, S. A., and Reeder, J. P.: Flight Measurements of the Longitudinal Stability, Stalling, and Lift Characteristics of an Airplane Having a 35° Sweptback Wing without Slots and with 40-Percent-Span Slots and a Comparison with Wind-Tunnel Data. NACA TN No. 1679, 1948.

3. Lockwood, Vernard E., and Watson, James M.: Stability and Control Characteristics at Low Speed of an Airplane Model Having a 38.7° Sweptback Wing with Aspect Ratio 4.51, Taper Ratio 0.54, and Conventional Tail Surfaces. NACA TN No. 1742, 1948.

TABLE I

AIRPLANE DIMENSIONS AND CHARACTERISTICS

Engine	Allison V-1710
Propeller:	
Diameter, ft	10.375
Number of blades	3
Engine-propeller gear ratio	2.23
Normal gross weight, lb	8700
Wing:	
Span, ft	33.6
Area, sq ft	250
Incidence (root section), deg	1.3
Airfoil section (normal to L.E.)	
Root	Modified 66,2x-116 (a=0.6)
Tip	Modified 66,2x-216 (a=0.6)
Mean aerodynamic chord, in.	93.6
Leading edge of M.A.C. (in. behind L.E. root chord)	39.3
Aspect ratio	4.51
Taper ratio	1.84
Dihedral, deg	0
Sweepback (at quarter-chord line), deg	35
Plain sealed wing flaps:	
Total area, sq ft	12.52
Span (along hinge line, each), in.	77.4
Travel (no load on system), deg	45
Ailerons:	
Span (along hinge line, each), in.	105
Area (behind hinge line, each), sq ft	6.51
Travel (no load on system), deg	±17
Horizontal tail:	
Span, in.	175
Total area, sq ft	46.53
Stabilizer area, sq ft	33.7
Total elevator area, sq ft	12.83
Elevator area (behind hinge line), sq ft	9.56
Distance from elevator hinge line to L.E. of M.A.C., in.	240.9
Elevator travel (no load on system), deg	
Upward	35
Downward	15
Vertical tail:	
Height along hinge line, in.	78.87
Fin area (above horizontal tail), sq ft	13.47
Total ventral-fin area, sq ft	17.10
Total rudder area, sq ft	10.26
Rudder area (behind hinge line), sq ft	8.3
Distance from rudder hinge line to L.E. of M.A.C., in.	263
Rudder travel (no load on system), deg	±30

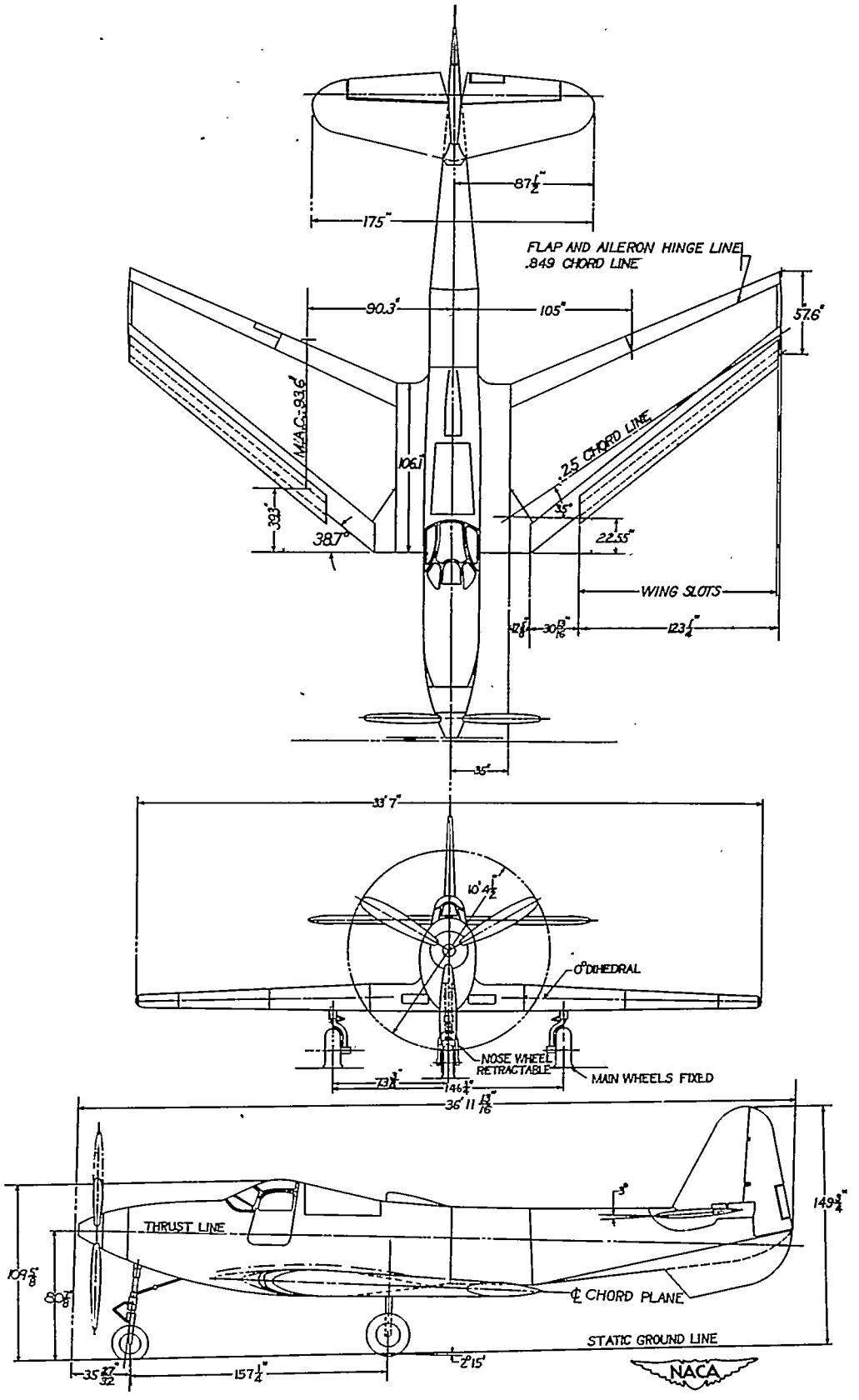

Figure 1.- Three-view drawing of test airplane.

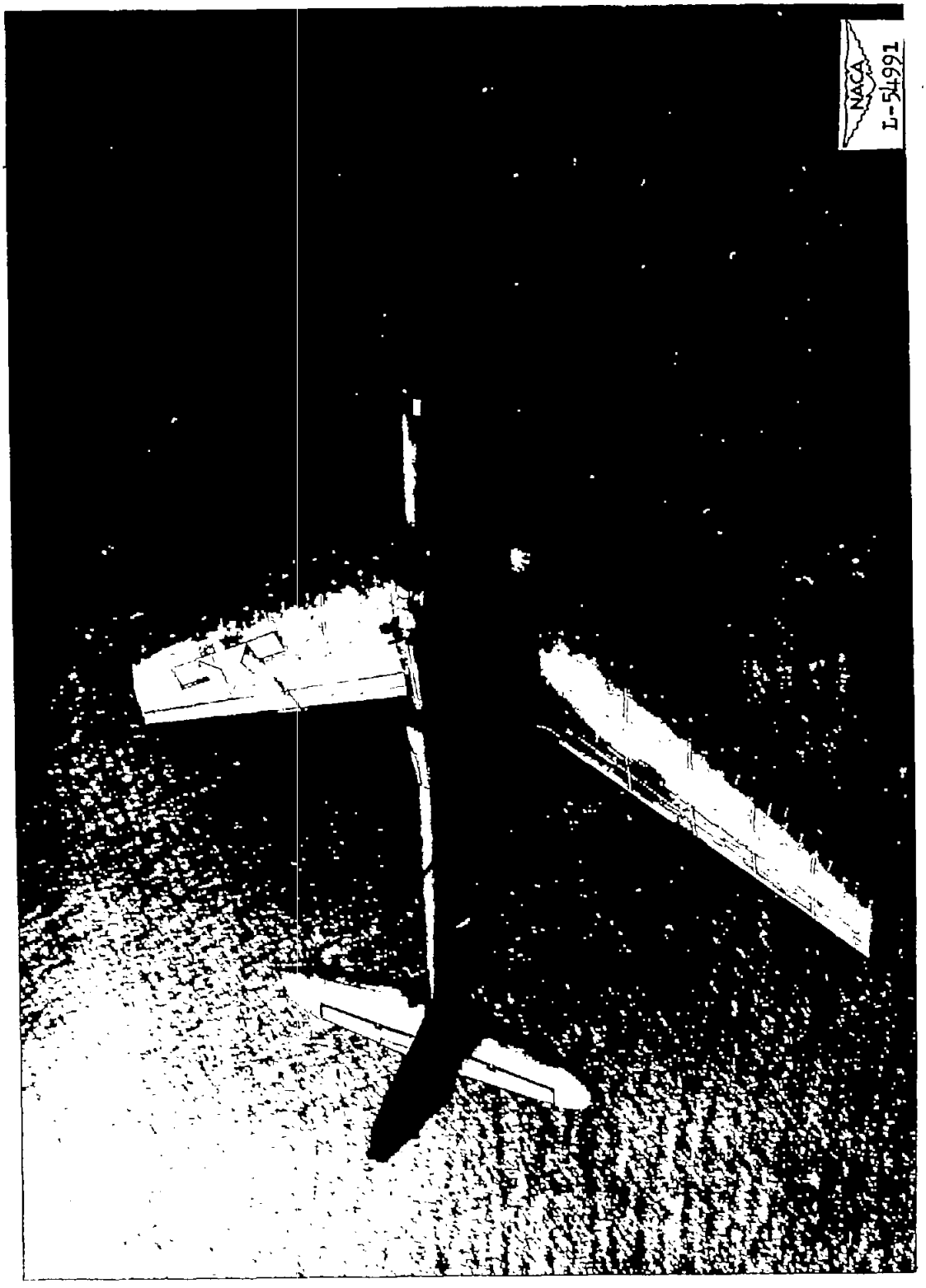

Figure 2.- Photograph of test airplane in flight.

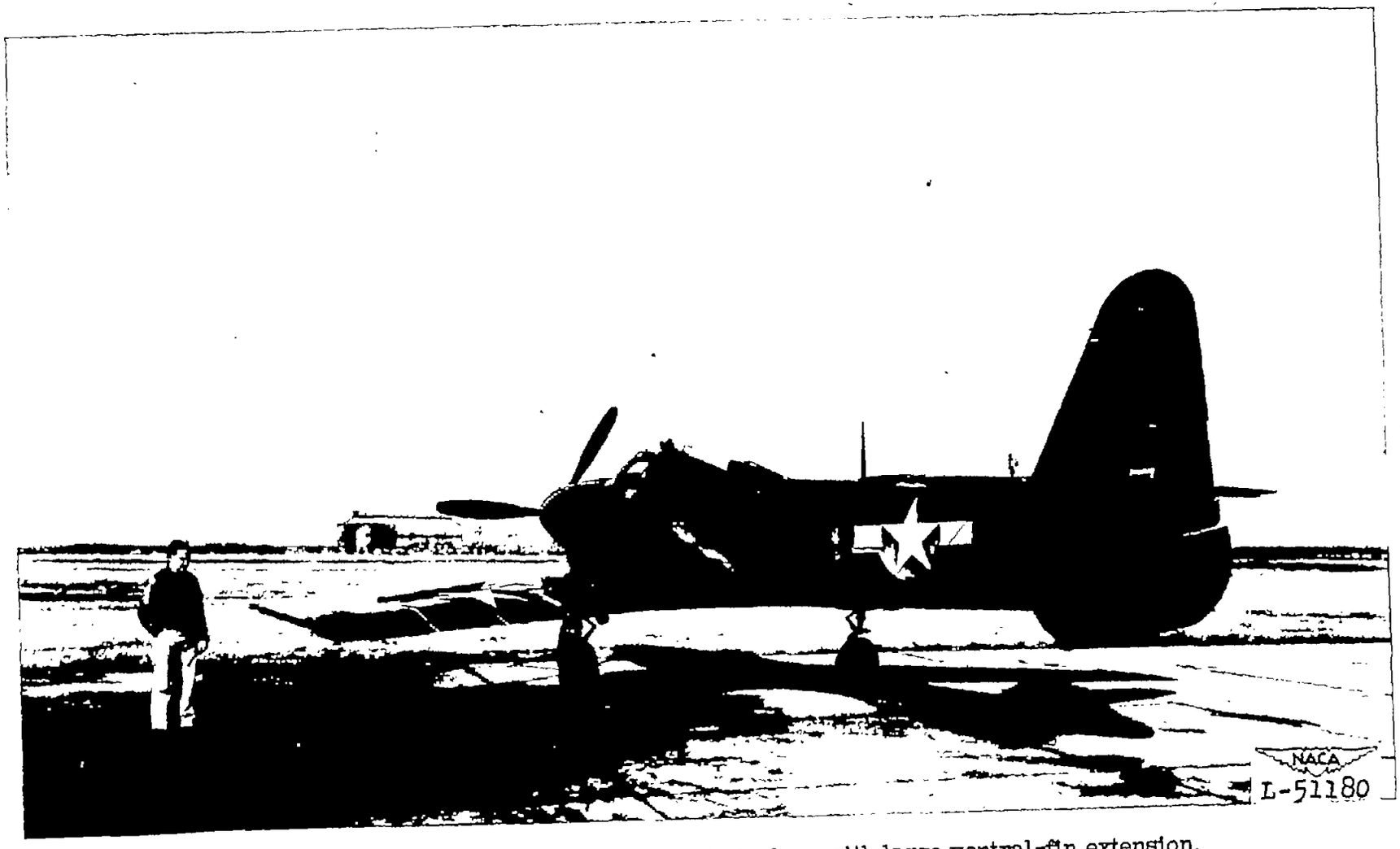

Figure 3.- Three-quarter rear view of test airplane with large ventral-fin extension.

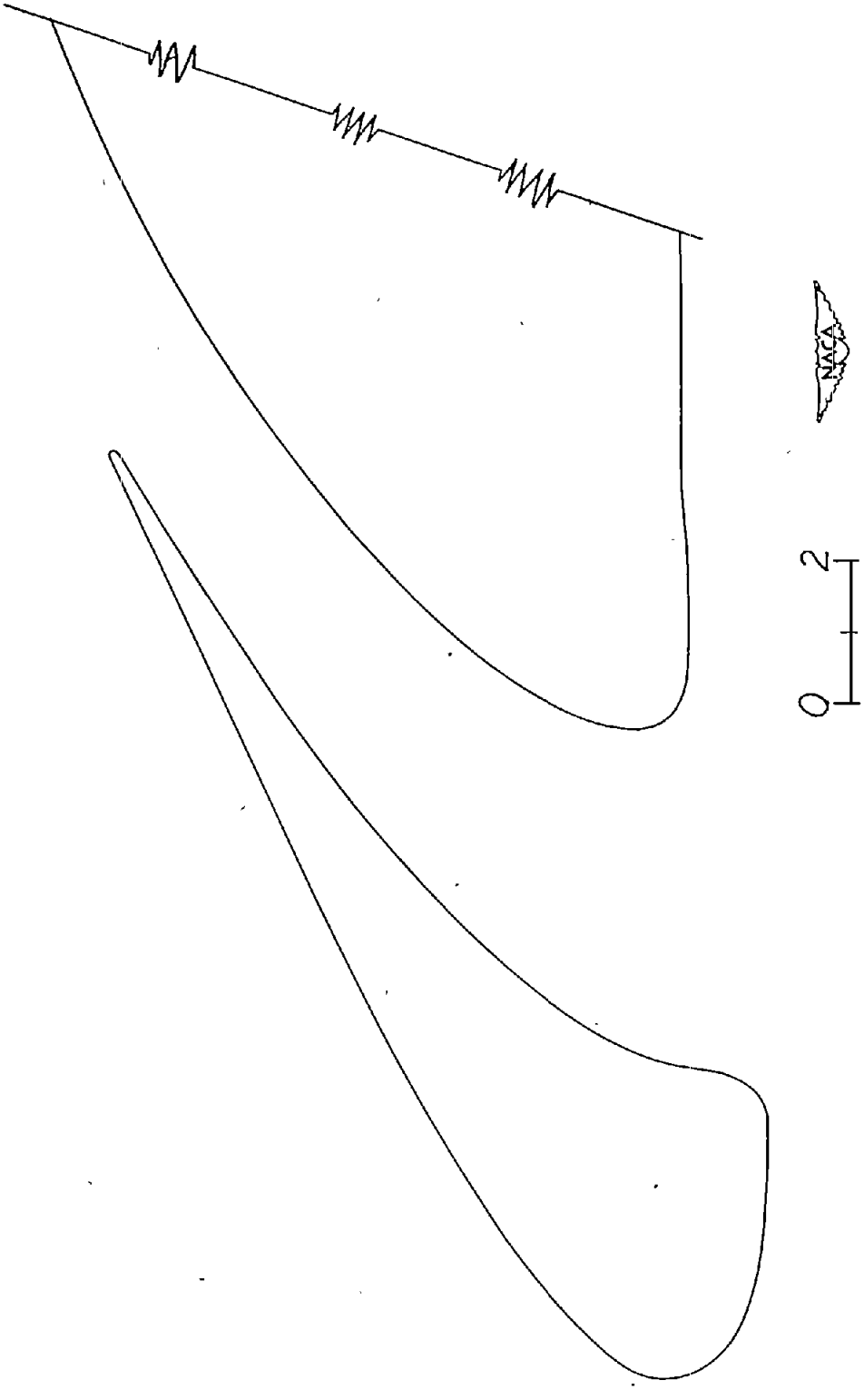

Figure 4.- Section of slot and forward part of wing in plane normal to wing leading edge.

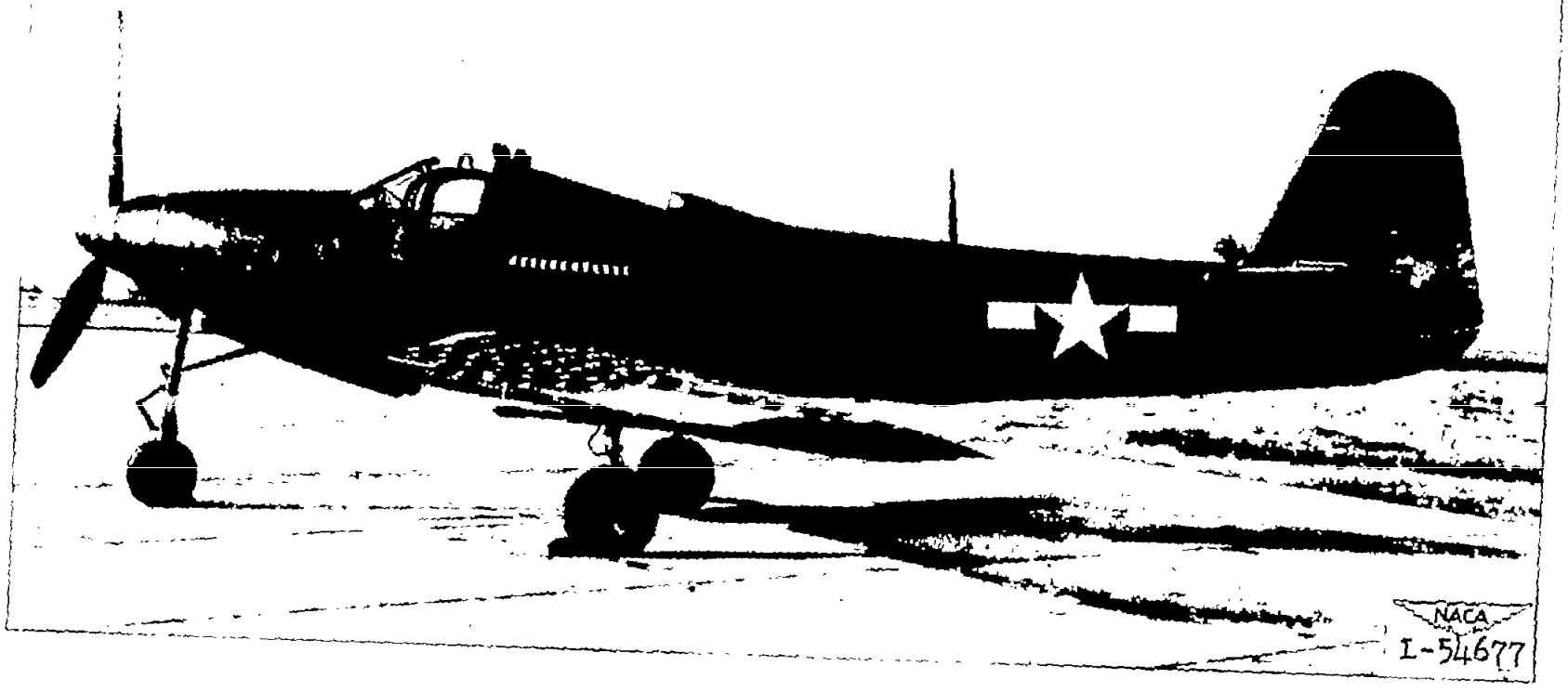

Figure 5.- Side view of test airplane without large ventral-fin extension.

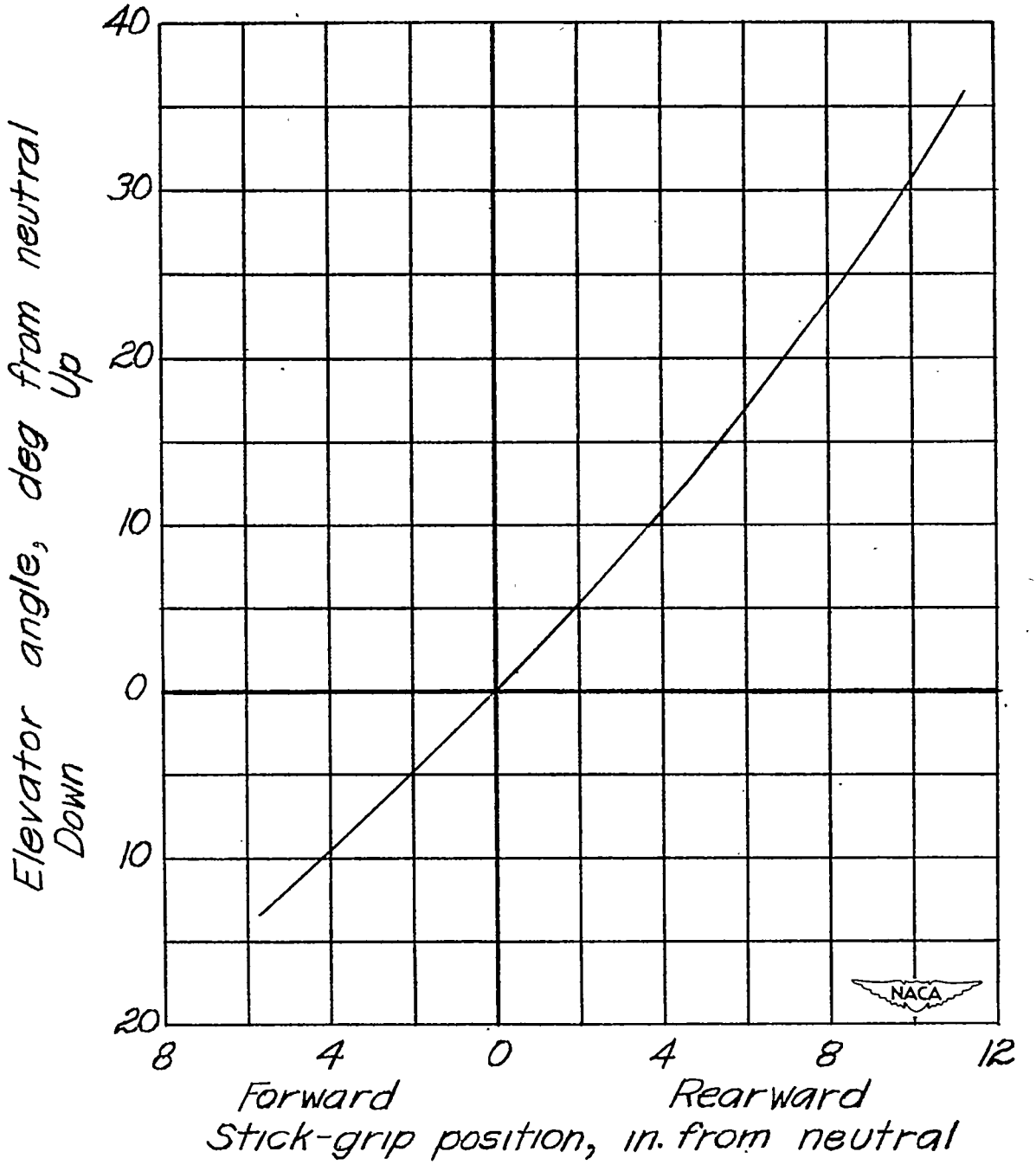

Figure 6.- Variation of elevator angle with stick-grip position. No load on system.

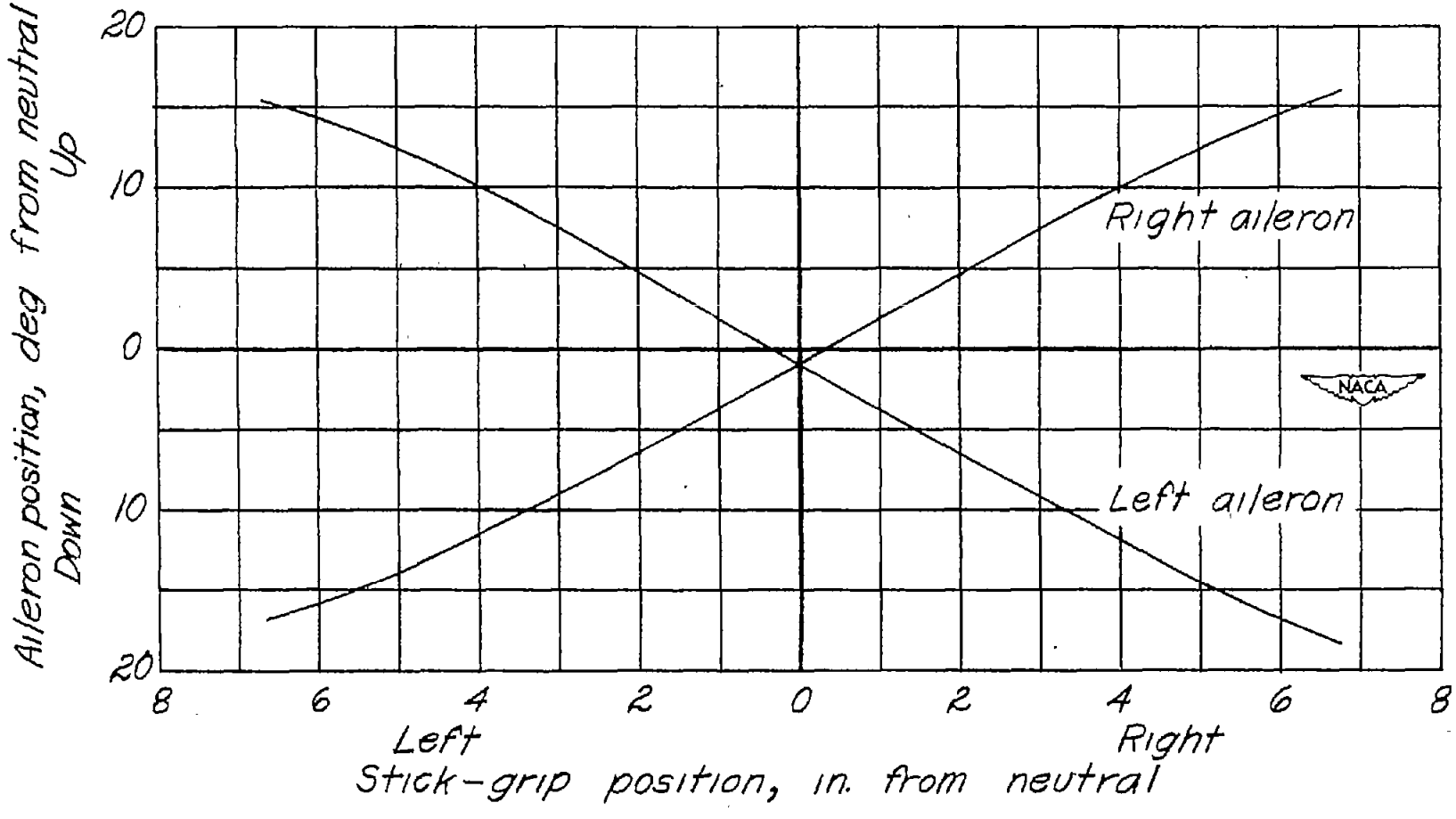

Figure 7.- Variation of left and right aileron position with stick-grip position. No load on system.

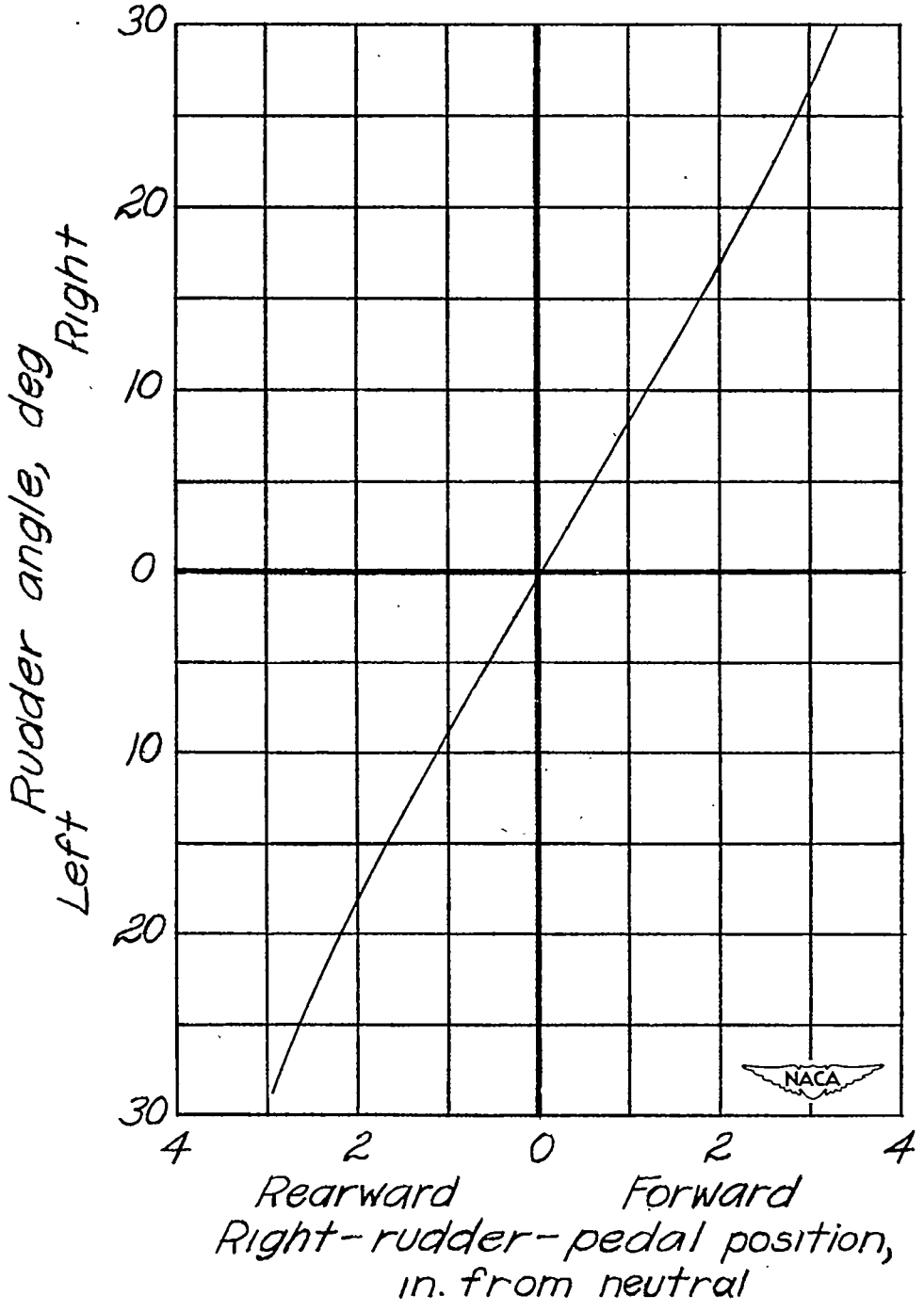

Figure 8.- Variation of rudder angle with right-rudder-pedal position. No load on system.

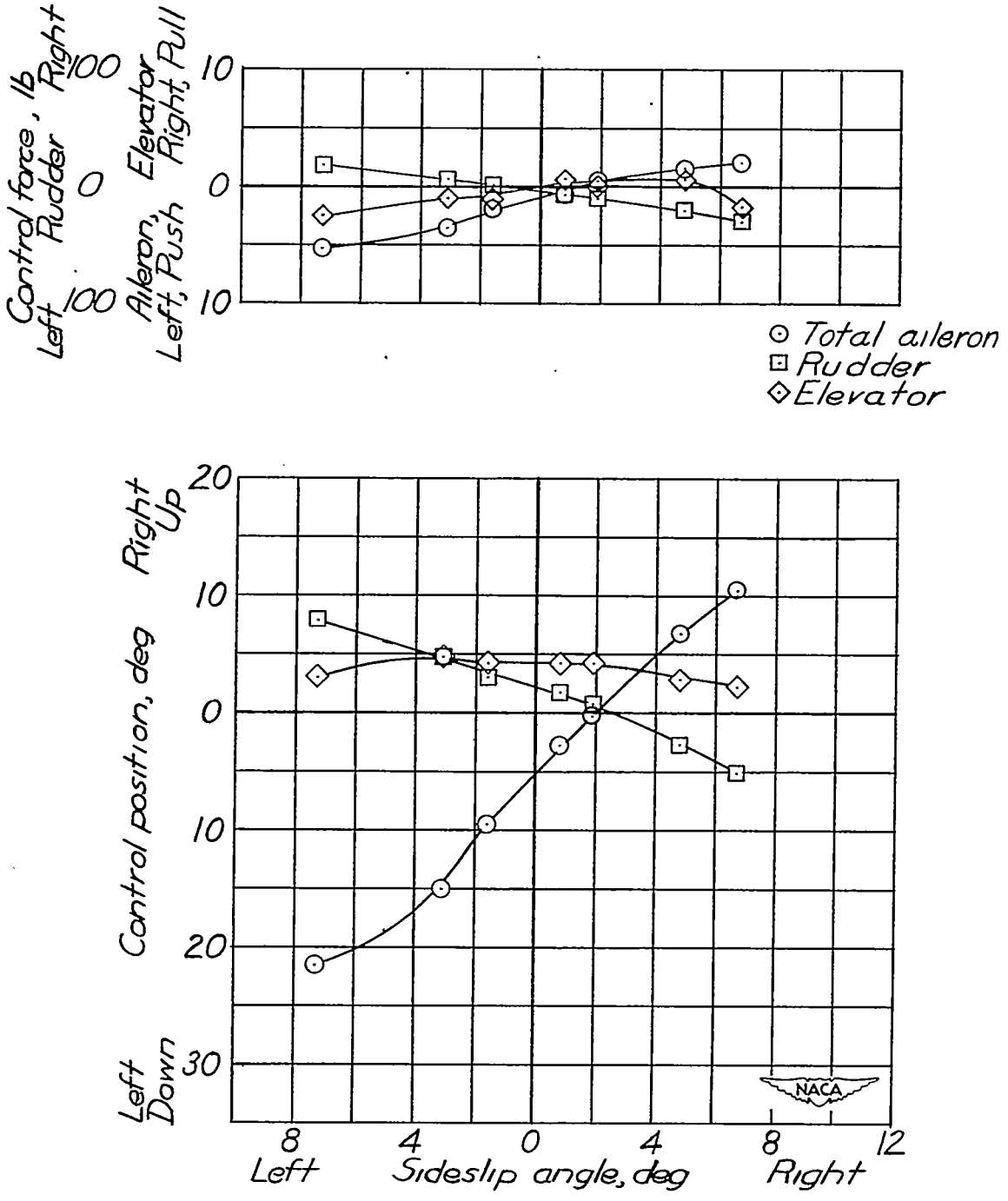

(a) V_c = 114 miles per hour; C_N = 1.08.

Figure 9.- Steady sideslip characteristics of test airplane without slots on wing. Flaps up; nose wheel up; engine idling.

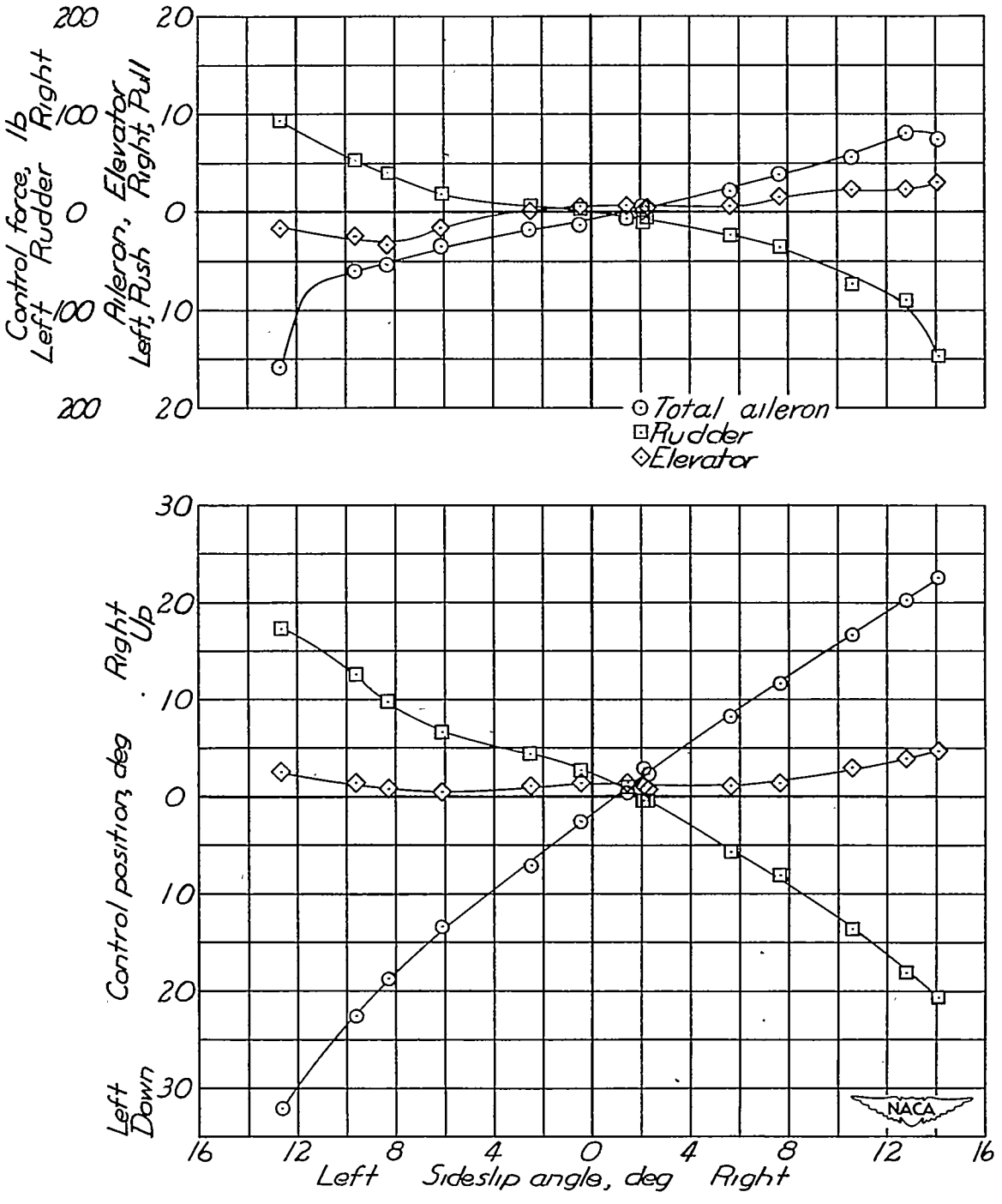

(b) V_c = 125 miles per hour; C_N = 0.90.

Figure 9.- Continued.

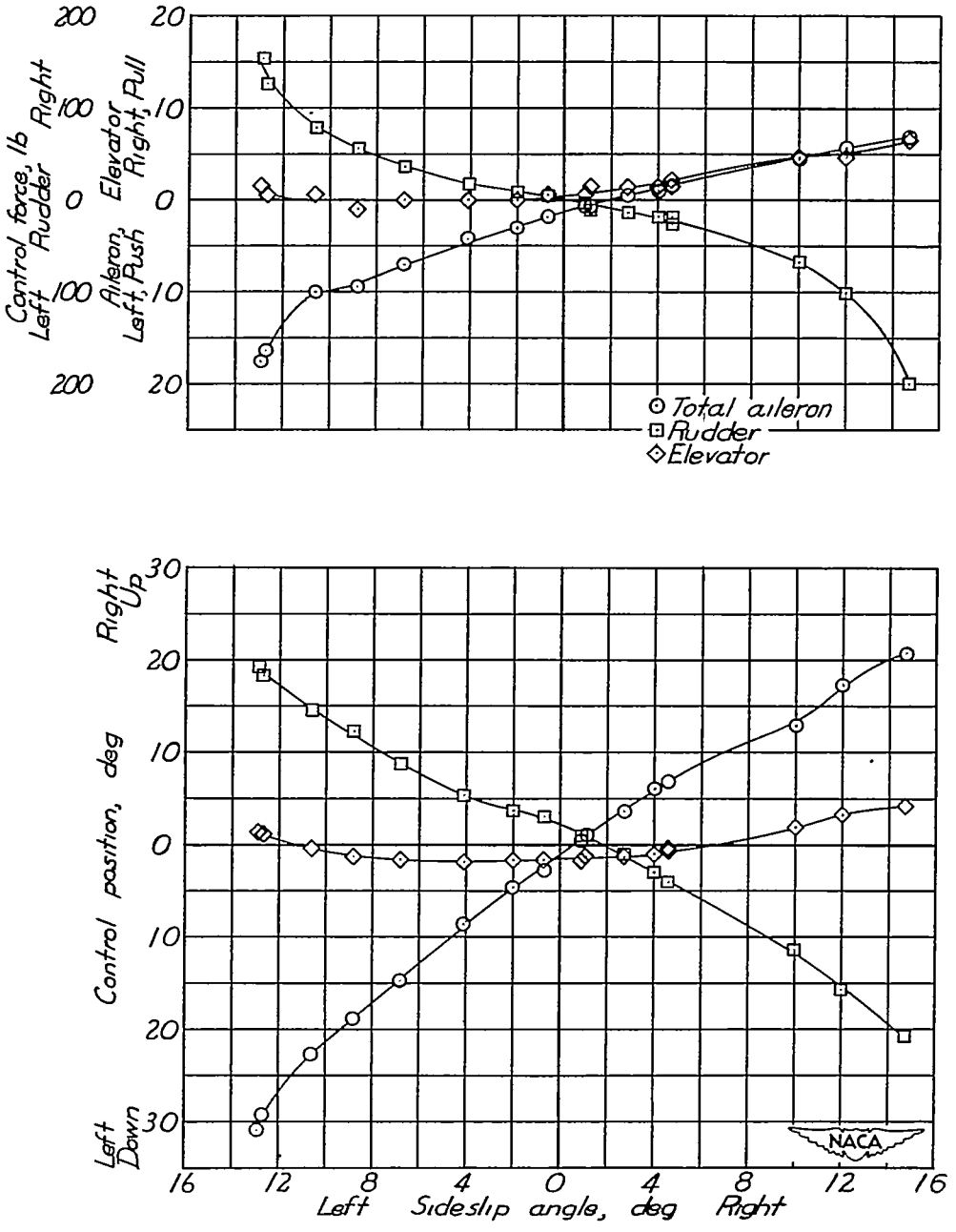

(c) V_c = 140 miles per hour; C_N = 0.73.

Figure 9.- Continued.

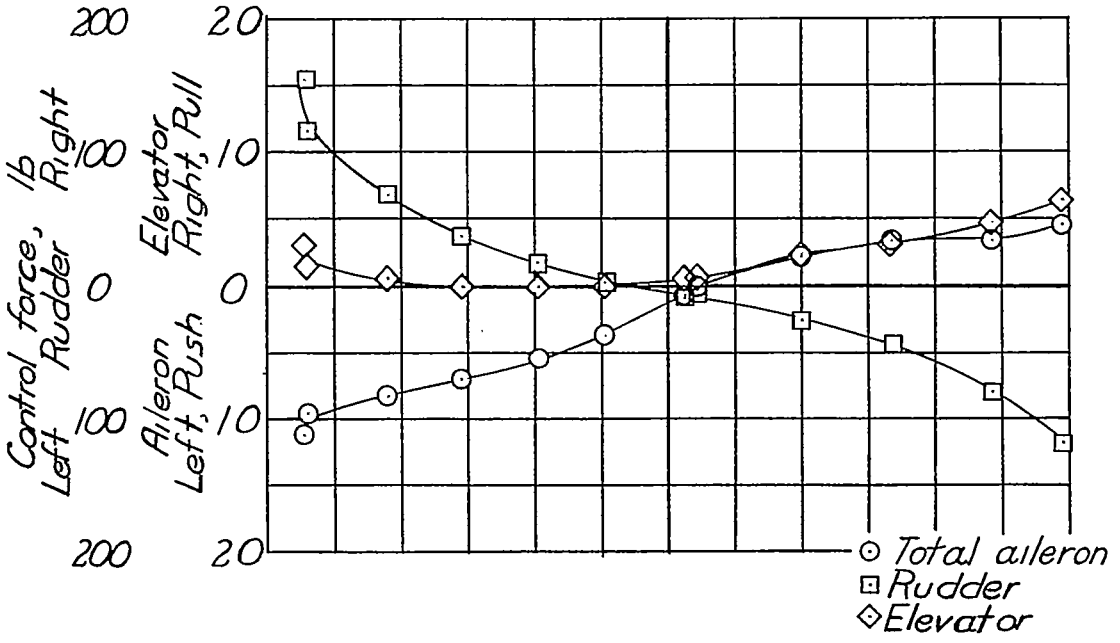

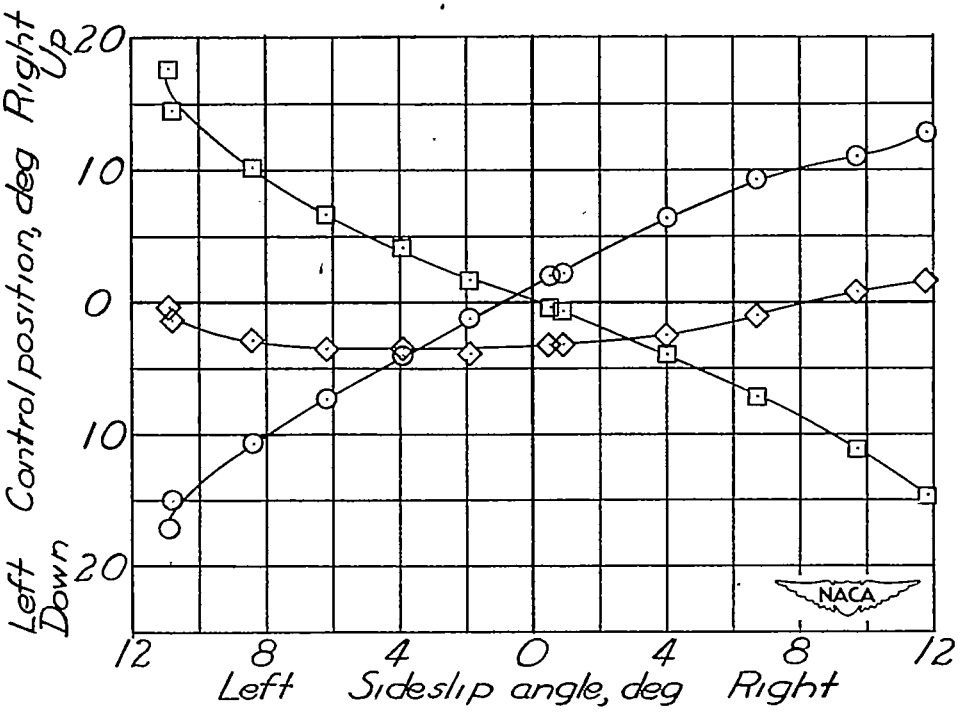

(d) V_c = 160 miles per hour; C_N = 0.55.

Figure 9.- Continued.

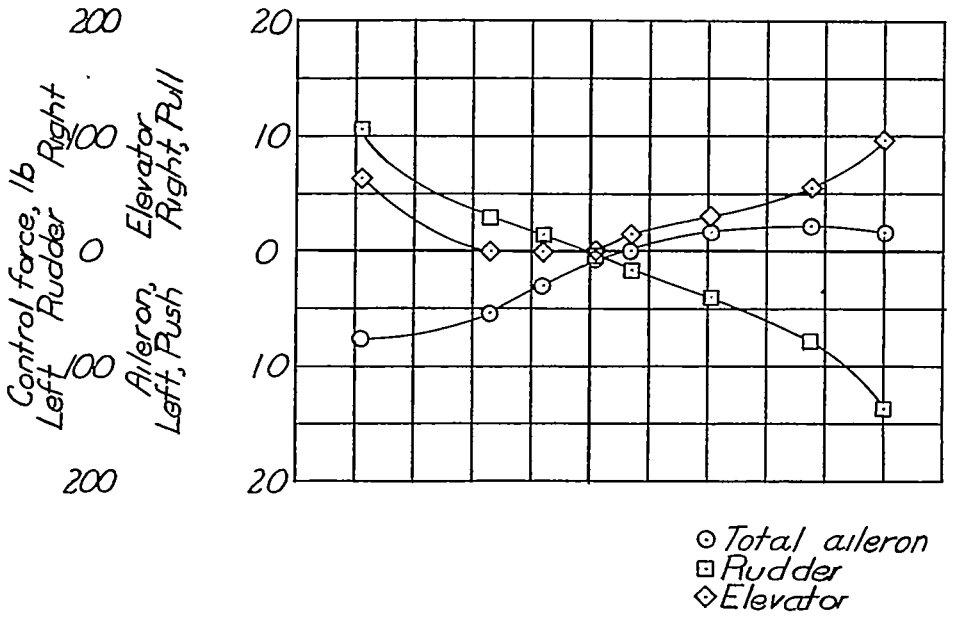

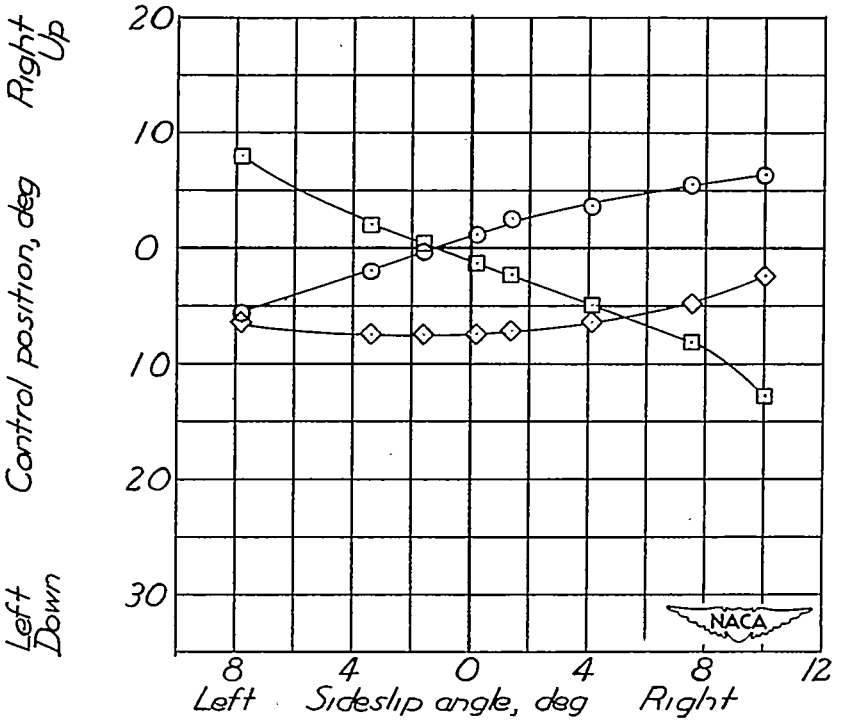

(e) V_c = 200 miles per hour; C_N = 0.35.

Figure 9.- Concluded.

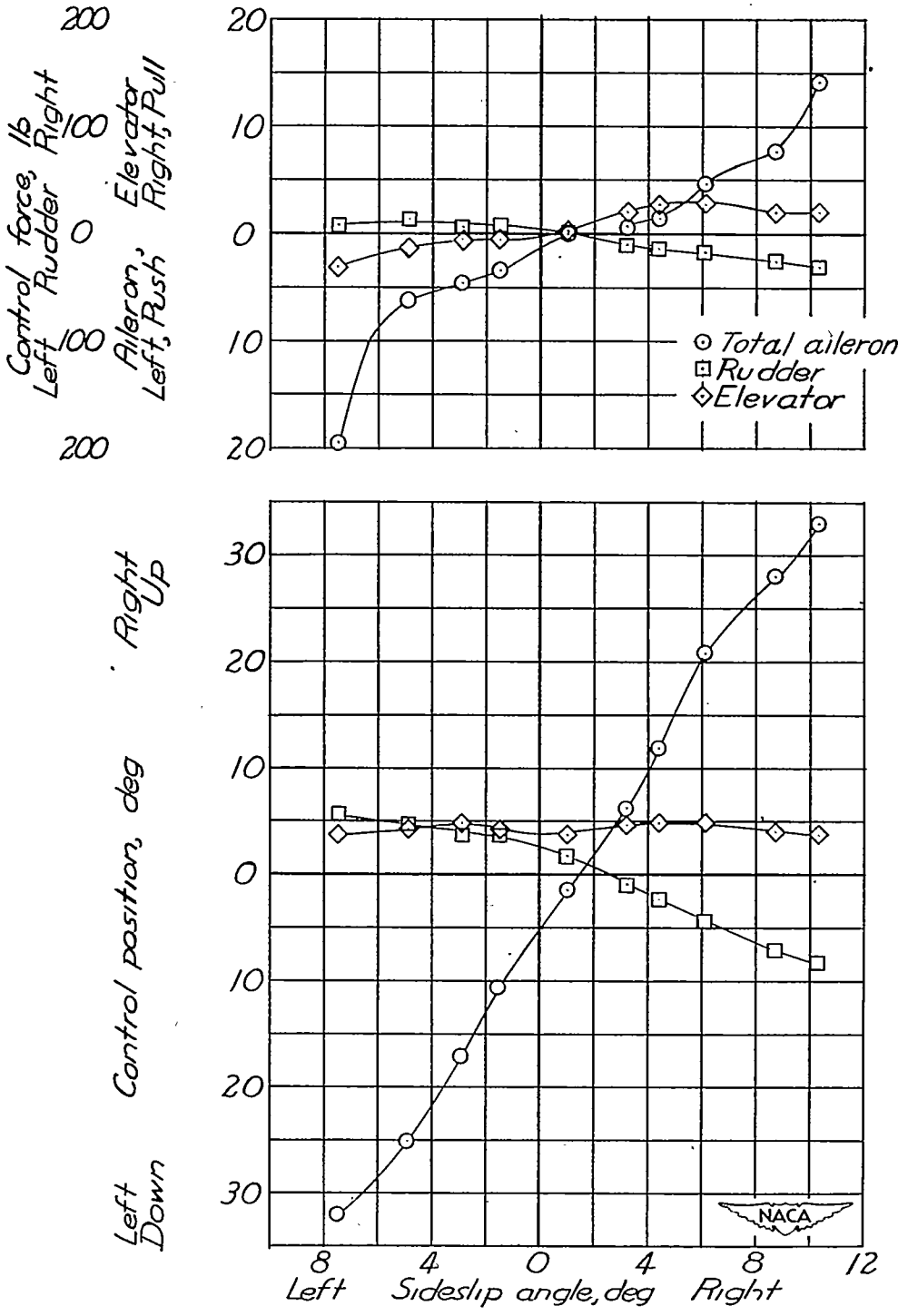

(a) V_c = 110 miles per hour; C_N = 1.14.

Figure 10.- Steady sideslip characteristics of test airplane without slots on wing. Flaps down; nose wheel down; engine idling.

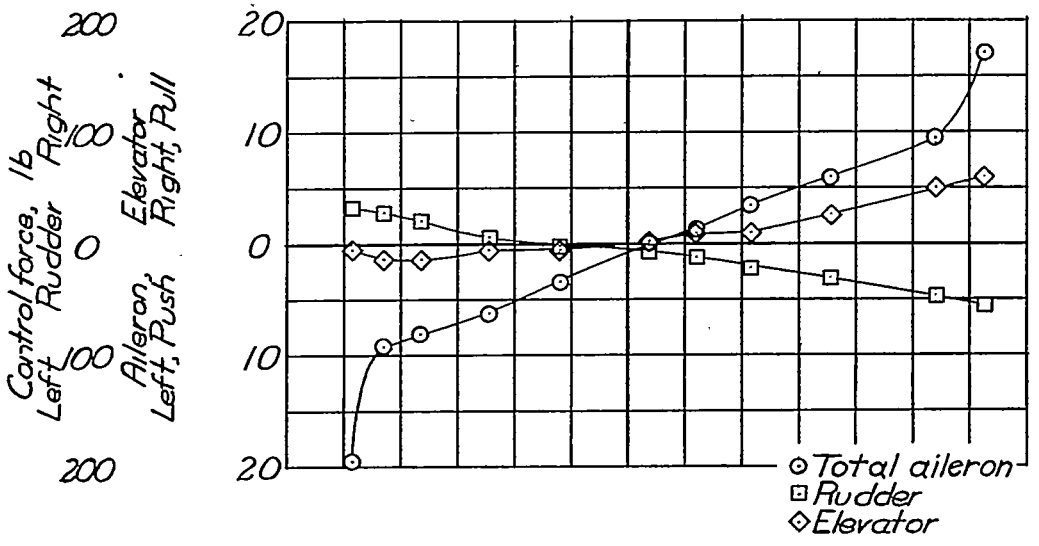

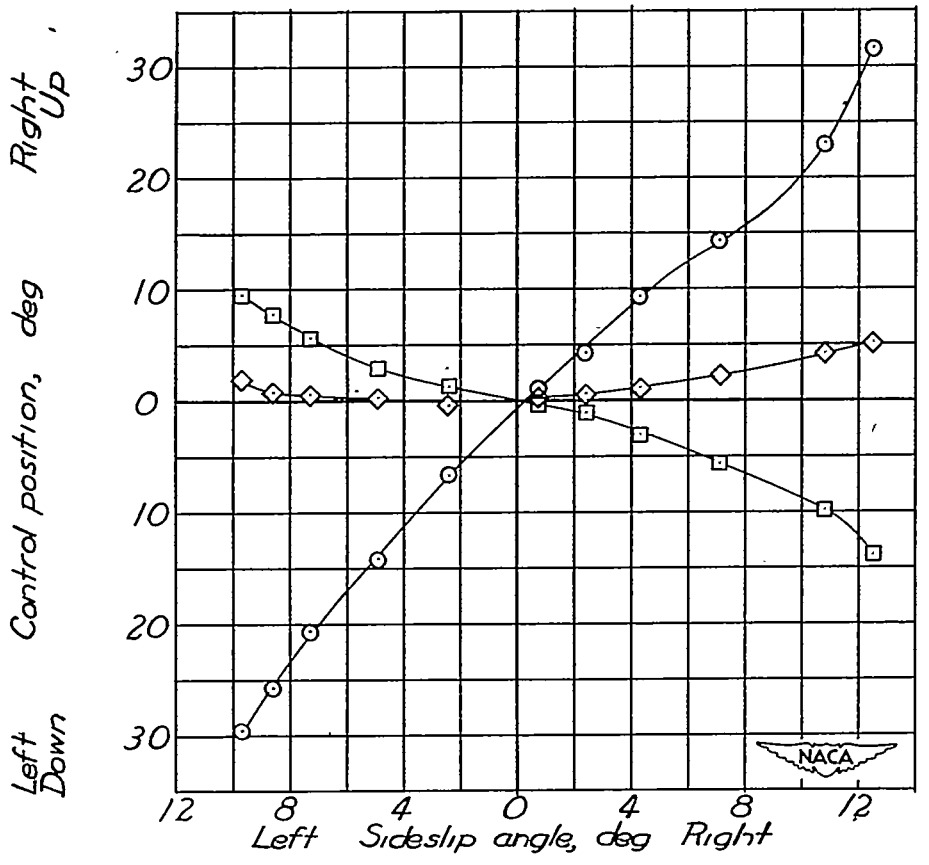

(b) V_c = 130 miles per hour; C_N = 0.82.

Figure 10.- Continued.

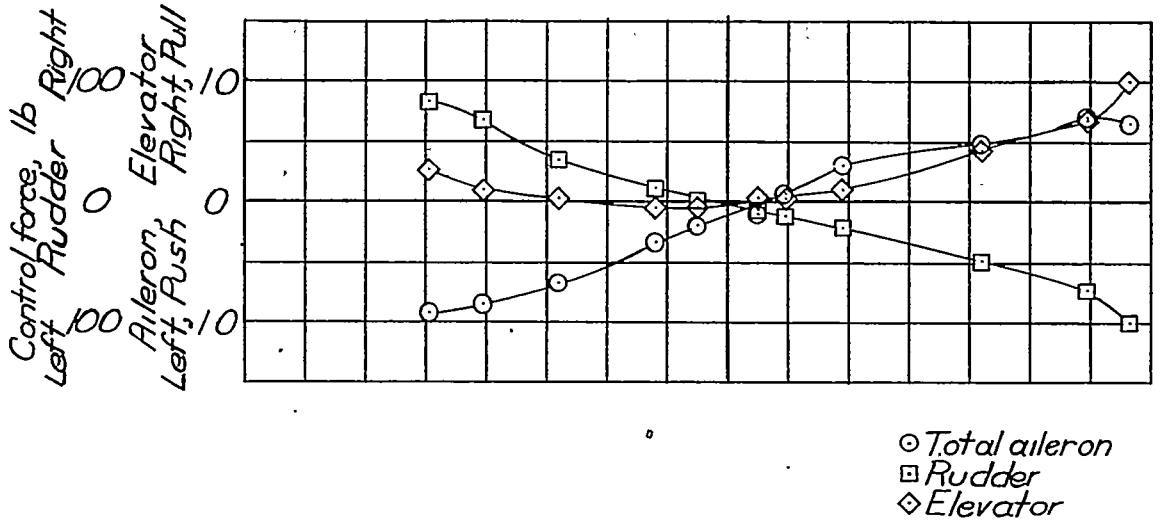

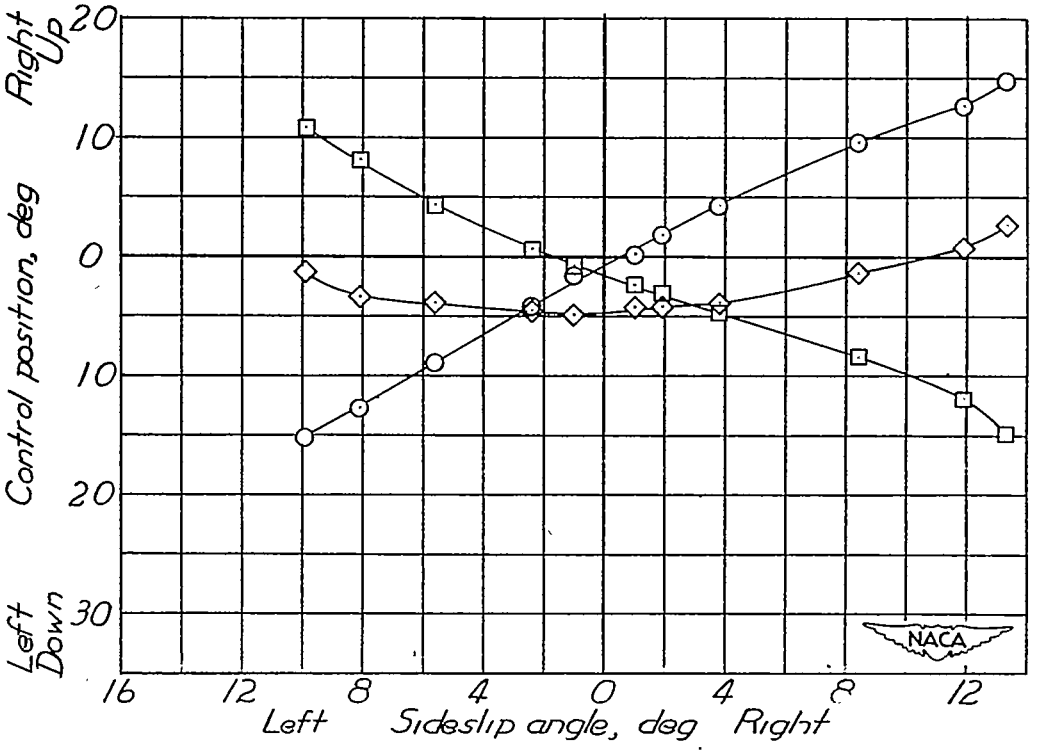

(c) V_c = 160 miles per hour; C_N = 0.55.

Figure 10.- Concluded.

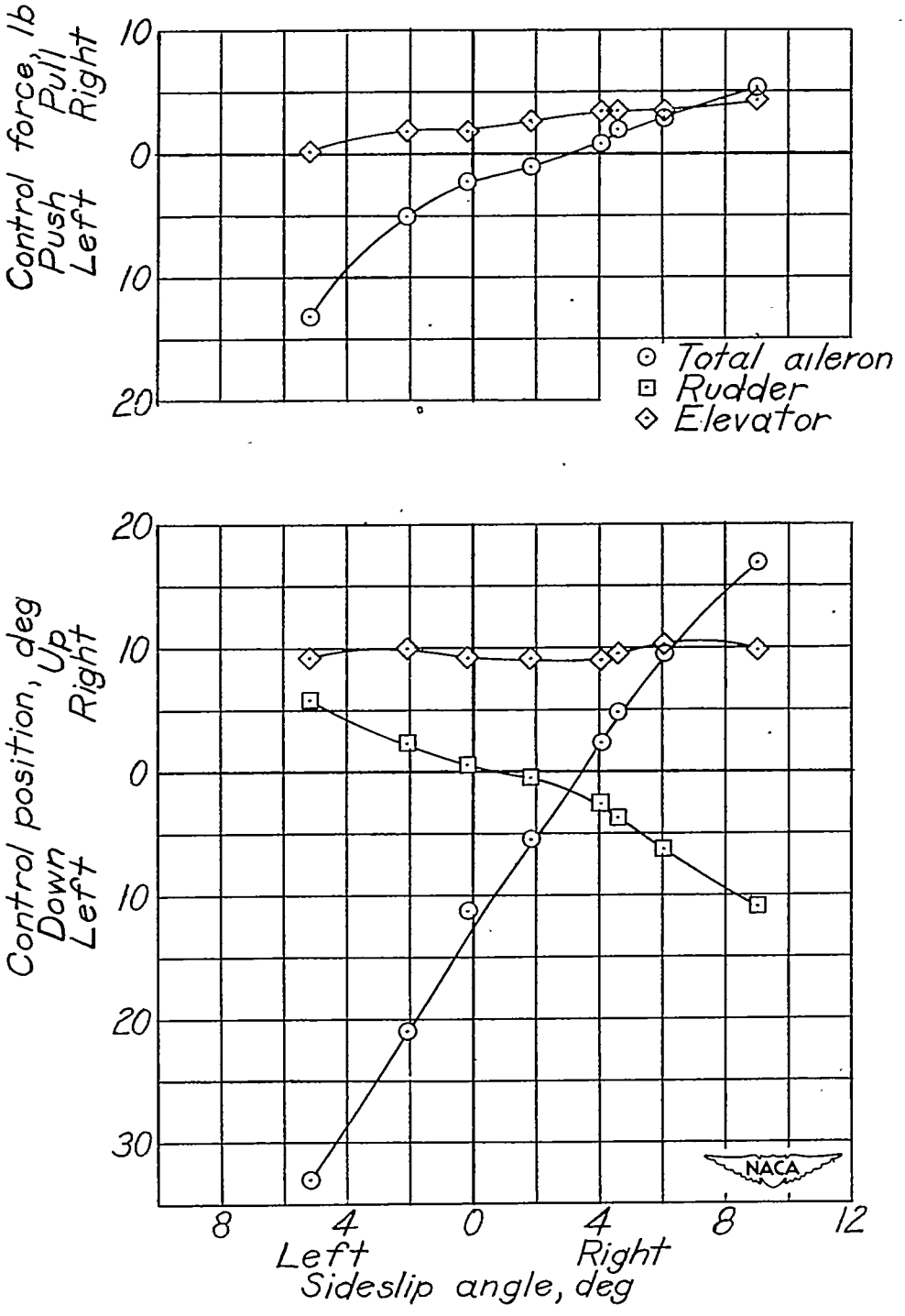

(a) V_c = 110 miles per hour; C_N = 1.15.

Figure 11.- Steady sideslip characteristics of test airplane with 80-percent-span slots on wing. Flaps up; nose wheel up; engine idling.

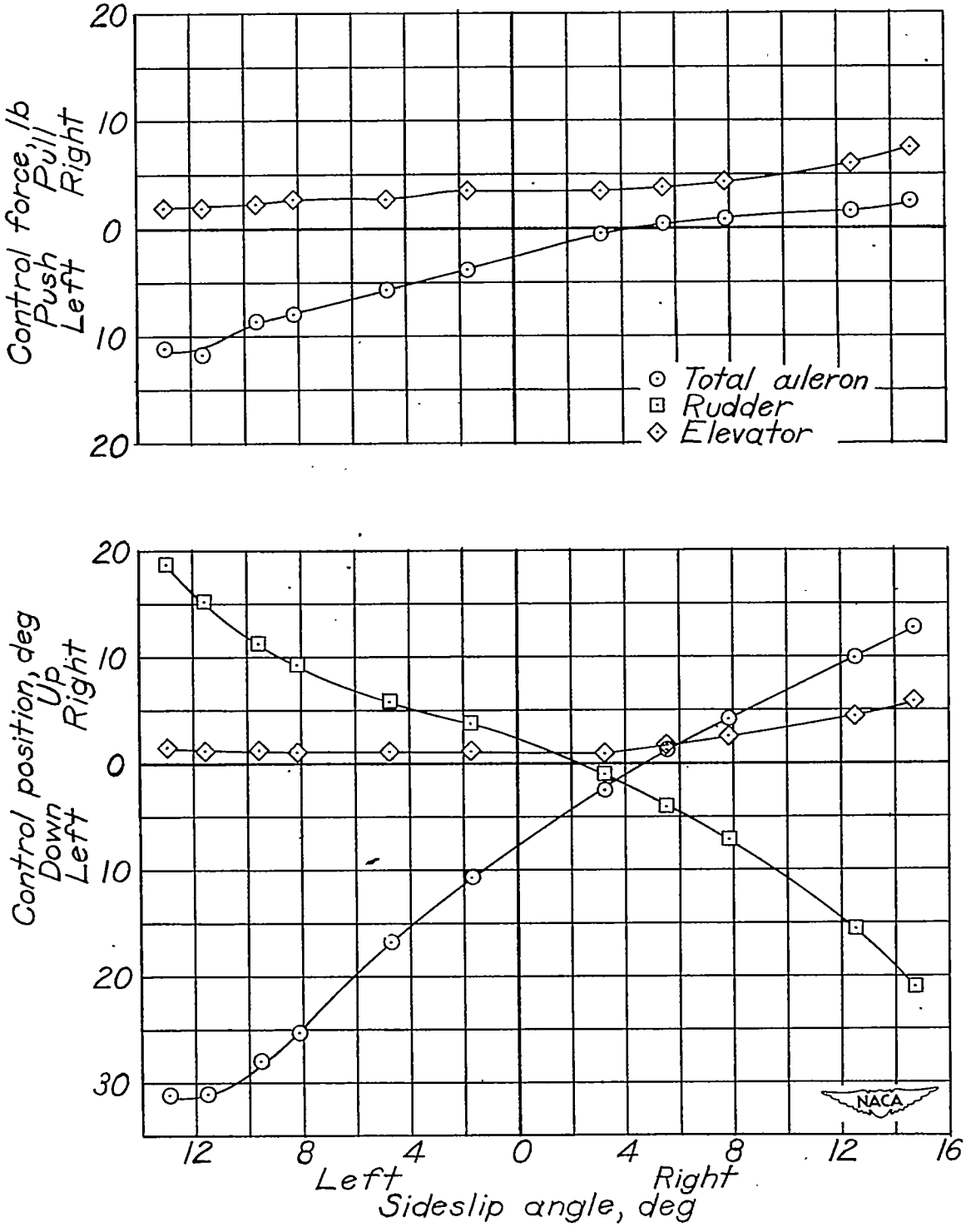

(b) V_c = 125 miles per hour; C_N = 0.88.

Figure 11.- Continued.

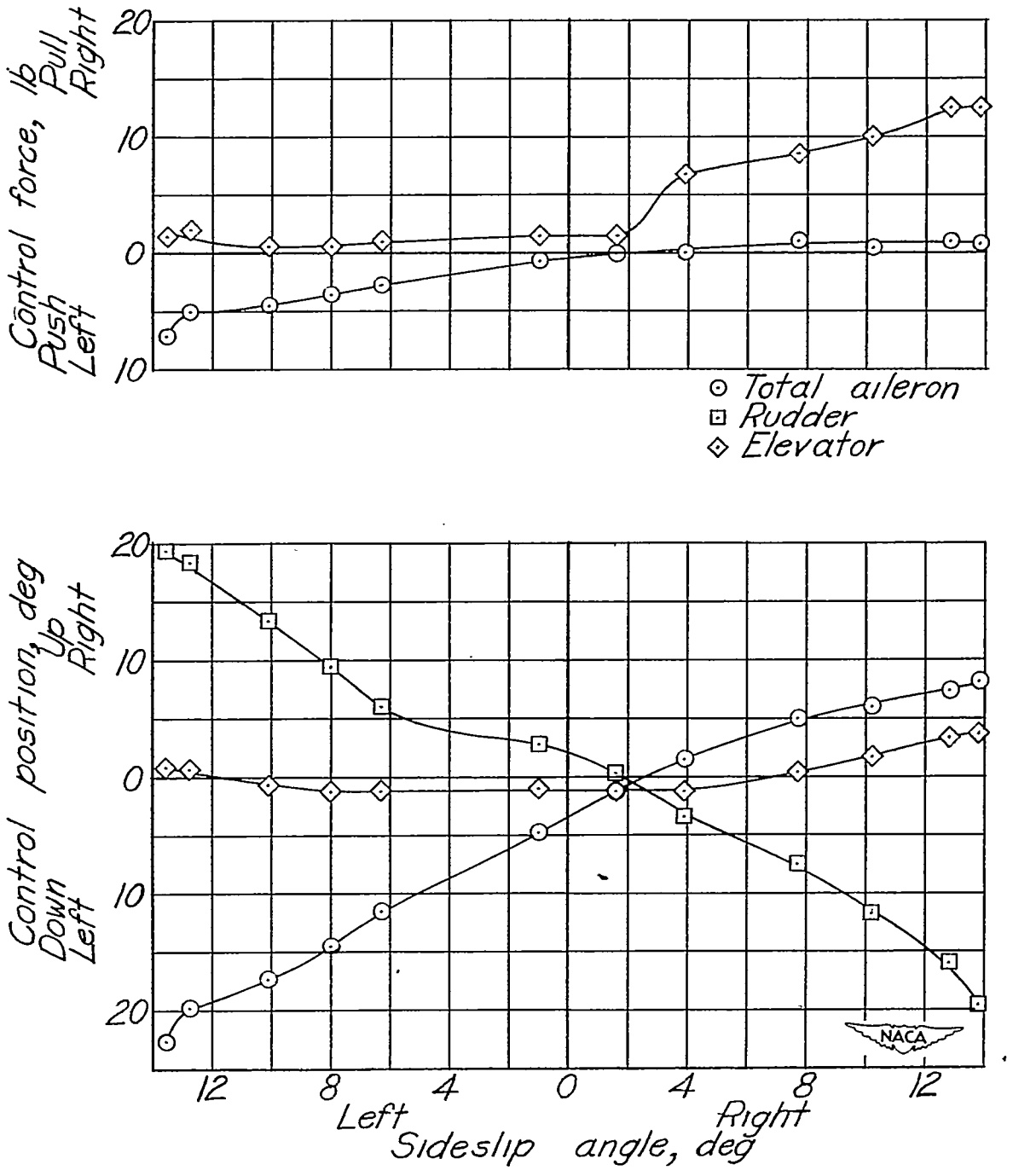

(c) V_c = 140 miles per hour; C_N = 0.73.

Figure 11.- Continued.

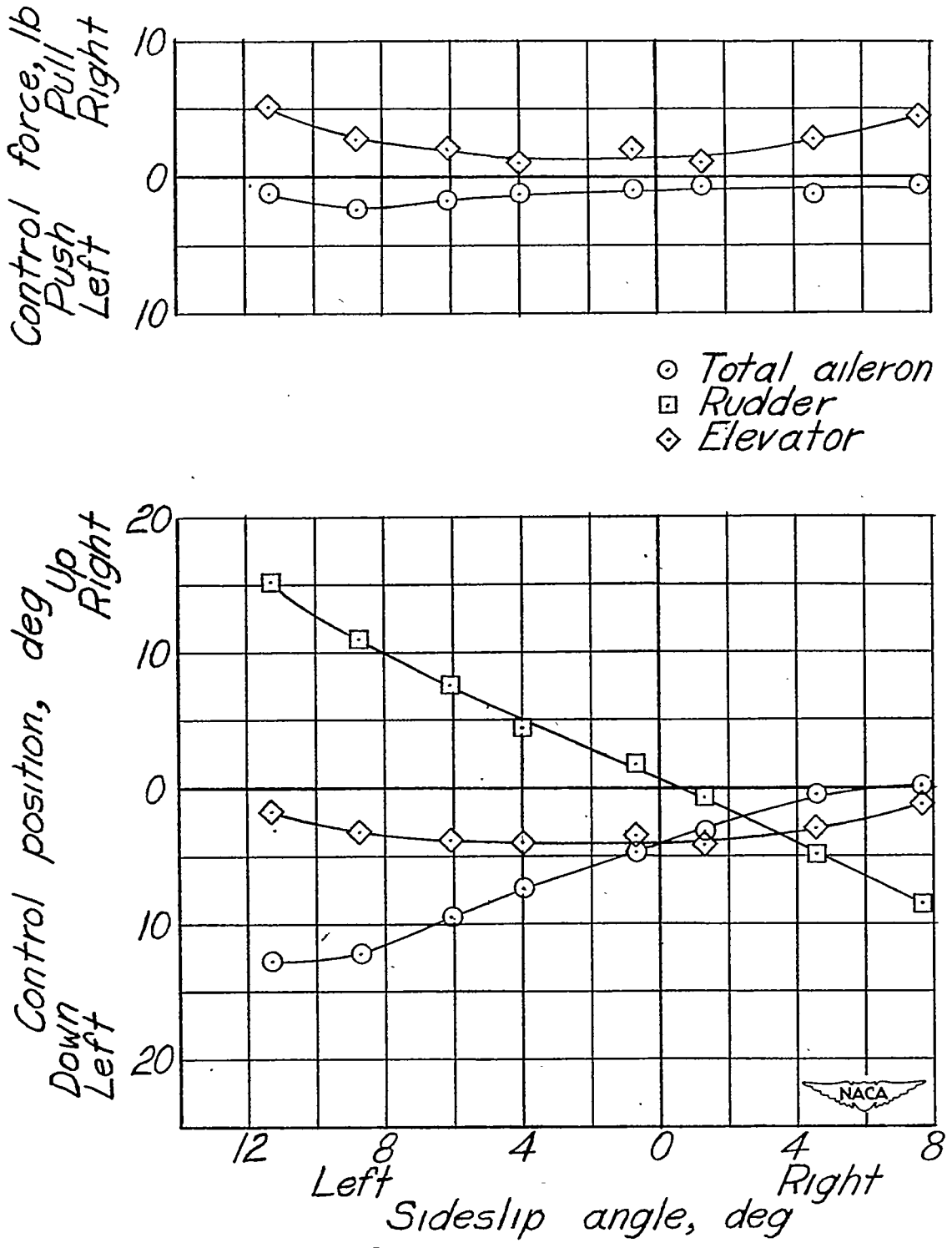

(d) V_c = 155 miles per hour; C_N = 0.56.

Figure 11.- Continued.

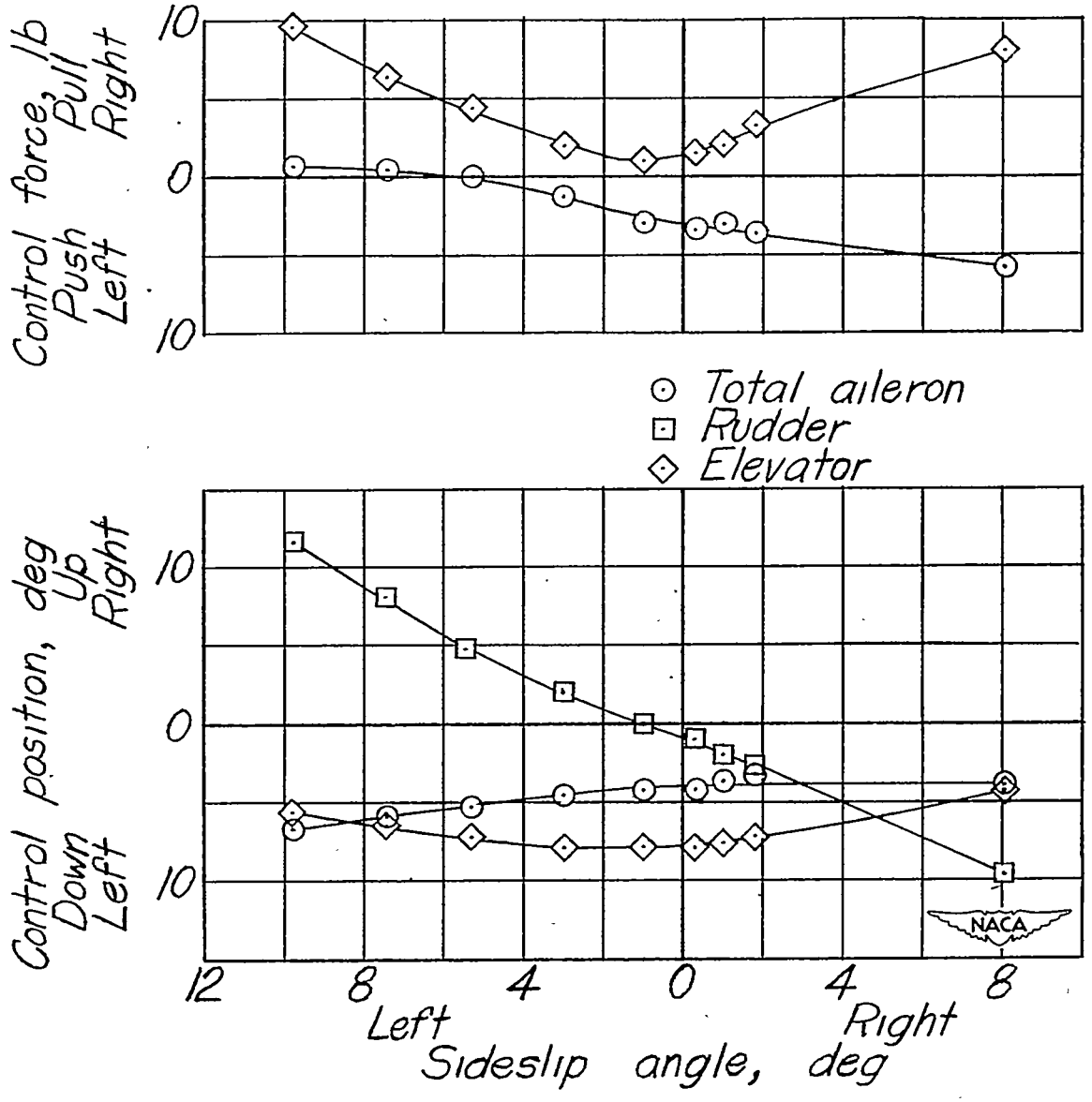

(e) V_c = 200 miles per hour; C_N = 0.35.

Figure 11.- Continued.

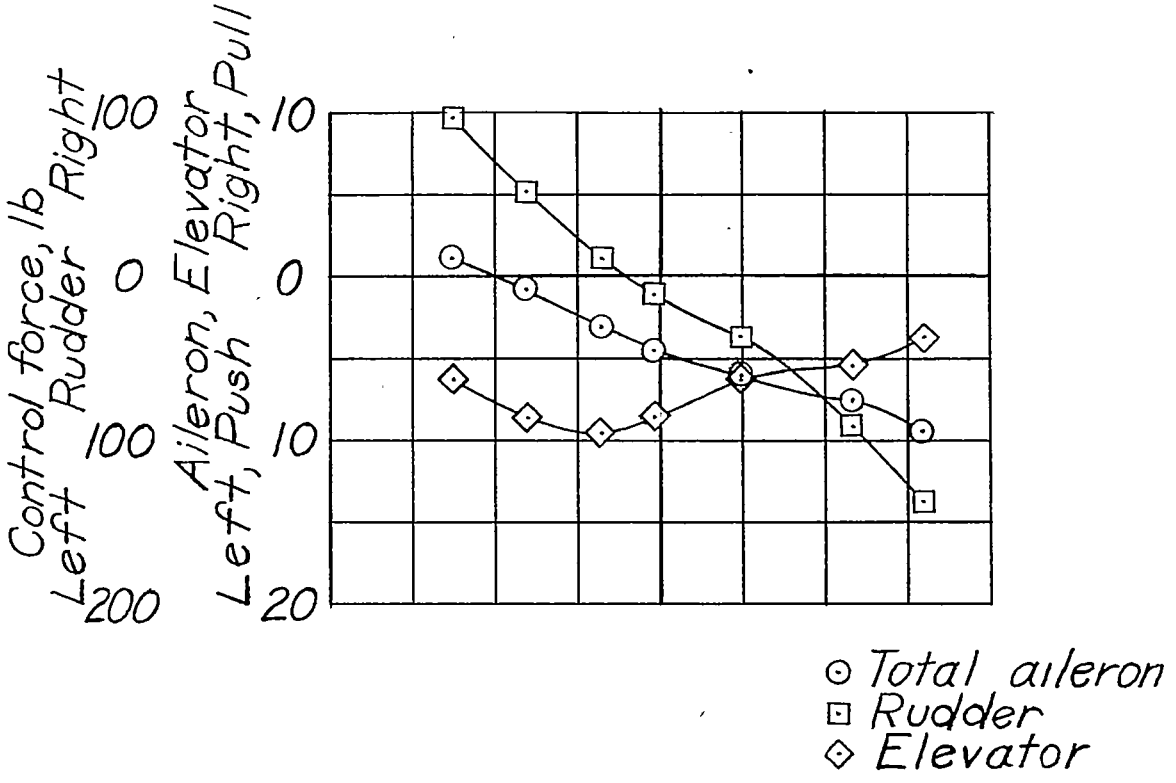

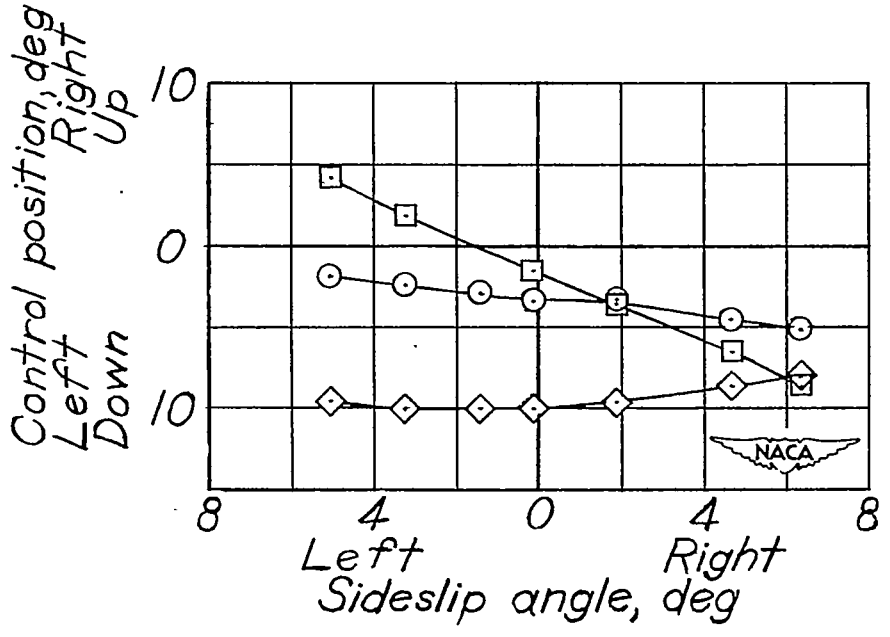

(f) V_c = 235 miles per hour; C_N = 0.25.

Figure 11.- Concluded.

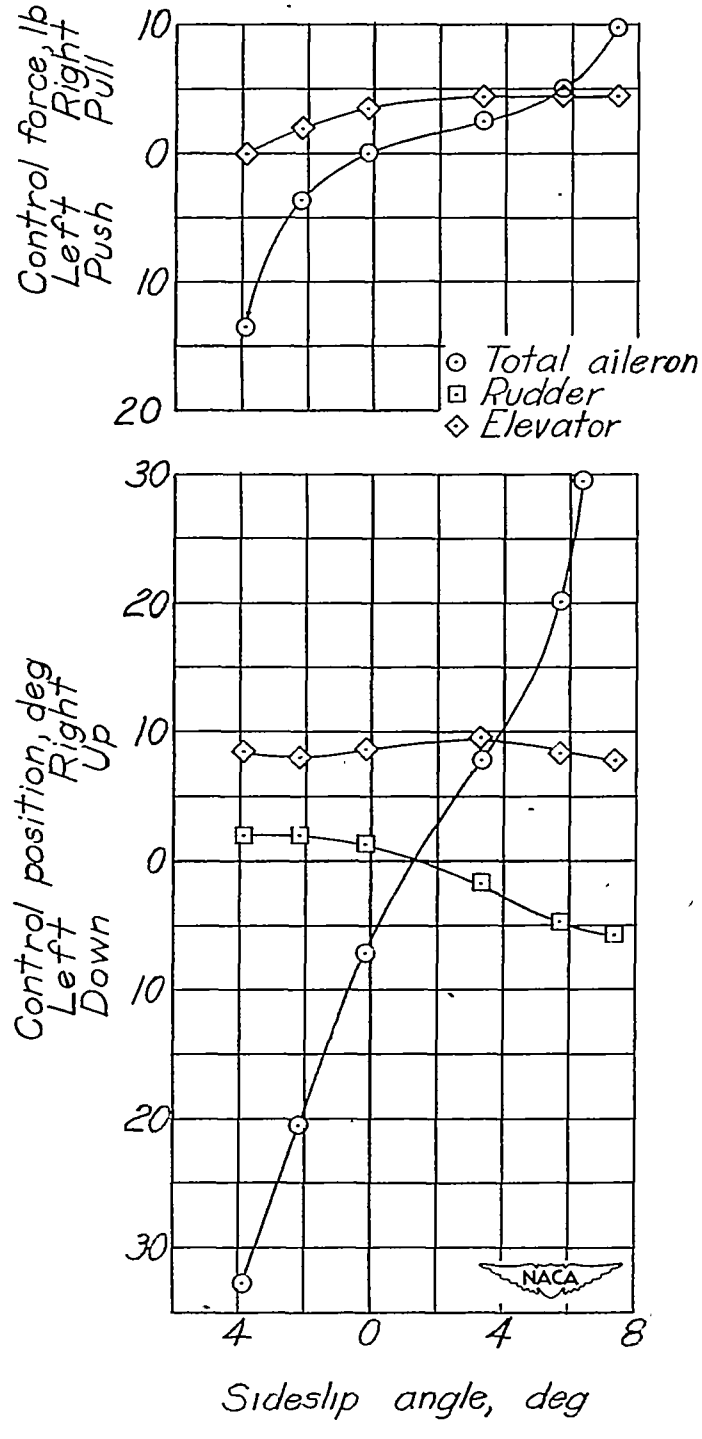

(a) V_c = 100 miles per hour; C_N = 1.38.

Figure 12.- Steady sideslip characteristics of test airplane with 80-percent-span slots on wing. Flaps down; nose wheel down; engine idling.

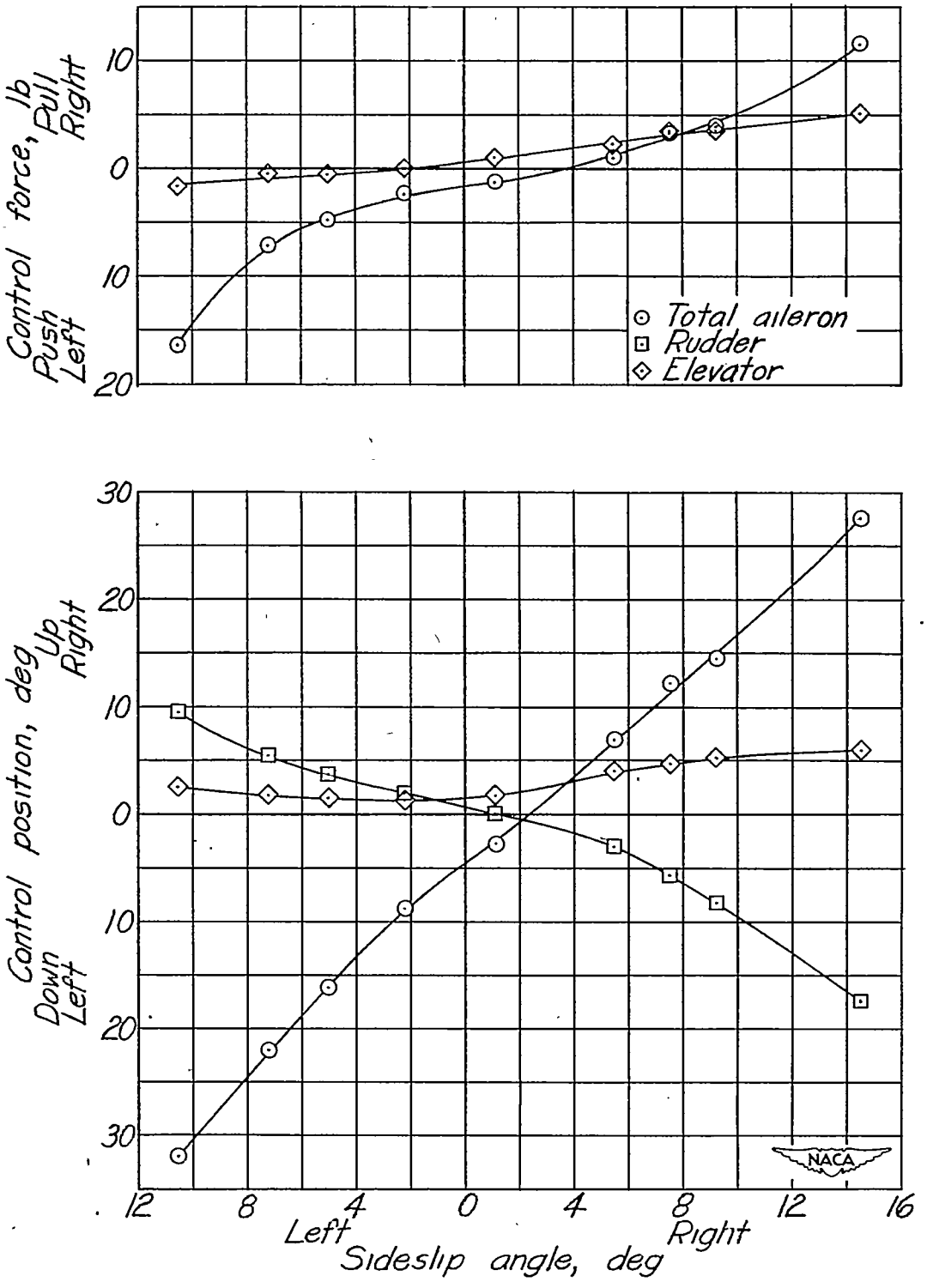

(b) V_c = 125 miles per hour; C_N = 0.87.

Figure 12.- Continued.

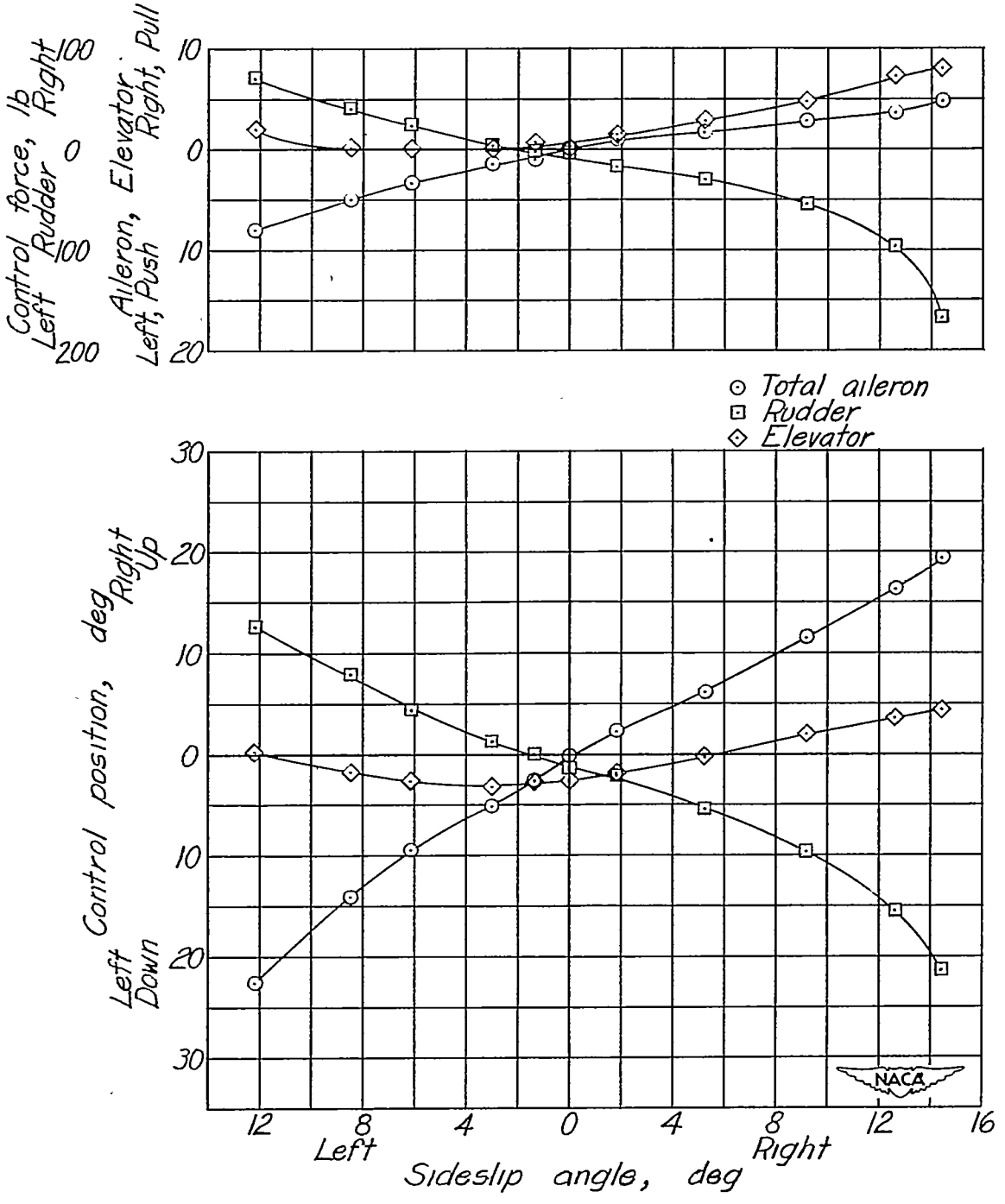

(c) V_c = 140 miles per hour; C_N = 0.71.

Figure 12.- Continued.

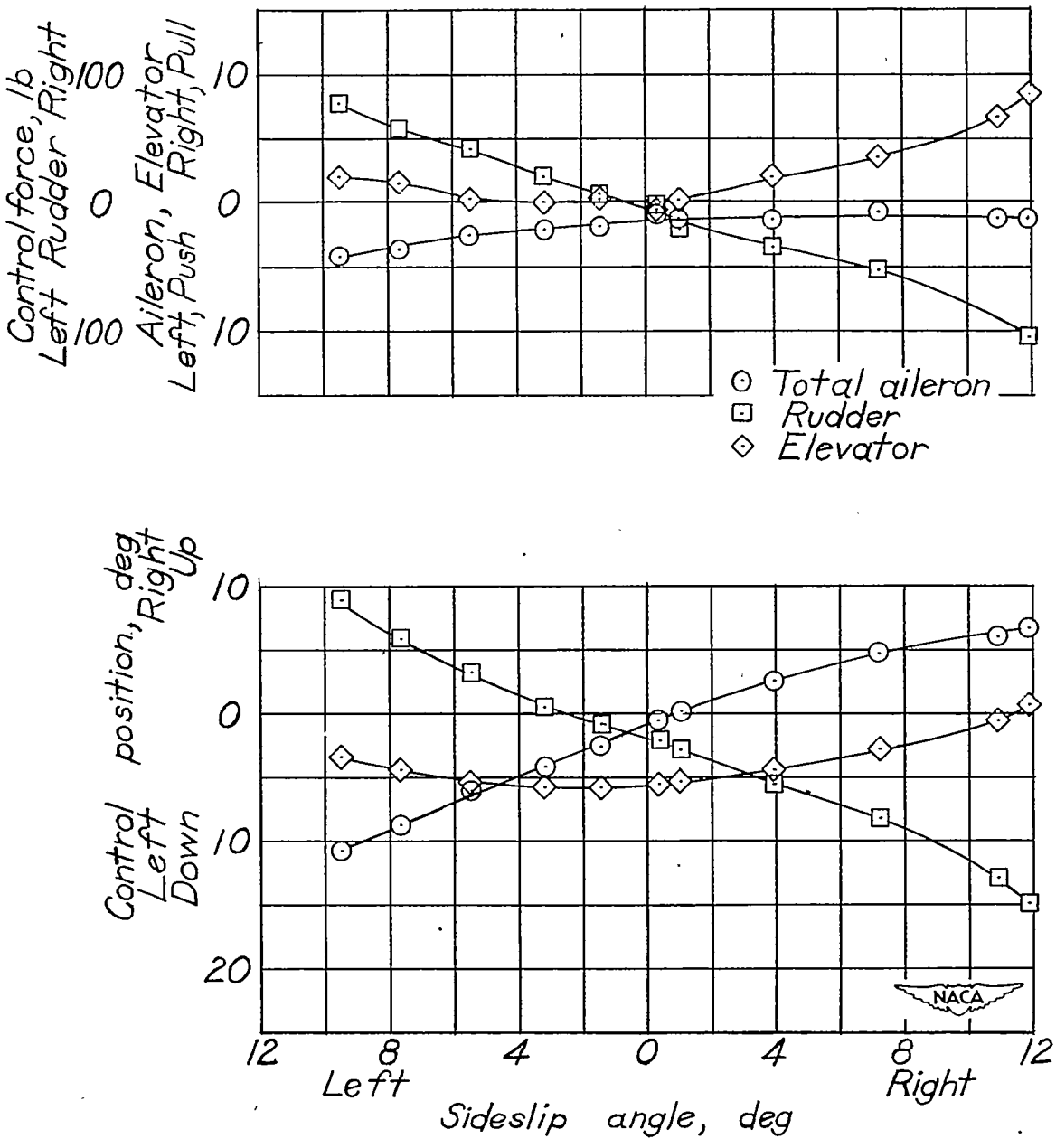

(d) V_c = 157 miles per hour; C_N = 0.56.

Figure 12.- Concluded.

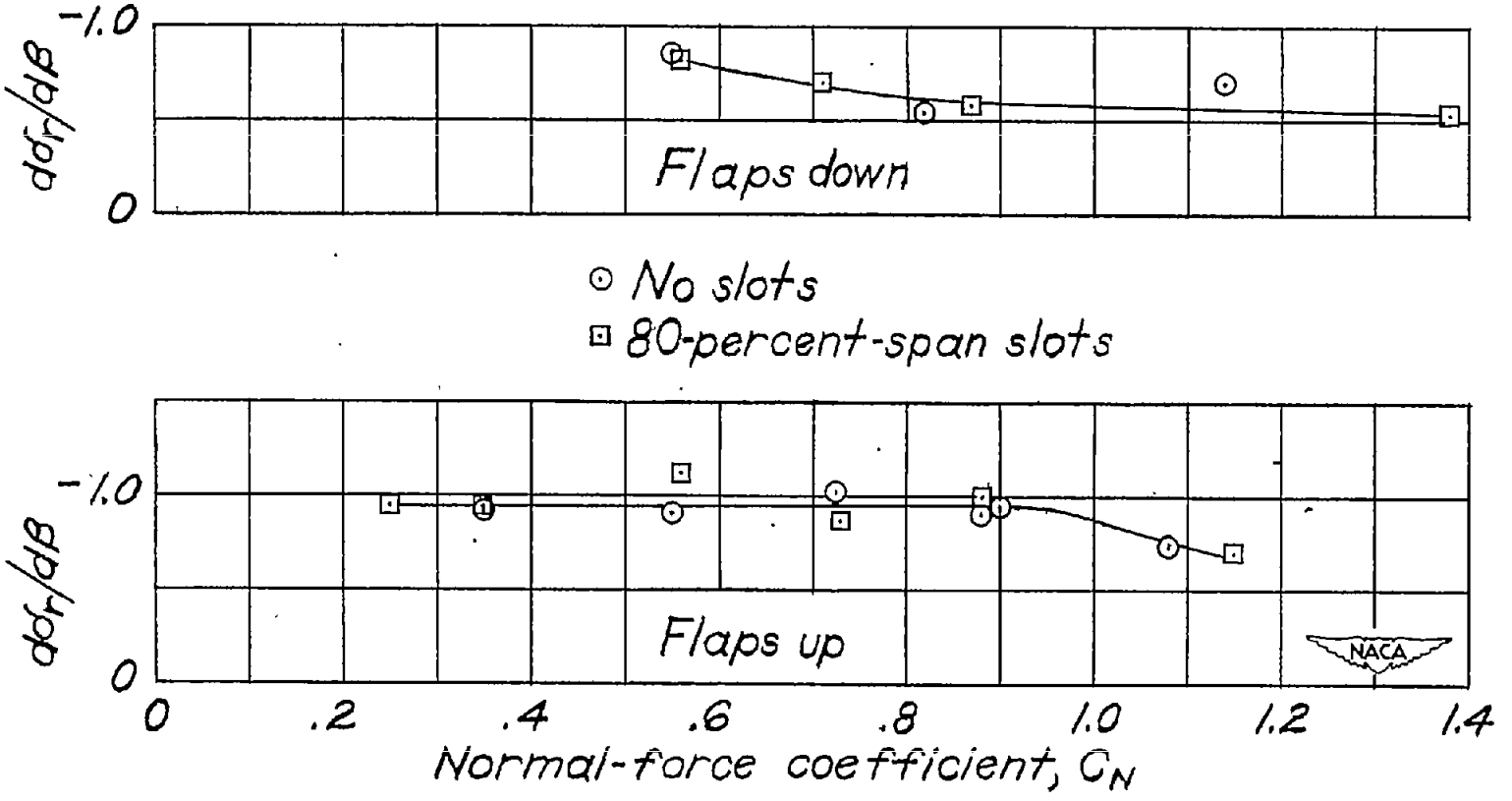

Figure 13.- Variation of $d\delta_r/d\beta$ with normal-force coefficient C_N as measured in steady sideslips. Engine idling.

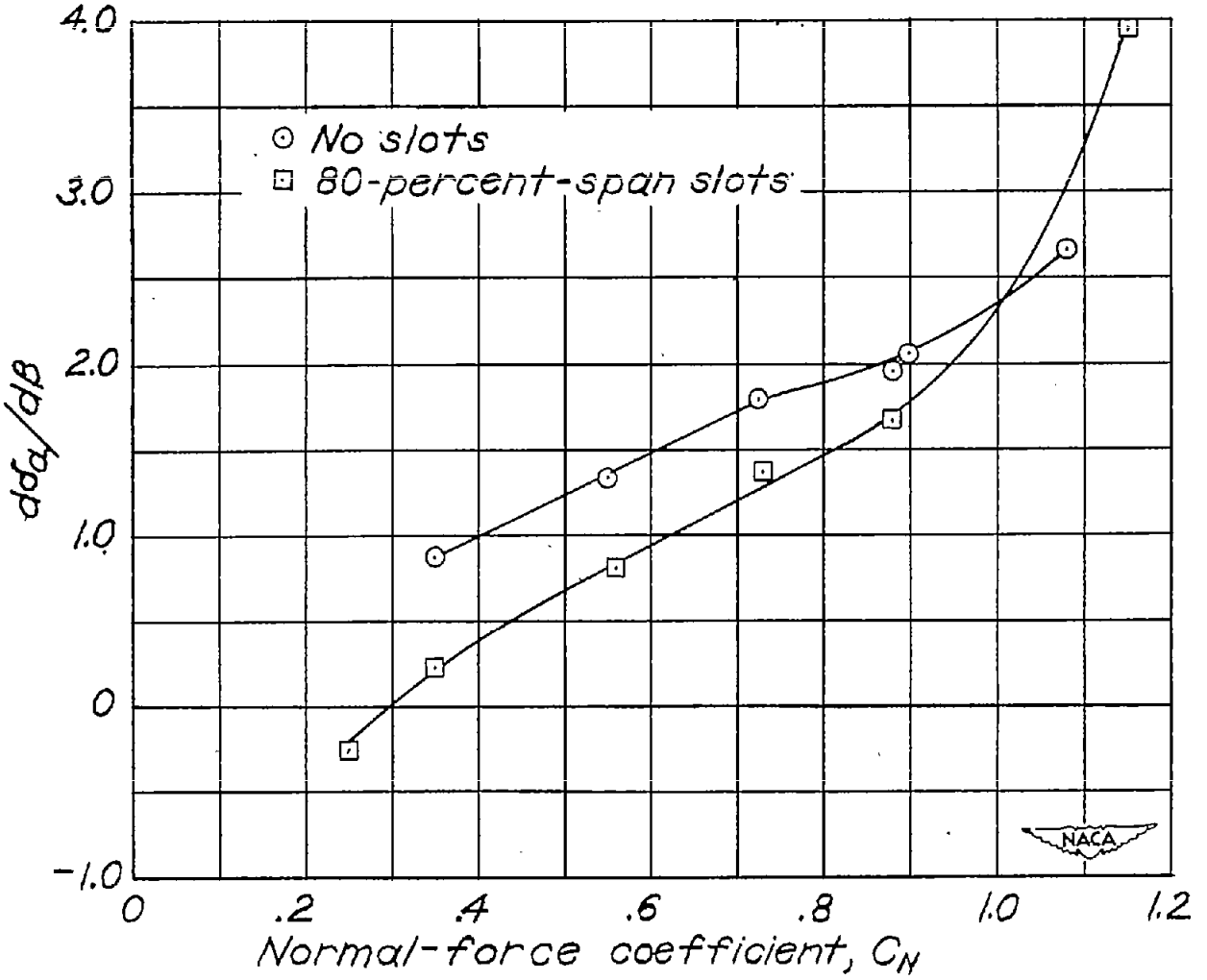

Figure 14.- Variation of $d\delta_a/d\beta$ with normal-force coefficient C_N as measured in steady sideslips. Flaps up; engine idling.

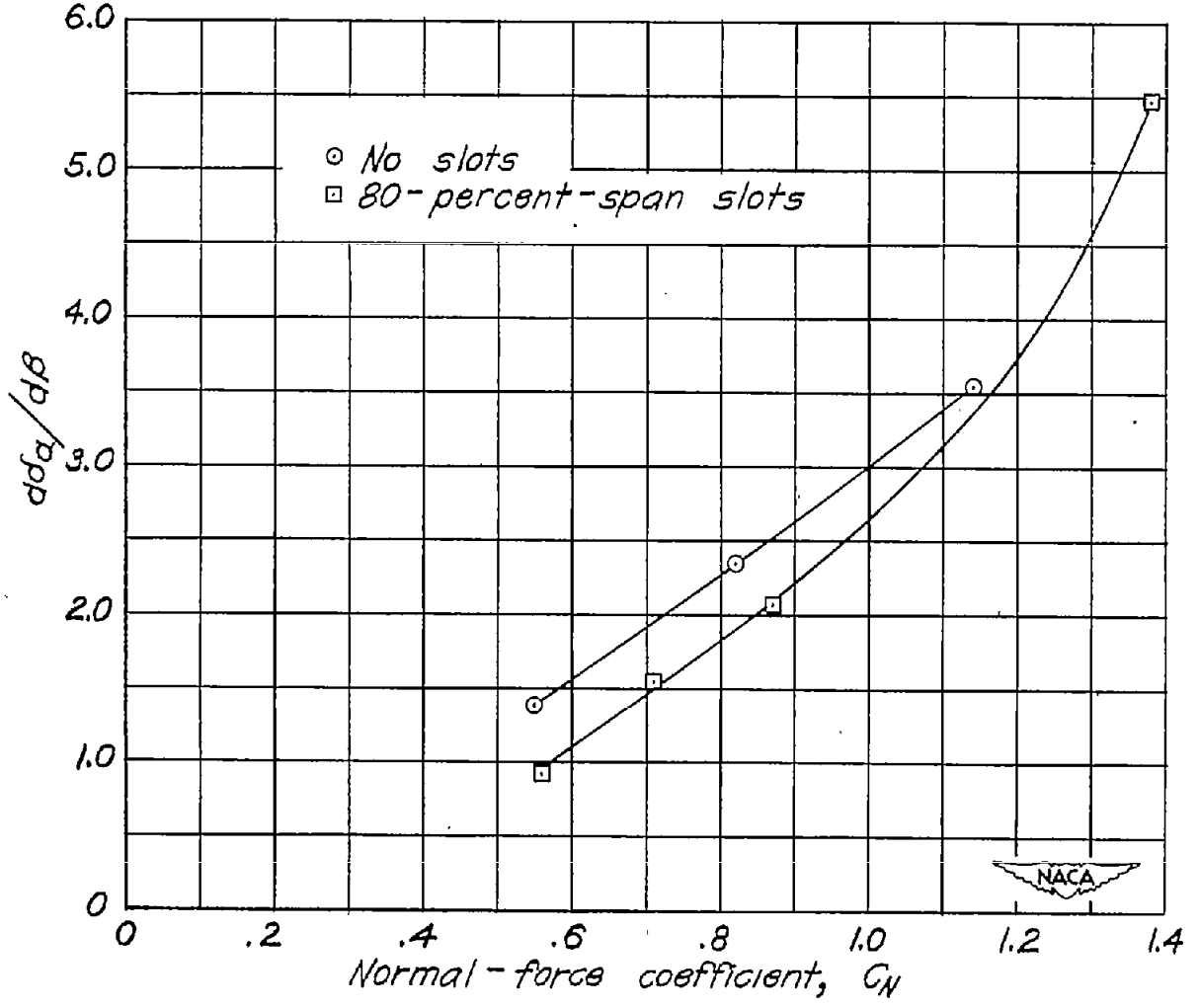

Figure 15.- Variation of $d\delta_a/d\beta$ with normal-force coefficient C_N as measured in steady sideslips. Flaps down; engine idling.

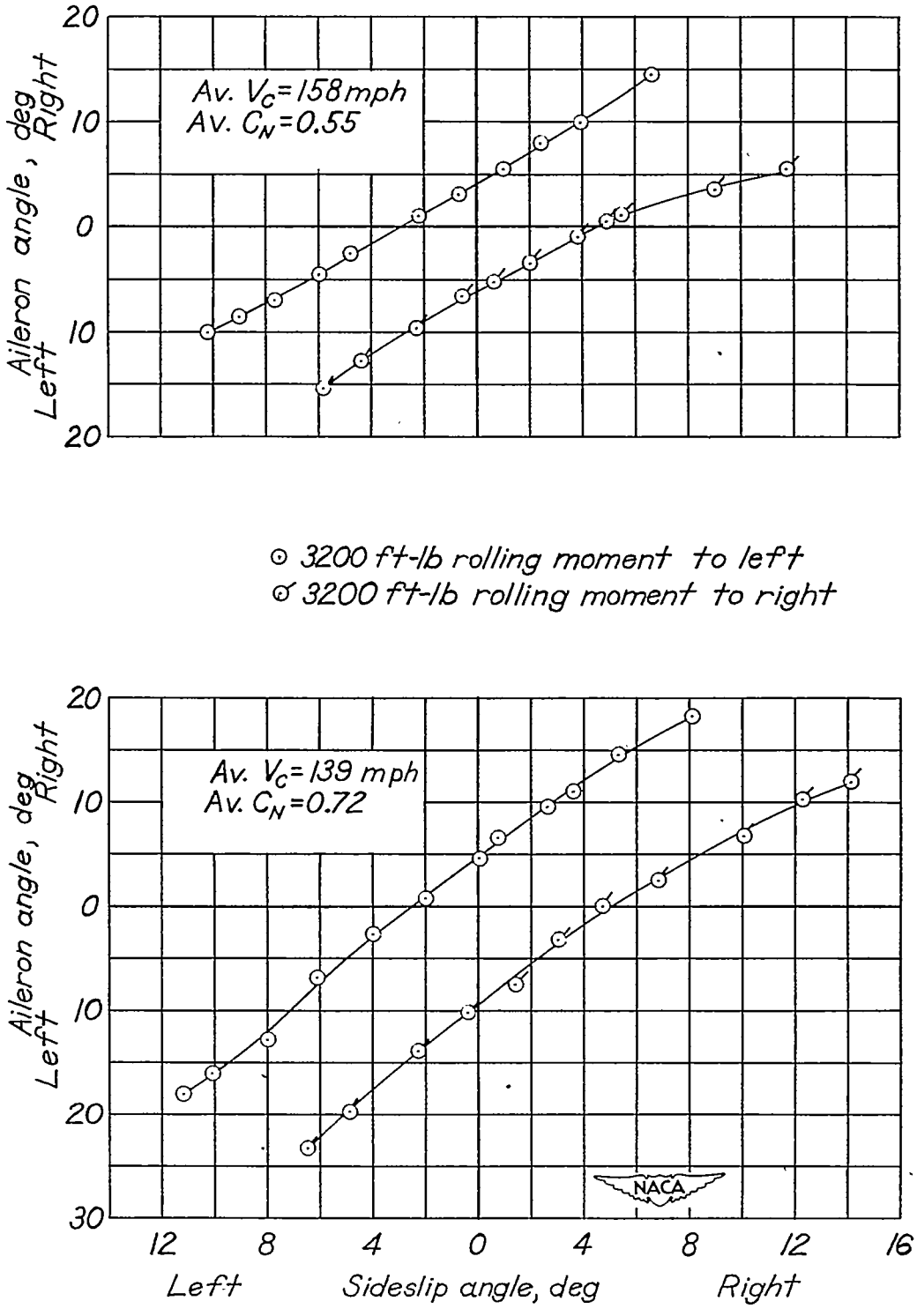

Figure 16.- Variation of aileron angle with sideslip angle in steady sideslips with airplane asymmetrically loaded. No slots; flaps up; nose wheel up; engine idling.

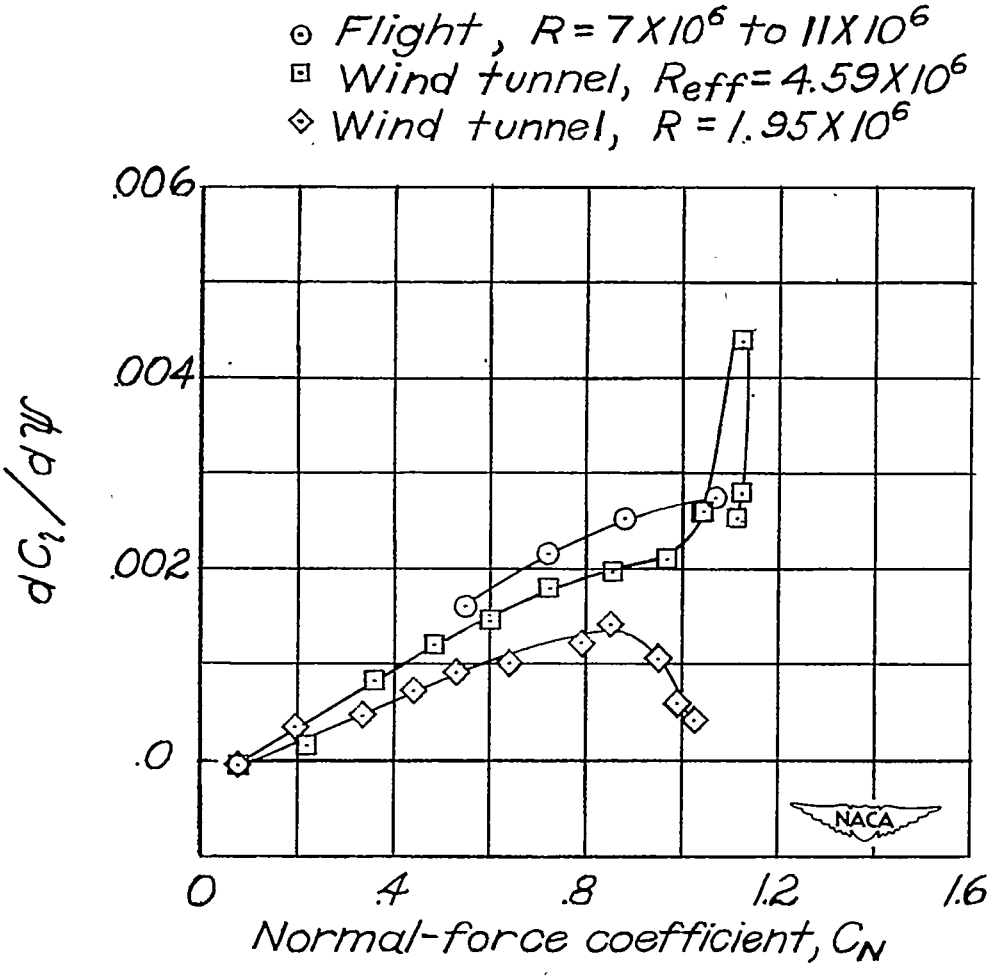

Figure 17.- Comparison of flight and wind-tunnel measurements of dihedral effect. No slots; flaps up; engine idling.

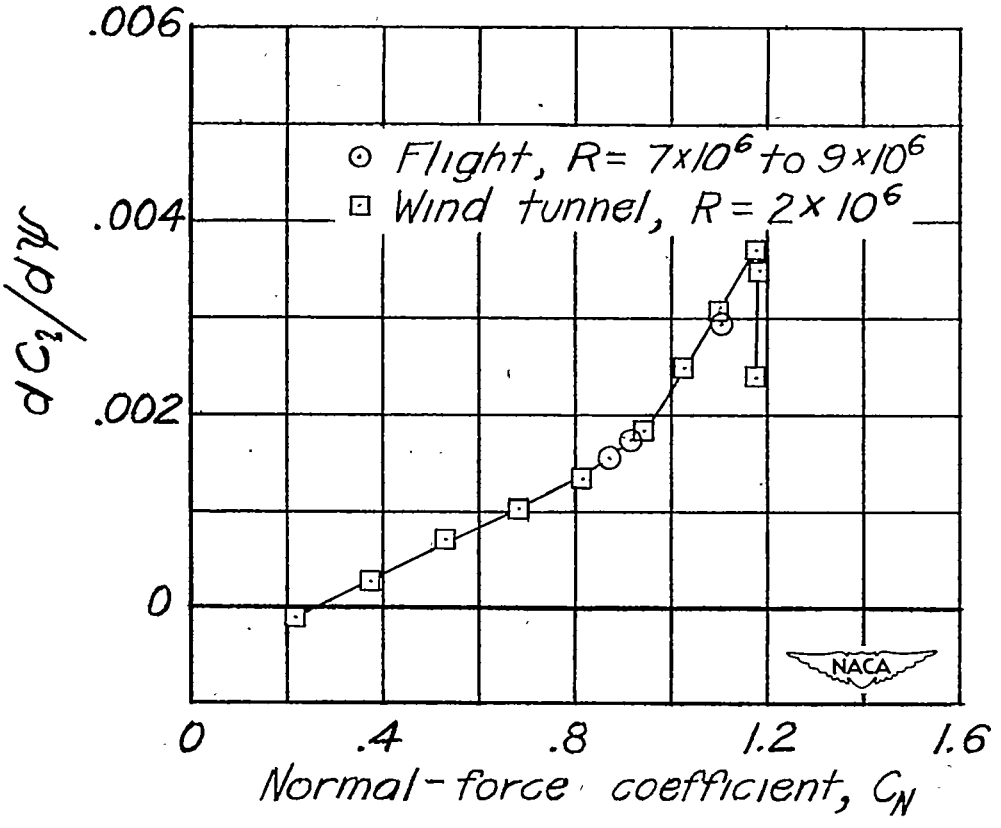

Figure 18.- Comparison of flight and wind-tunnel measurements of dihedral effect. 80-percent-span slots; flaps up; engine idling.

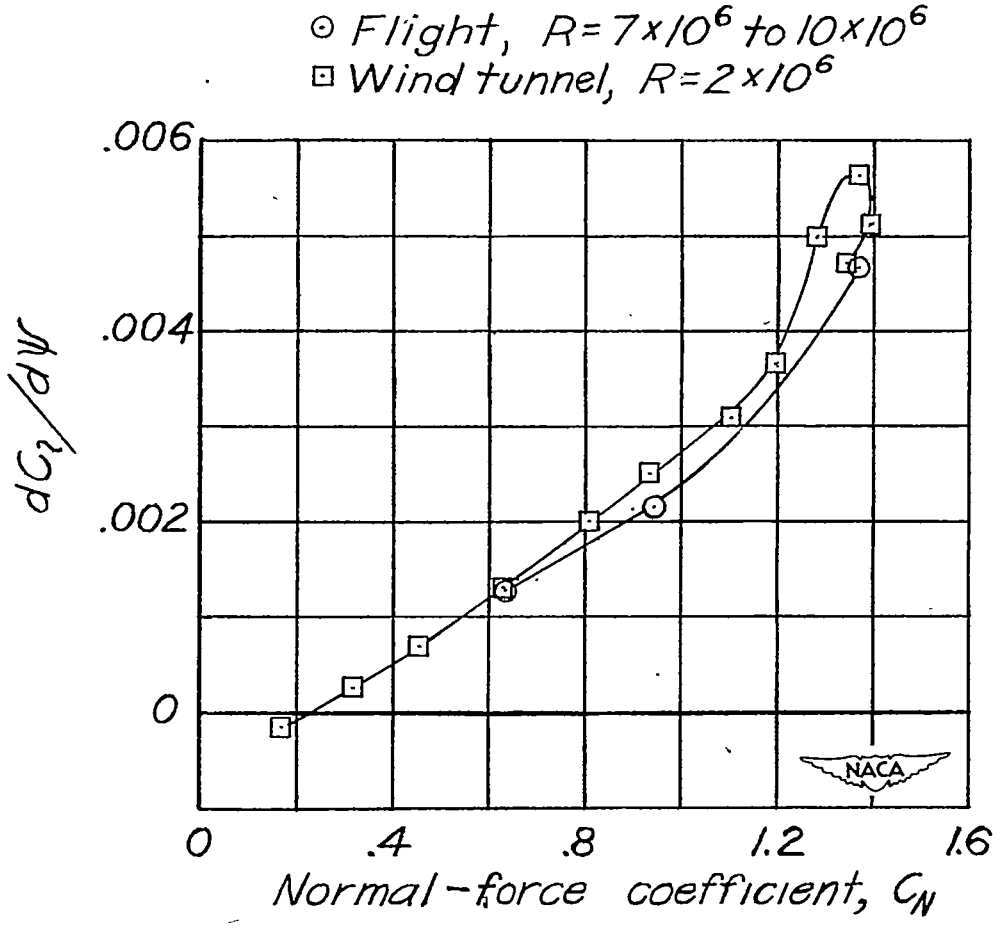

Figure 19.- Comparison of flight and wind-tunnel measurements of dihedral effect. 80-percent-span slots; flaps down; engine idling.

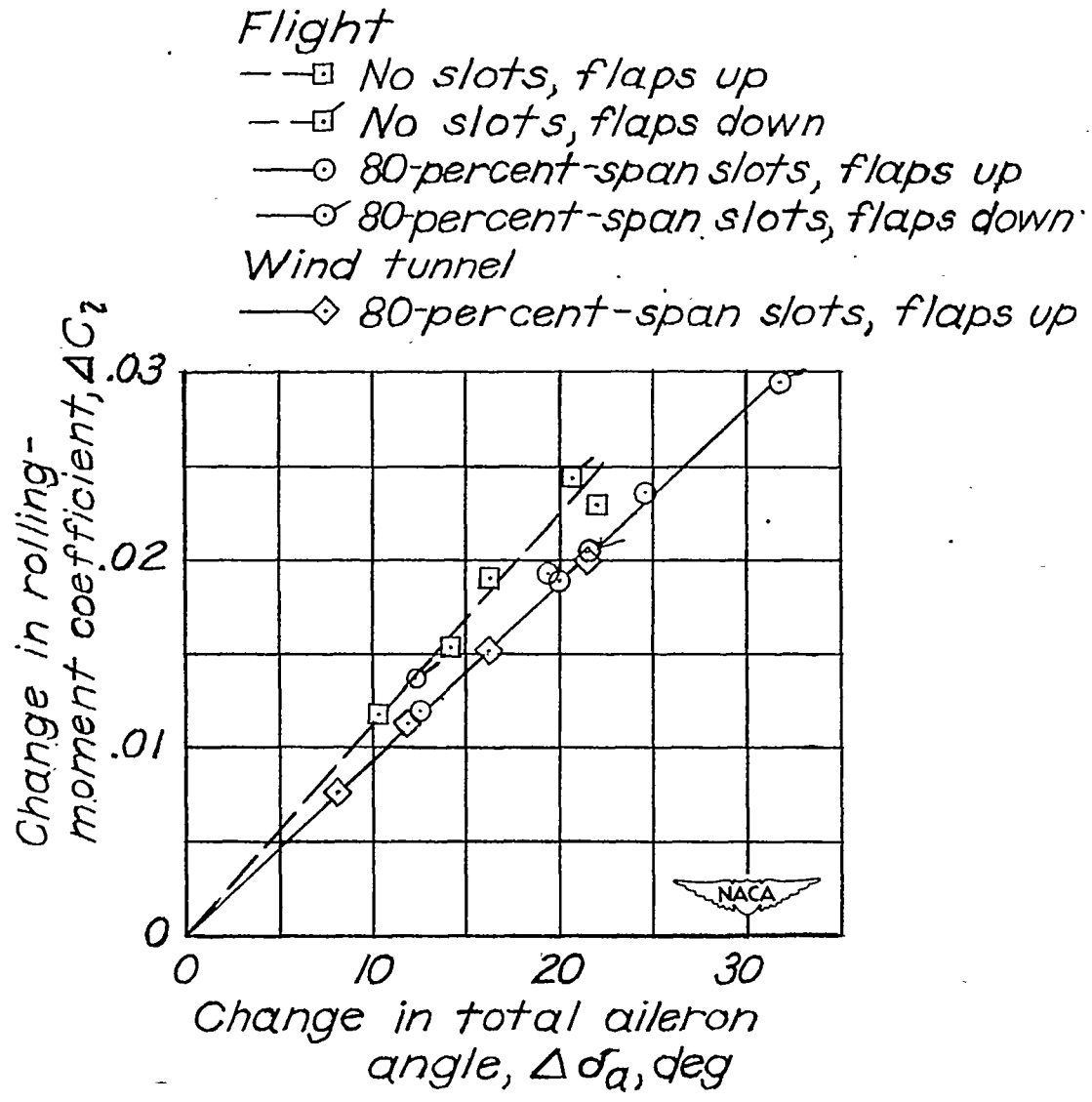

Figure 20.- Change in rolling-moment coefficient ΔC_l with change in total aileron angle $\Delta \delta_a$. Engine idling.

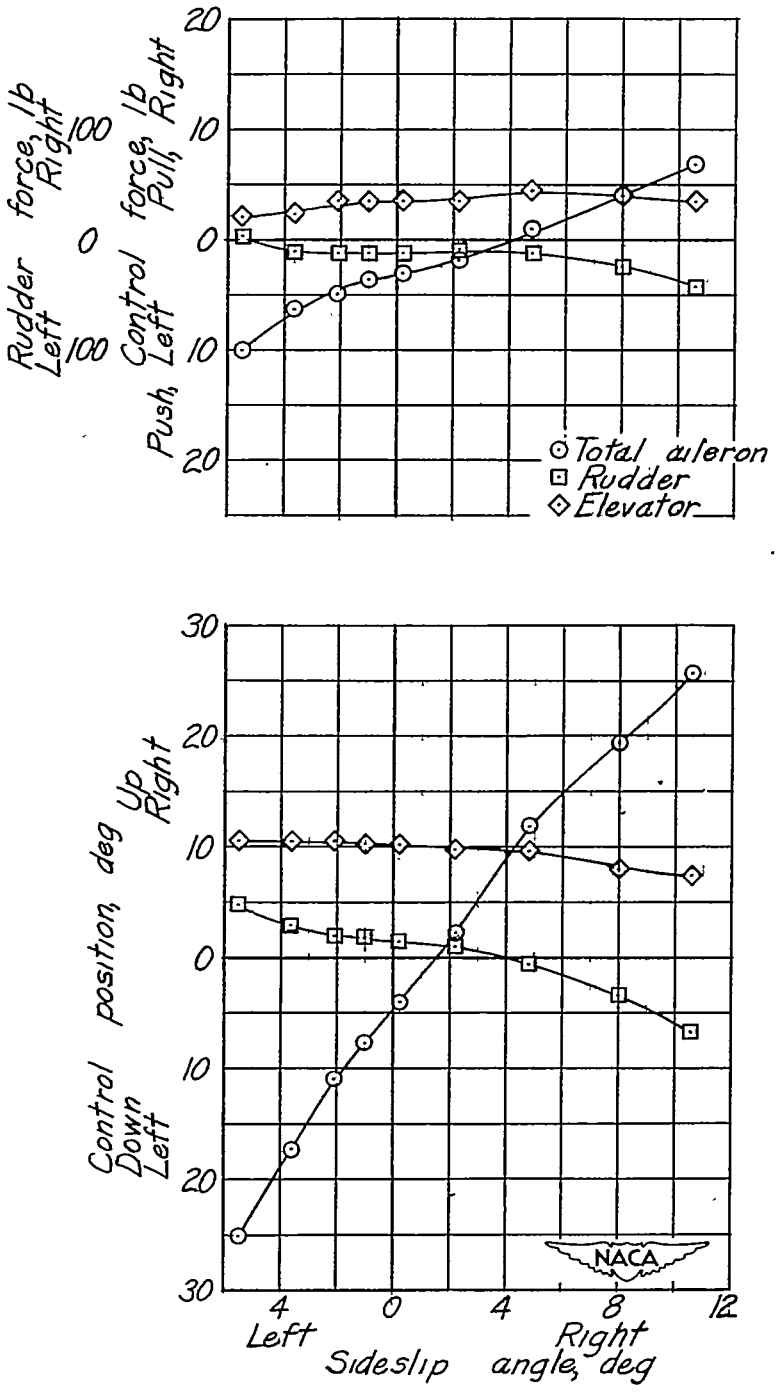

(a) V_c = 111 miles per hour; C_N = 1.13.

Figure 21.- Steady sideslip characteristics of test airplane with 80-percent-span slots. Ventral-fin extension off; flaps up; nose wheel up; engine idling.

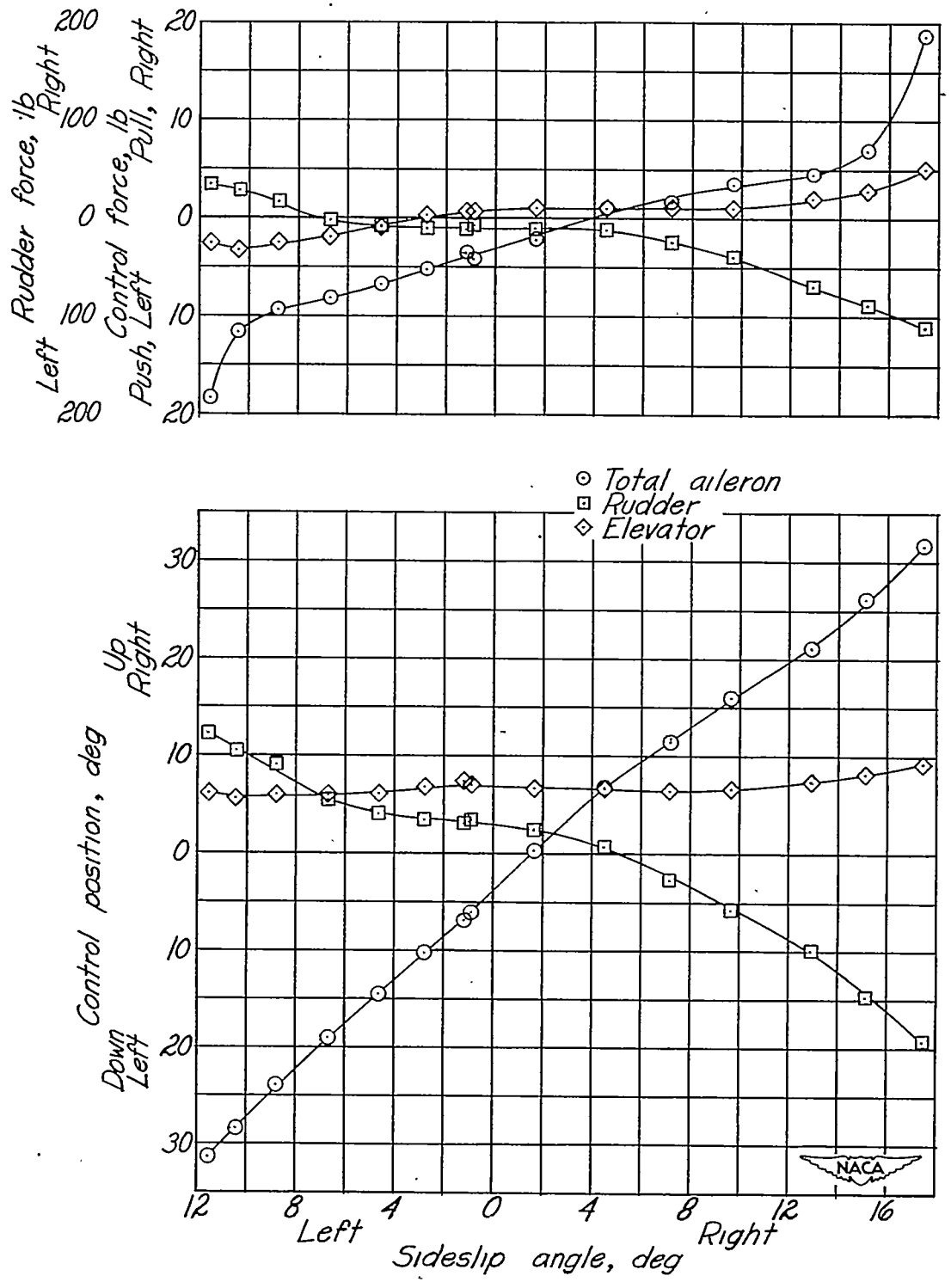

(b) V_c = 120 miles per hour; C_N = 1.00

Figure 21.- Continued.

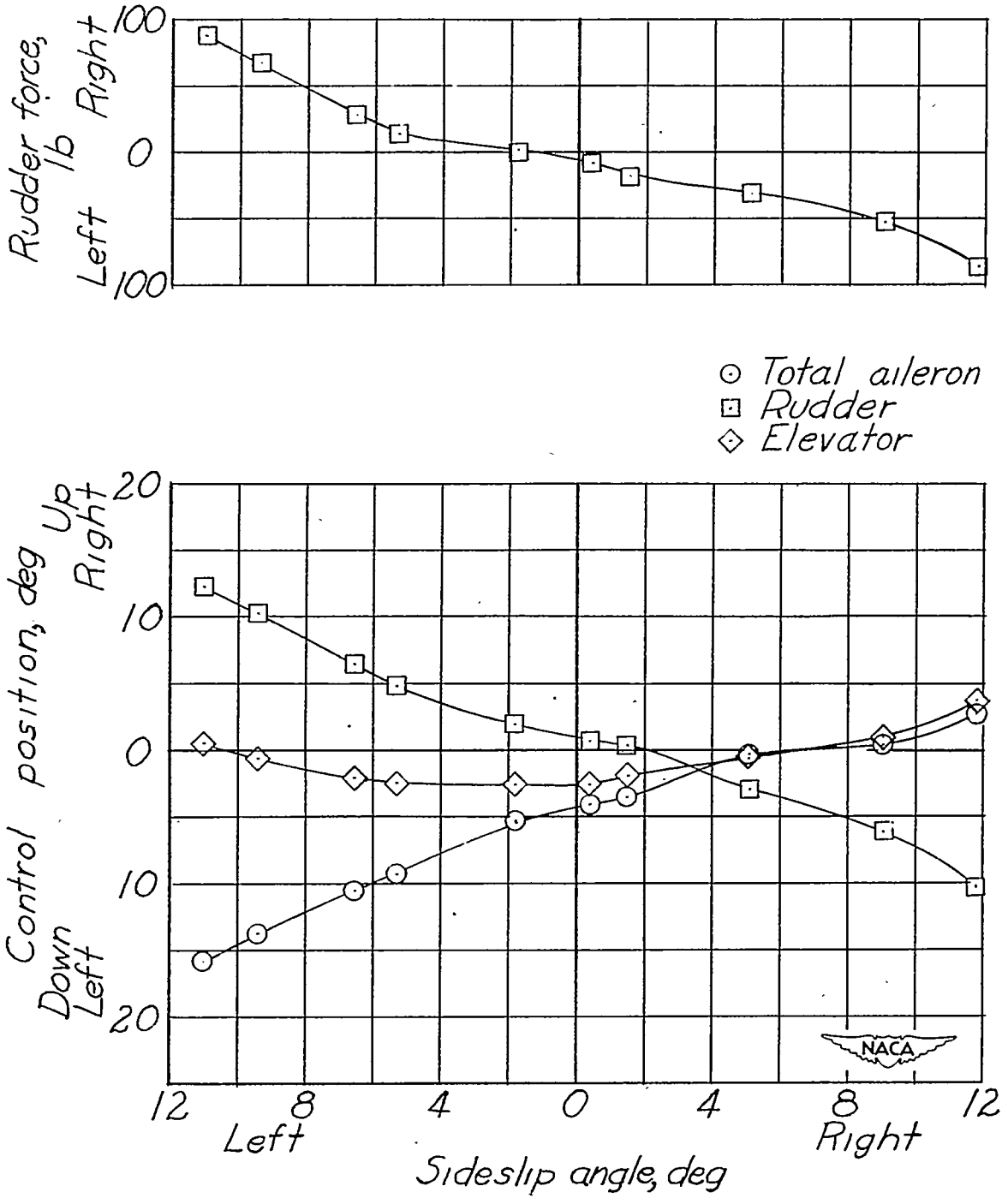

(c) V_c = 137 miles per hour; C_N = 0.75.

Figure 21.- Continued.

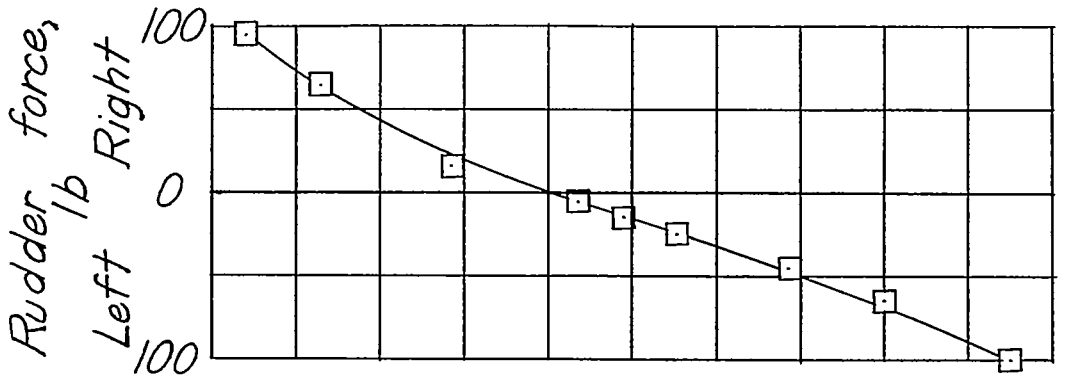

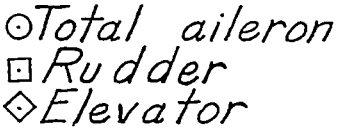

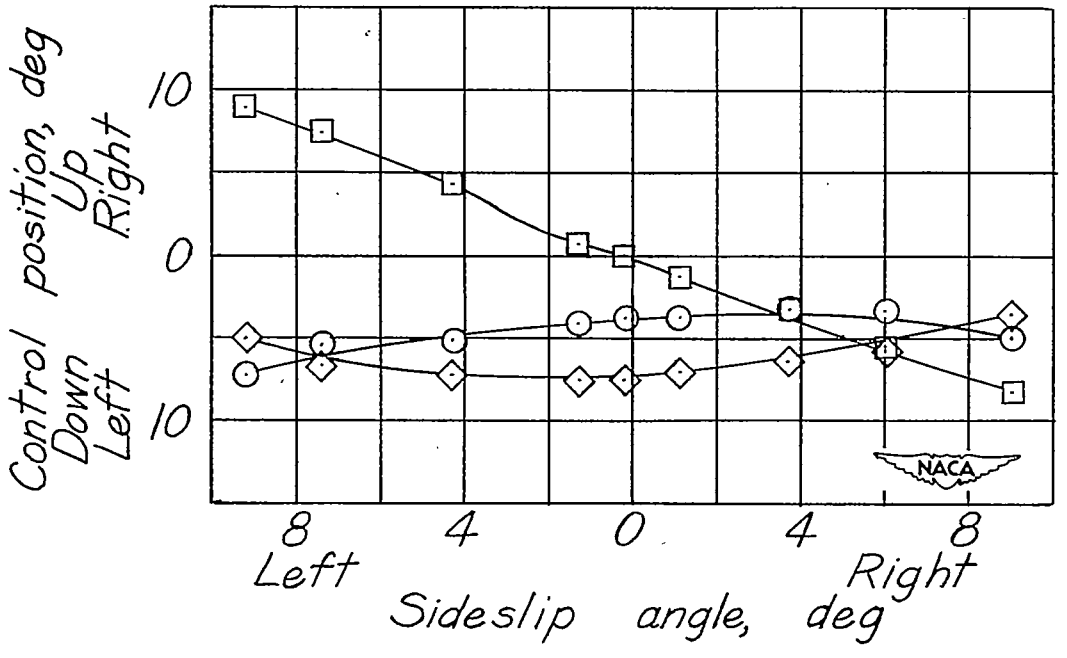

(d) V_c = 200 miles per hour; C_N = 0.36.

Figure 21.- Concluded.

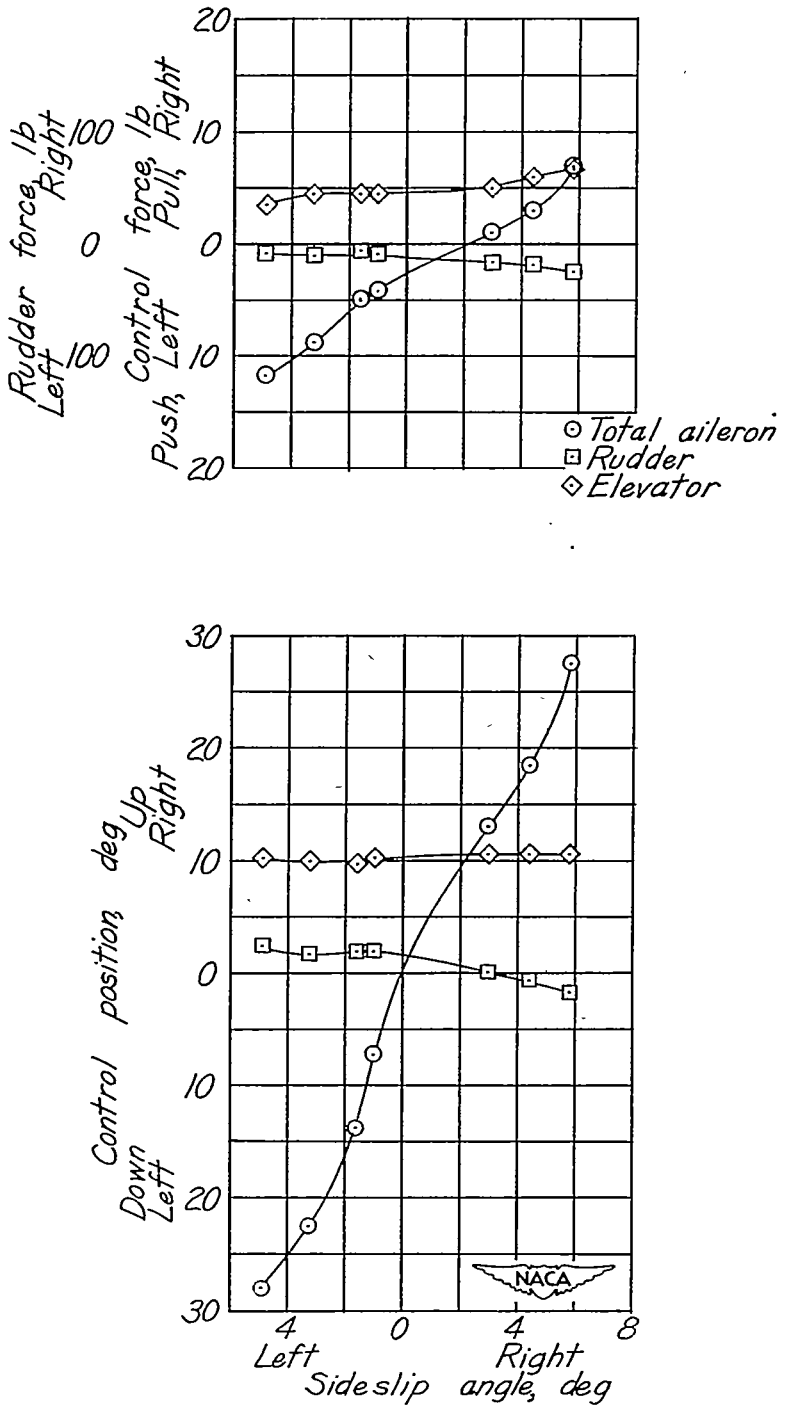

(a) V_c = 100 miles per hour; C_N = 1.37.

Figure 22.- Steady sideslip characteristics of test airplane with 80-percent-span slots. Ventral-fin extension off; flaps down; nose wheel down; engine idling.

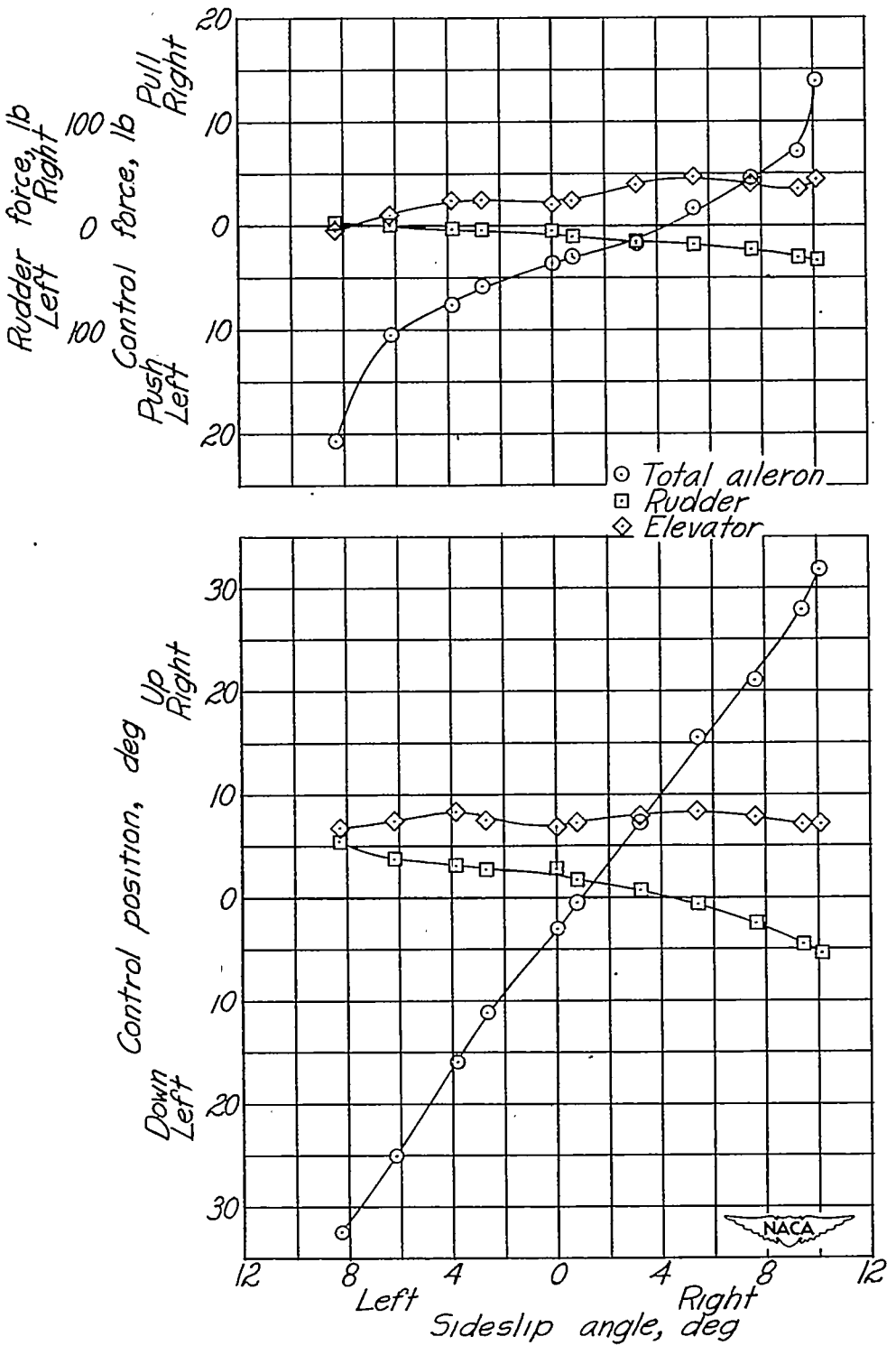

(b) V_c = 110 miles per hour; C_N = 1.14.

Figure 22.- Continued.

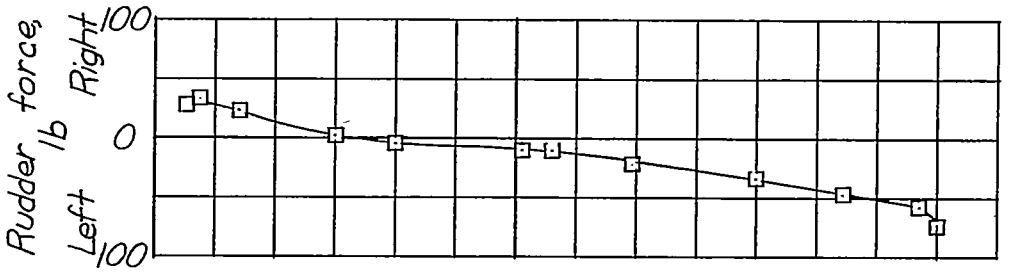

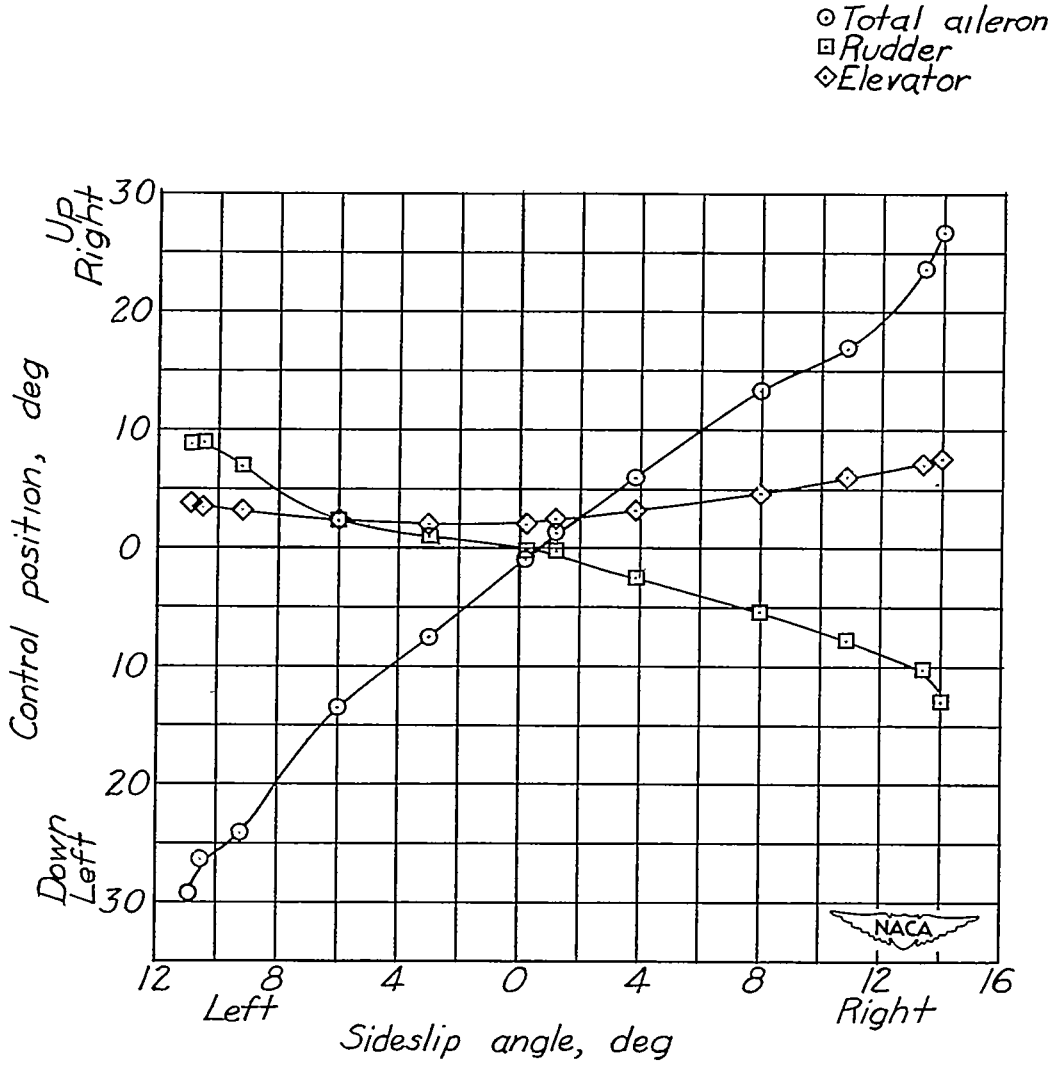

(c) V_c = 120 miles per hour; C_N = 0.84.

Figure 22.- Continued.

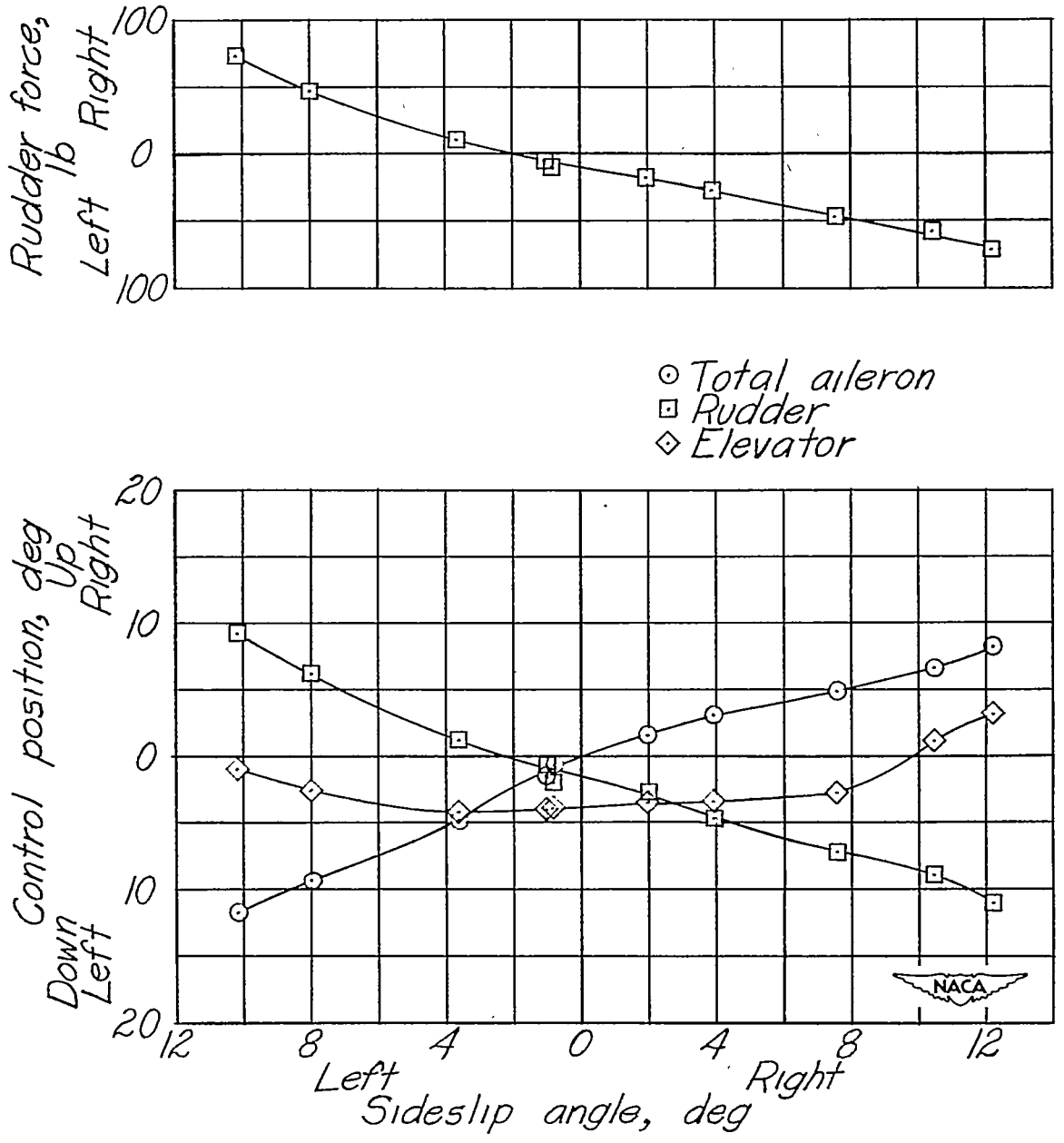

(d) V_c = 160 miles per hour; C_N = 0.55.

Figure 22.- Concluded.

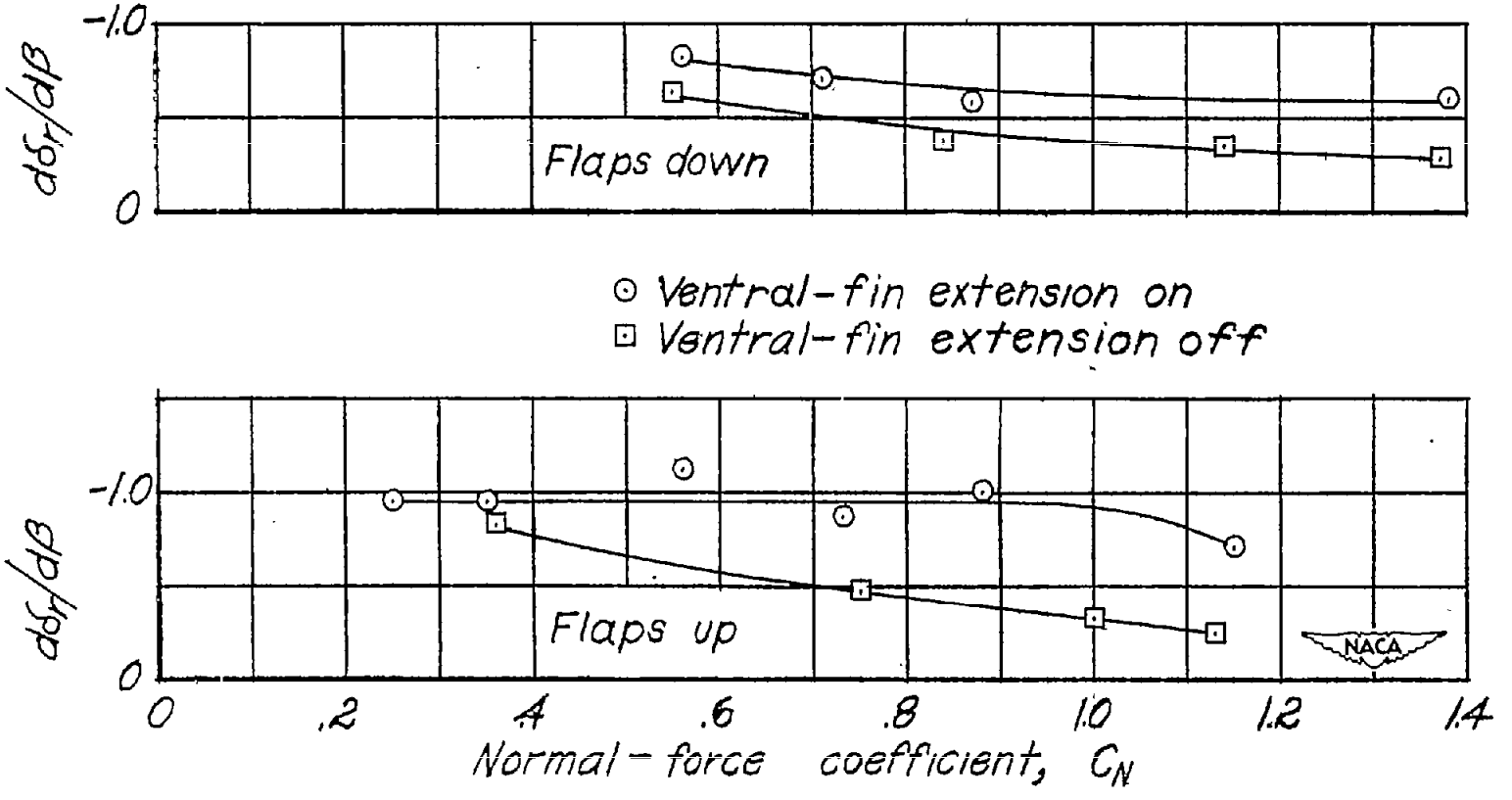

Figure 23.- Variation of $d\delta_r/d\beta$ with normal-force coefficient C_N as measured in steady sideslips. 80-percent-span slots; engine idling.

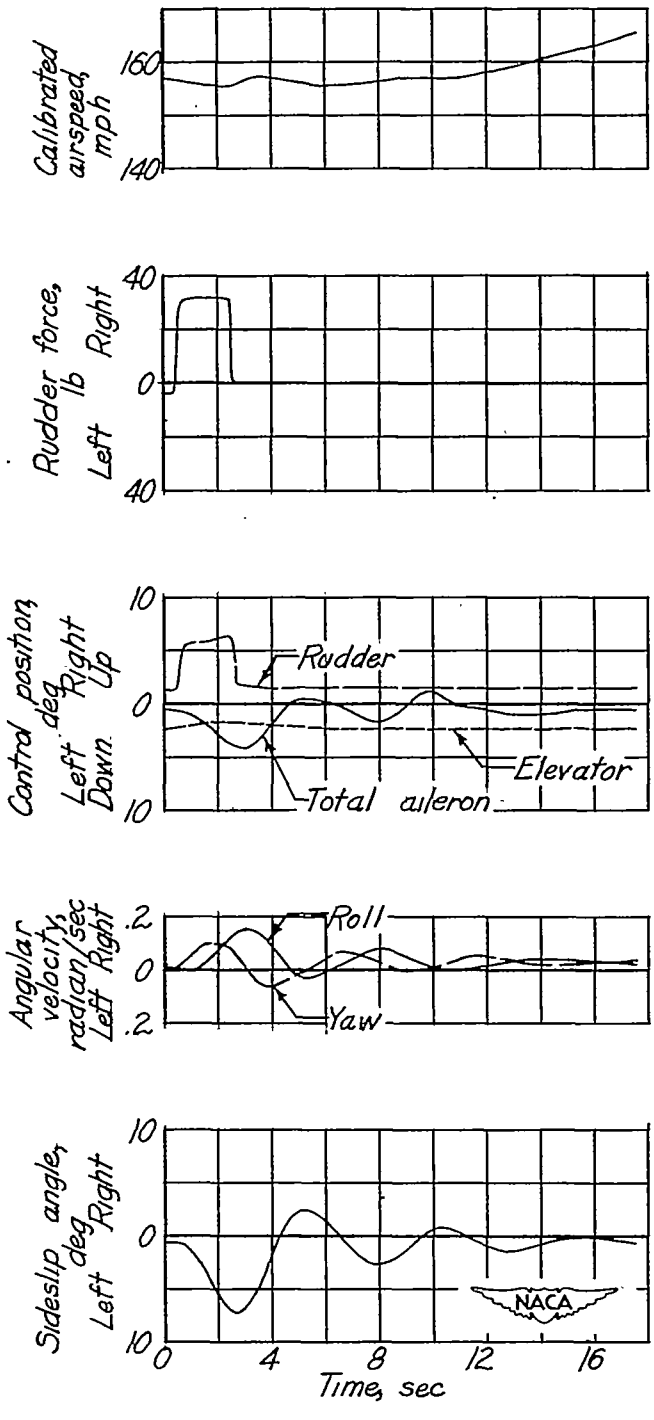

(a) Pilot did not attempt to damp oscillation.

Figure 24.- Time history of oscillation resulting from abrupt deflection and release of rudder. Control stick free; ventral-fin extension off; 80-percent-span slots; flaps up; nose wheel up; engine idling.

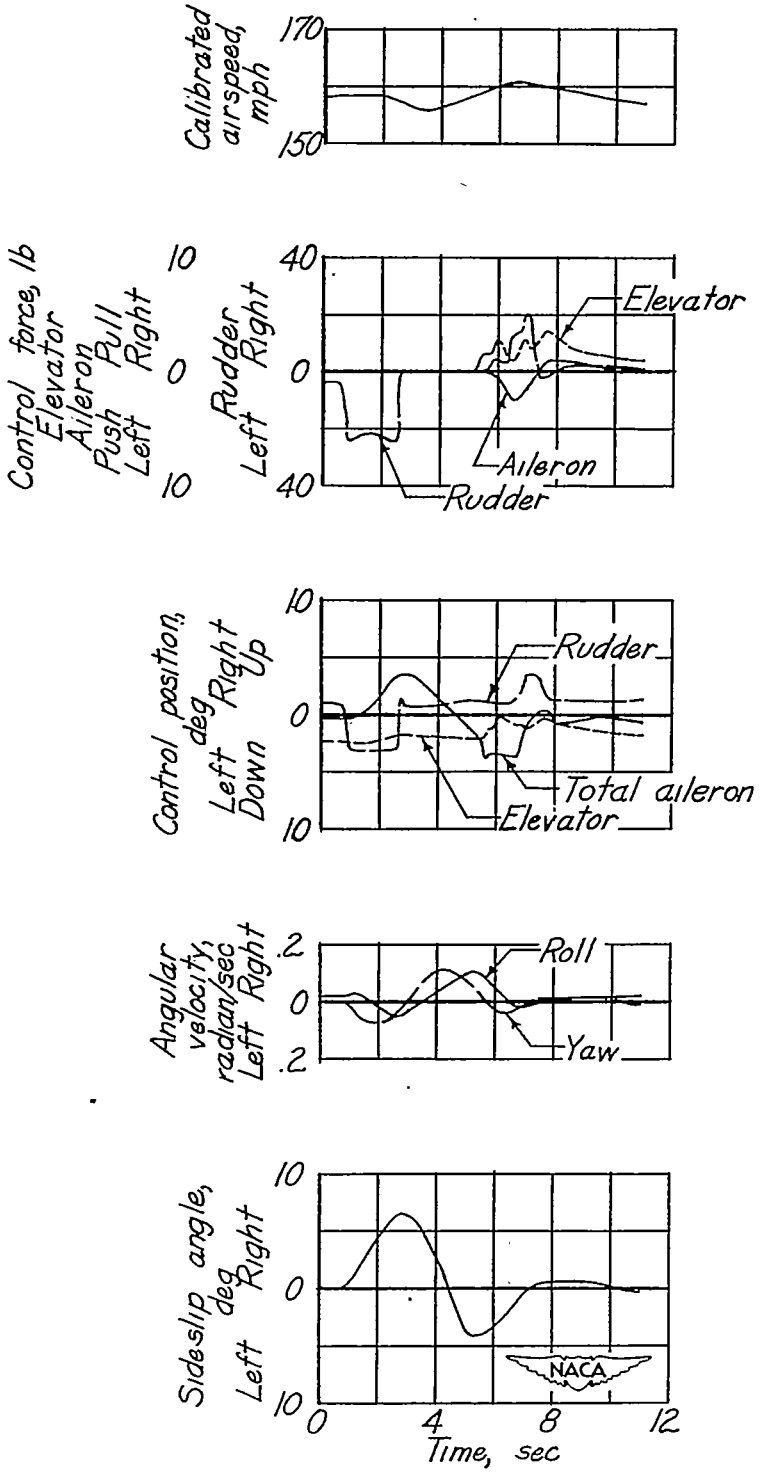

(b) Pilot applied coordinated rudder and aileron to damp oscillation.

Figure 24.- Concluded.

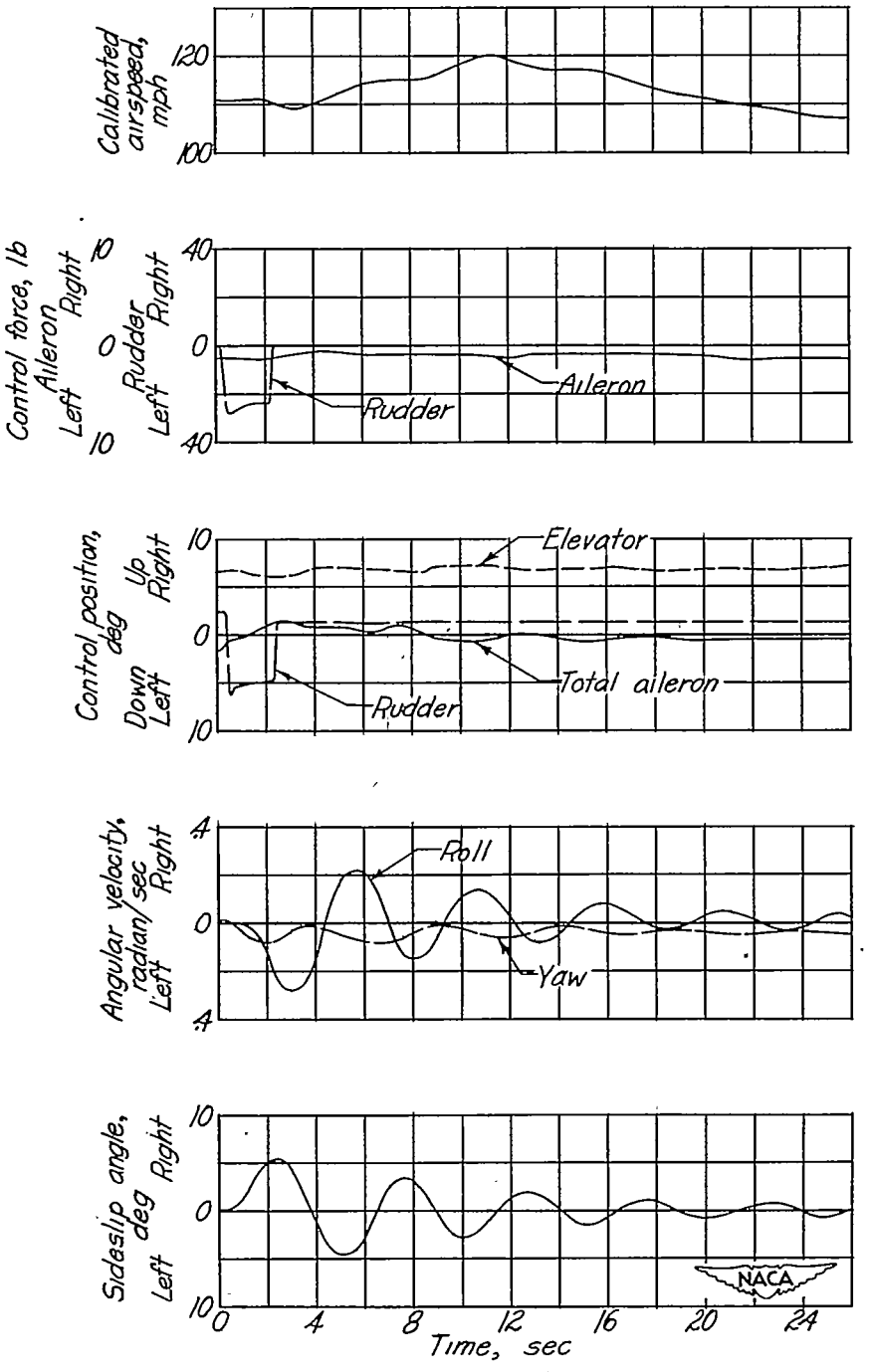

(a) Pilot did not attempt to damp oscillation.

Figure 25.- Time history of oscillation resulting from abrupt deflection and release of rudder. Pilot attempted to hold control stick fixed; ventral-fin extension off; 80-percent-span slots; flaps down; nose wheel down; engine idling.

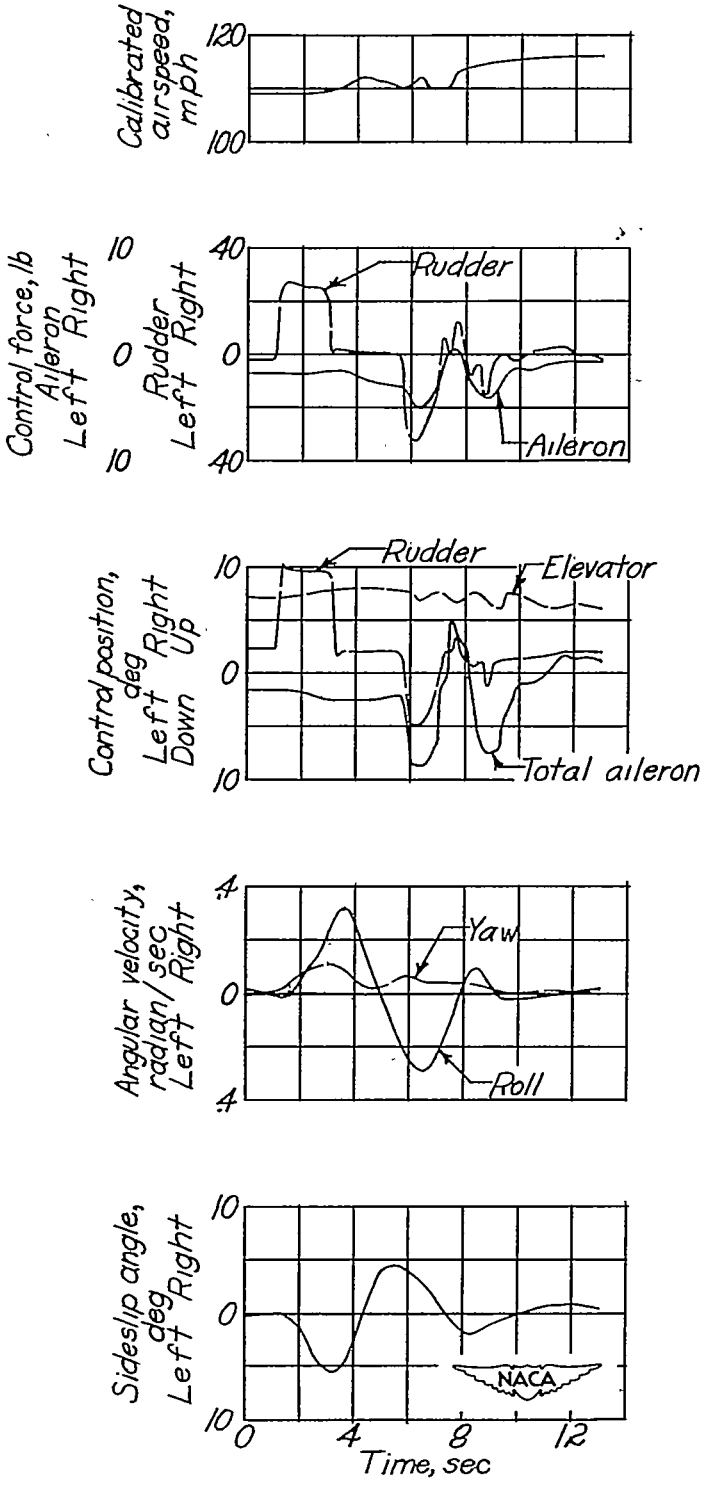

(b) Pilot applied coordinated rudder and aileron to damp oscillation.

Figure 25.- Concluded.

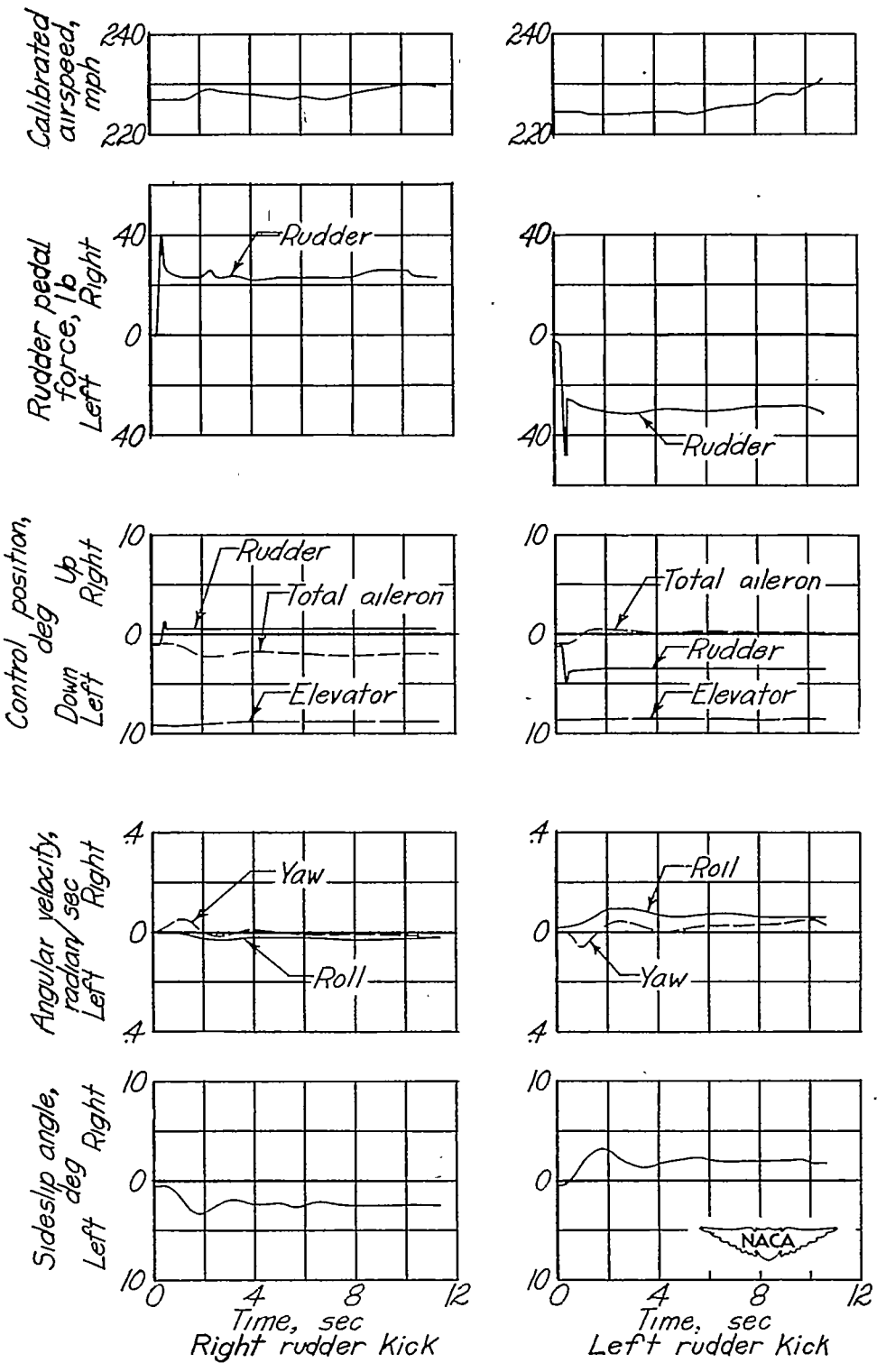

Figure 26.- Time histories of right and left rudder kicks. Control stick free; 80-percent-span slots; flaps up; nose wheel up; engine idling.

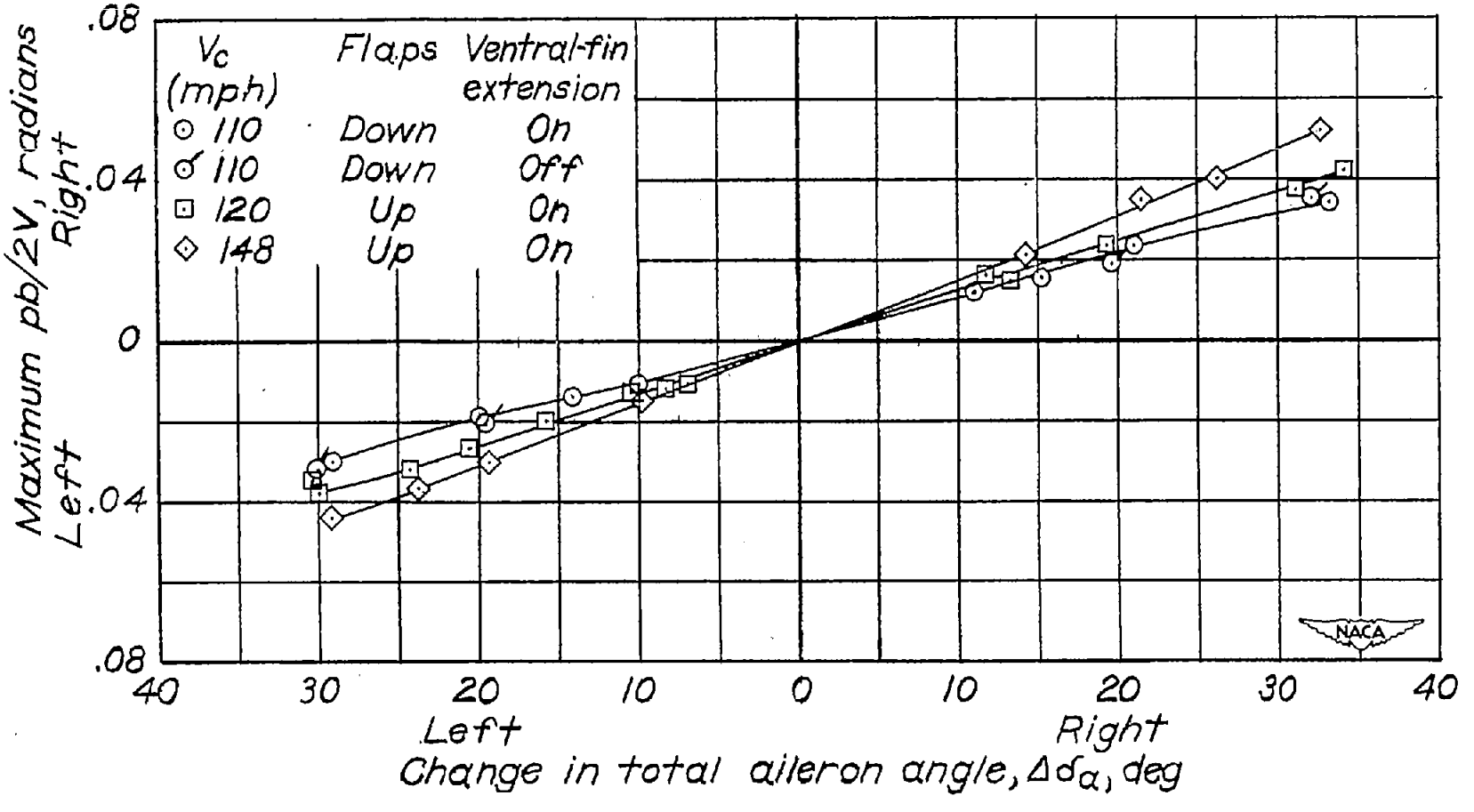

Figure 27.- Variation of maximum pb/2V with change in total aileron angle in rudder-fixed aileron rolls. 80-percent-span slots; engine idling.

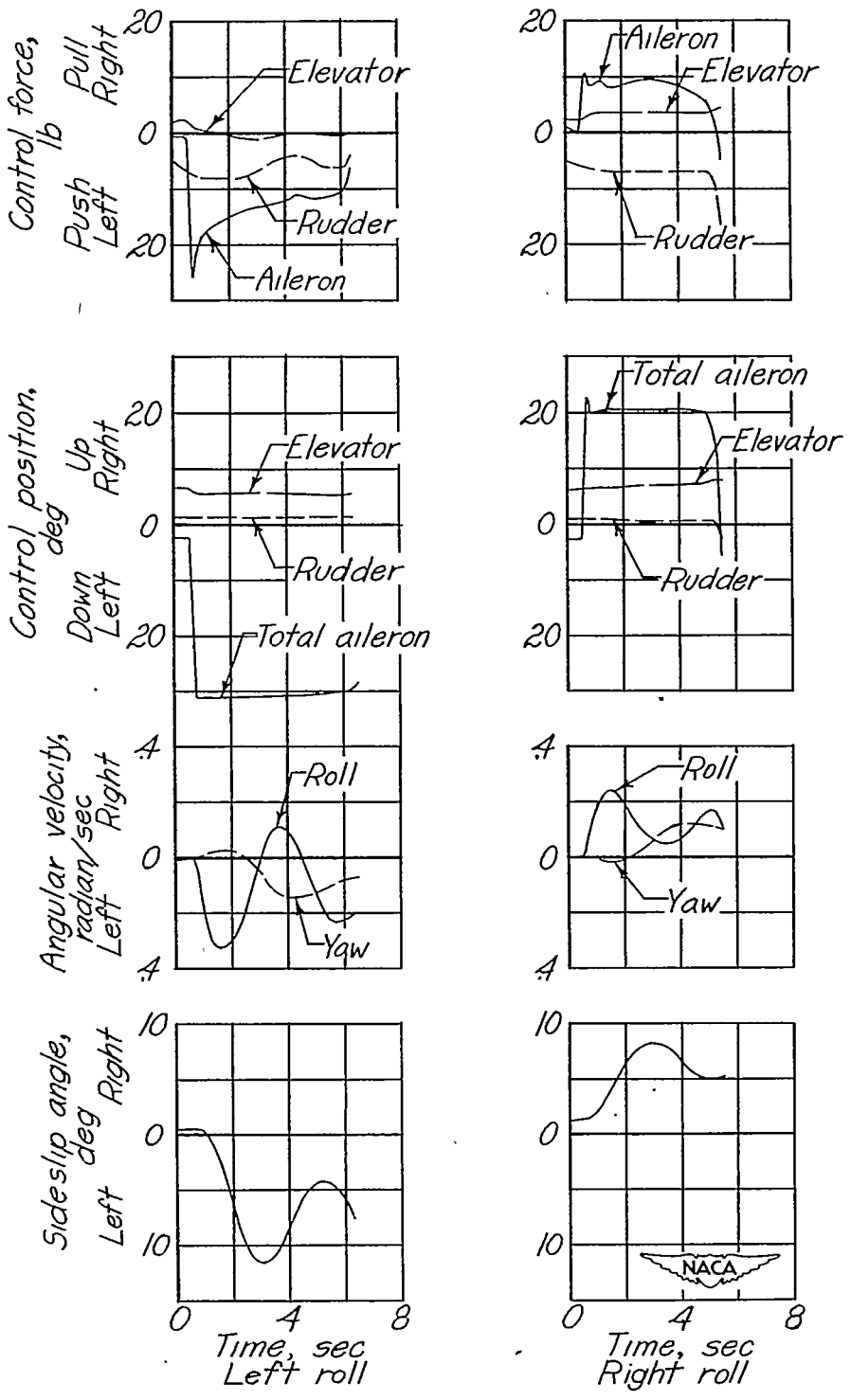

Figure 28.- Time histories of left and right aileron rolls with rudder fixed. V_c = 110 miles per hour; 80-percent-span slots; flaps down; nose wheel down; engine idling.

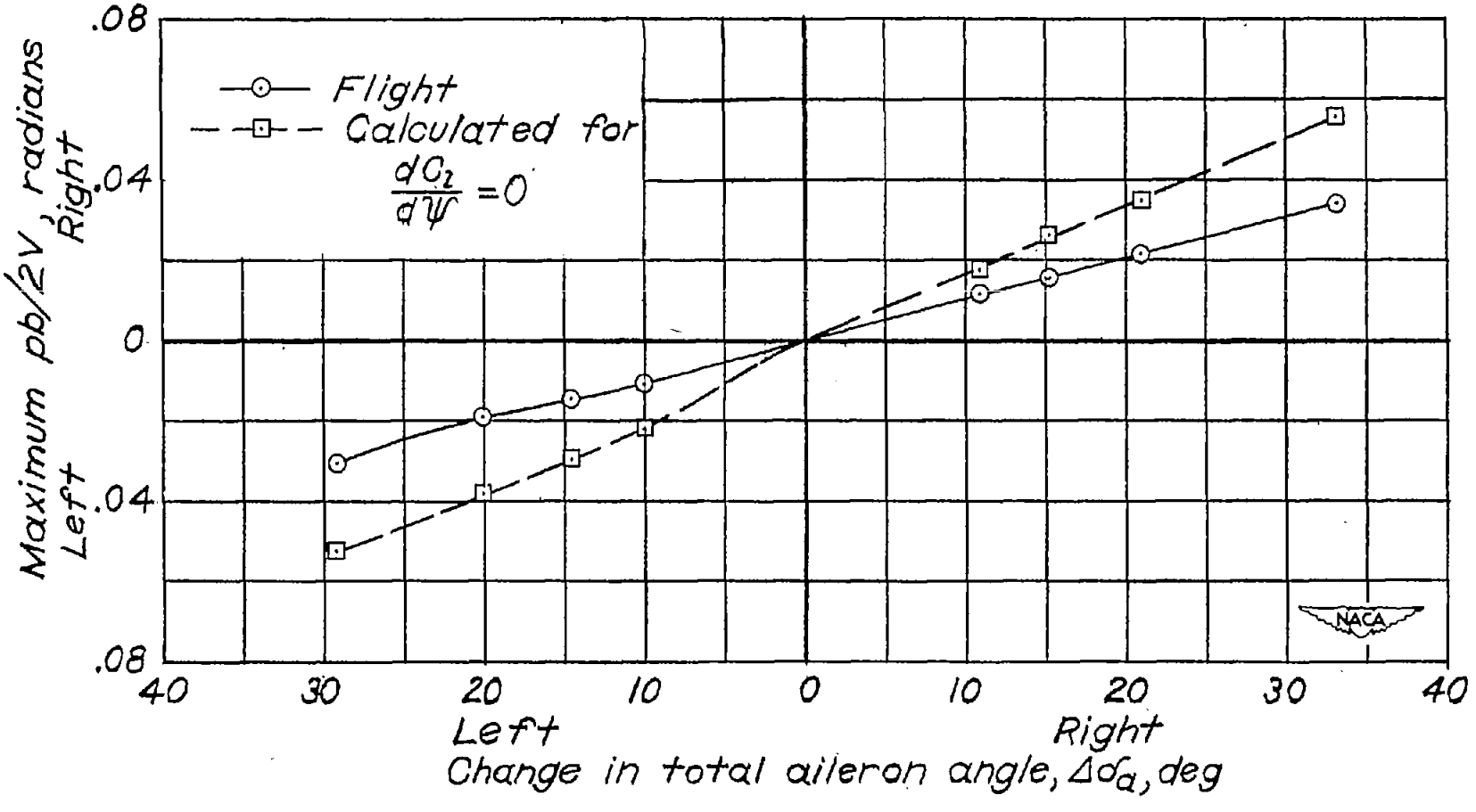

Figure 29.- Reduction in pb/2V due to dihedral effect in rudder-fixed aileron rolls. V_c = 110 miles per hour; 80-percent-span slots; flaps down; nose wheel down; engine idling.

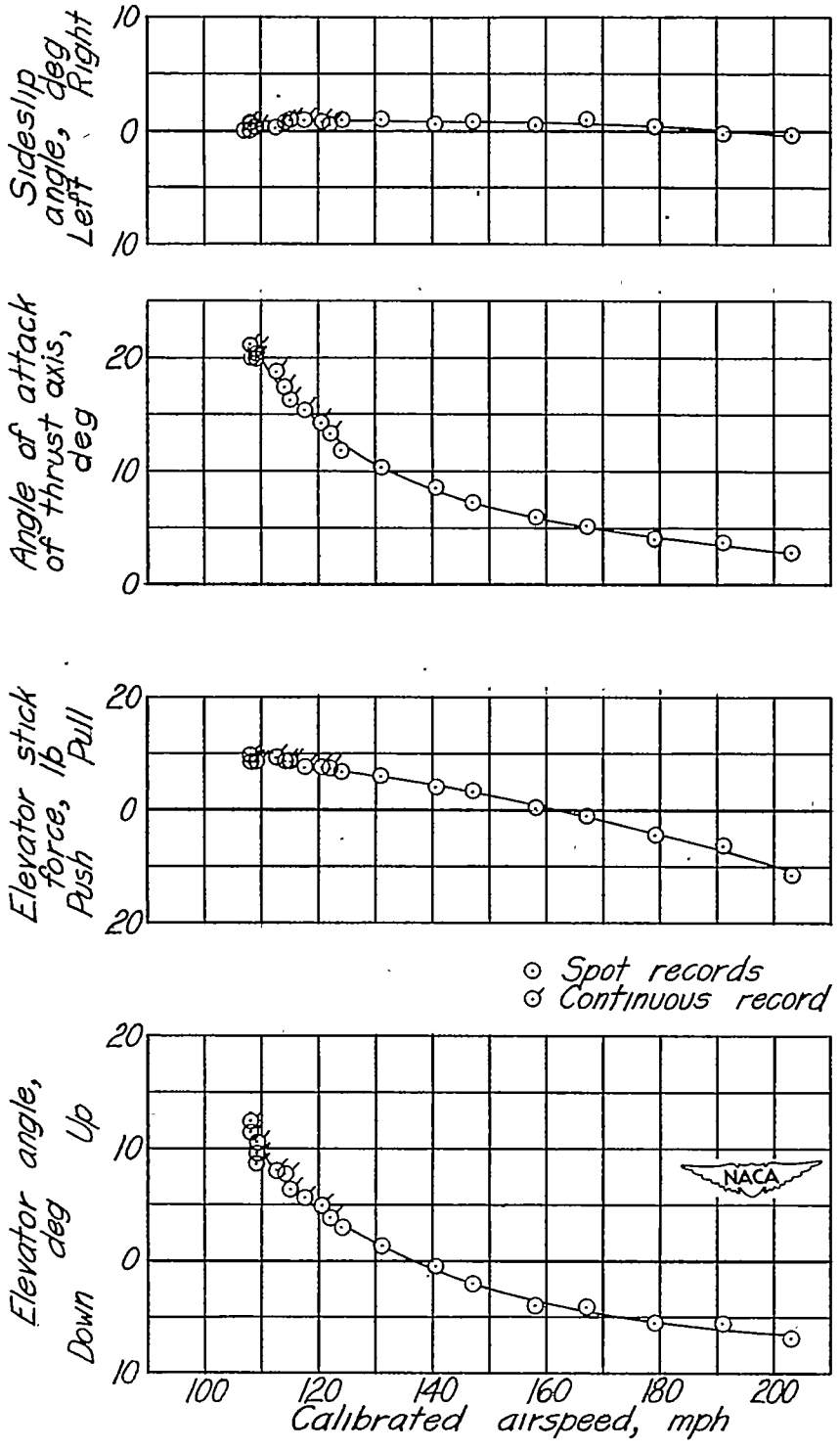

Figure 30.- Static longitudinal stability characteristics of test airplane with 80-percent-span slots on wing. Flaps up; nose wheel up; engine idling; center of gravity at 26.6 percent mean aerodynamic chord.

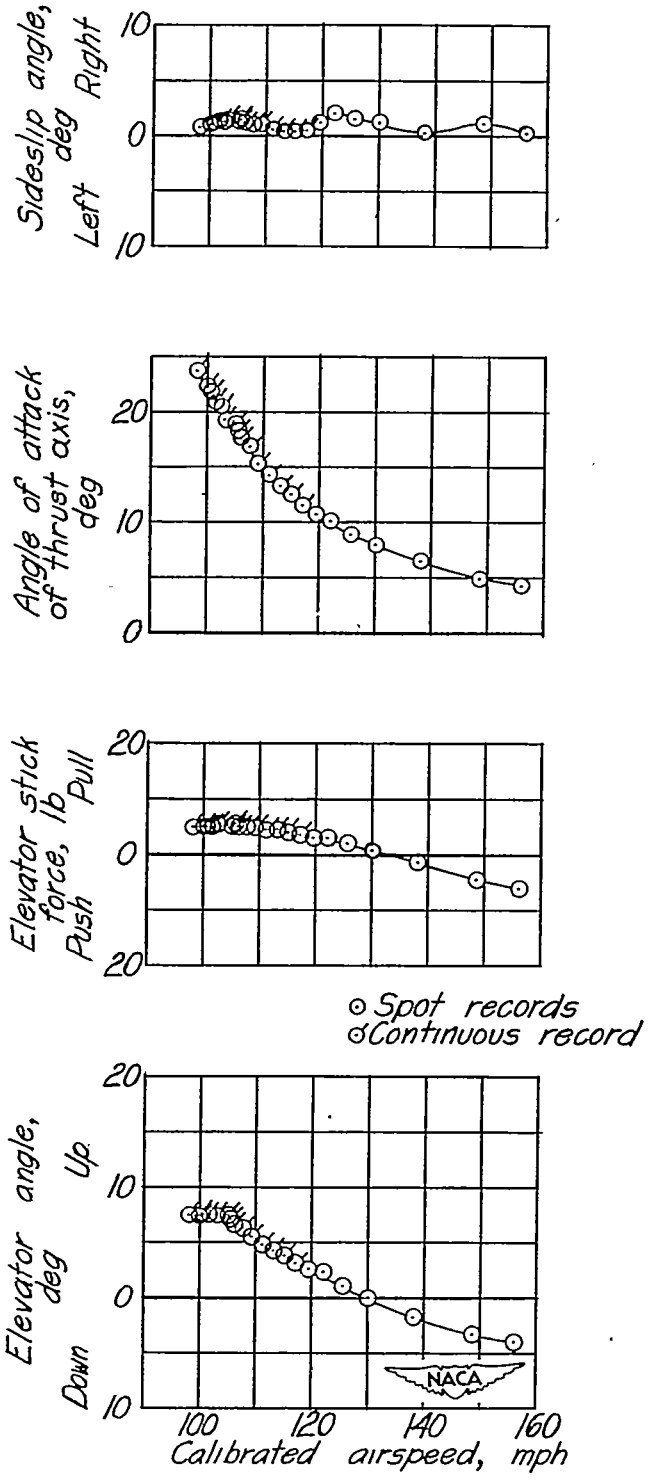

Figure 31.- Static longitudinal stability characteristics of test airplane with 80-percent-span slots on wing. Flaps down; nose wheel down; engine idling; center of gravity at 27.1 percent mean aerodynamic chord.

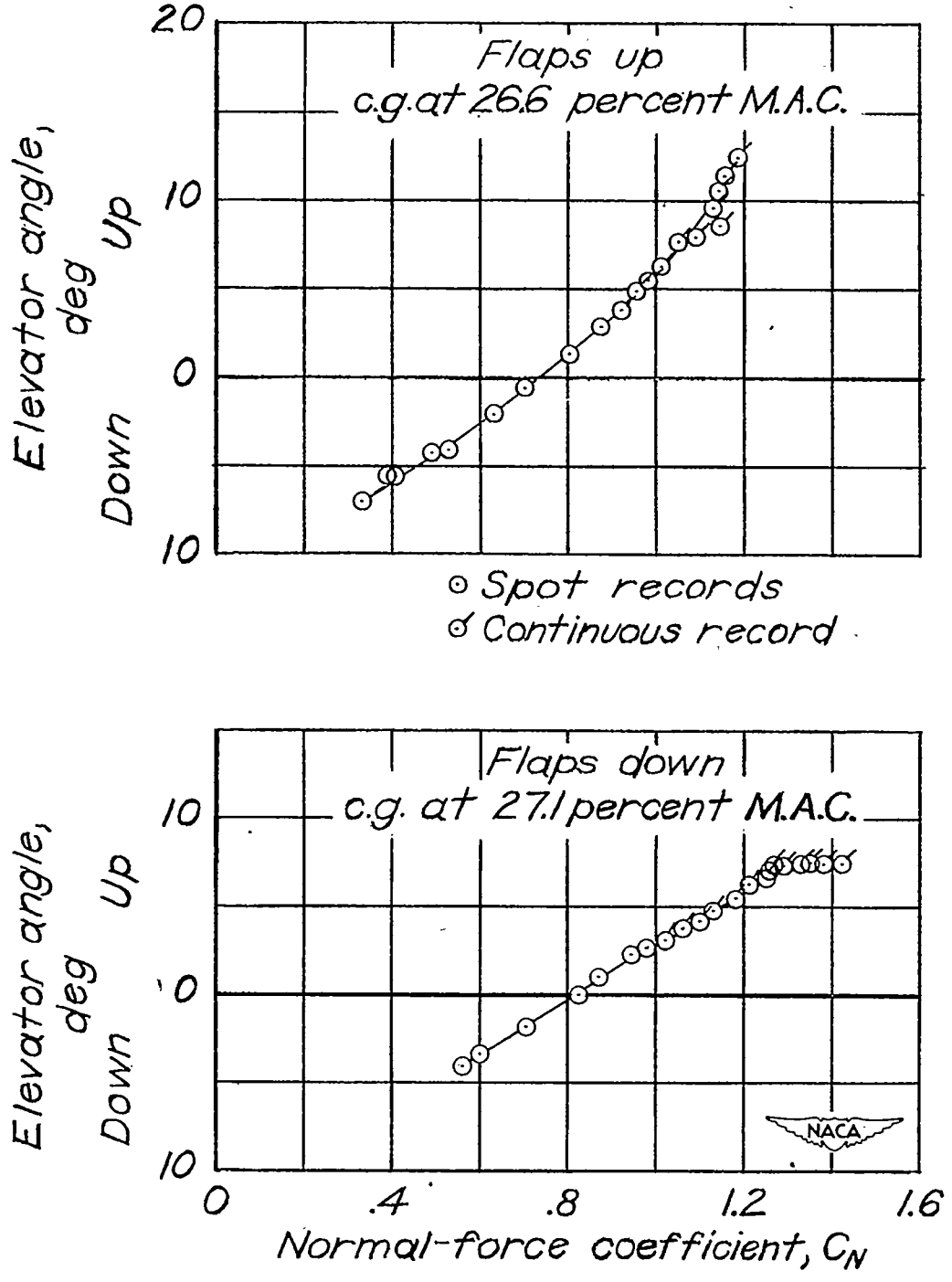

Figure 32.- Variation of elevator angle required for trim with normal-force coefficient for test airplane with 80-percent-span slots on wing. Engine idling.

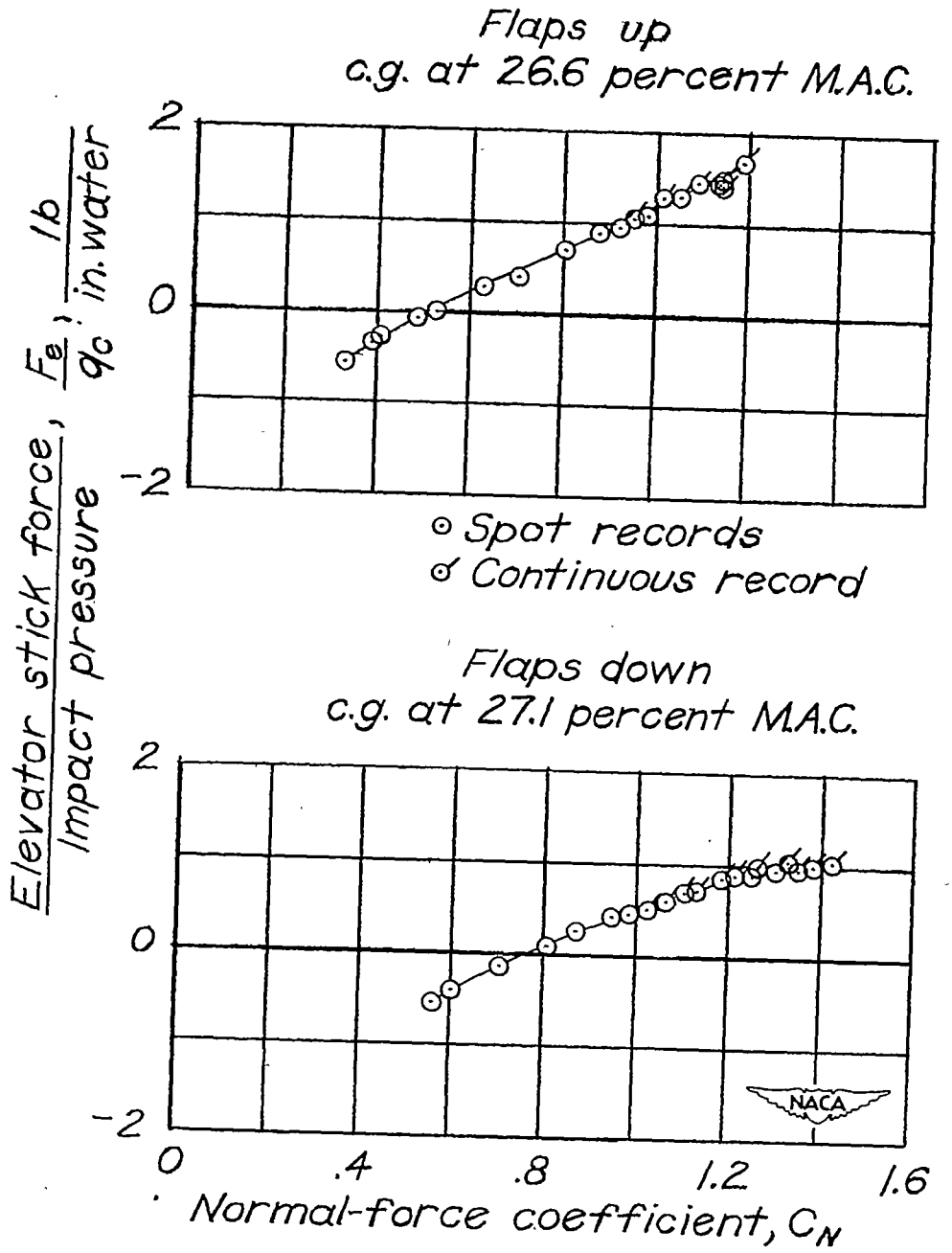

Figure 33.- Variation of elevator stick force divided by impact pressure with normal-force coefficient for test airplane with 80-percent-span slots on wing. Engine idling.

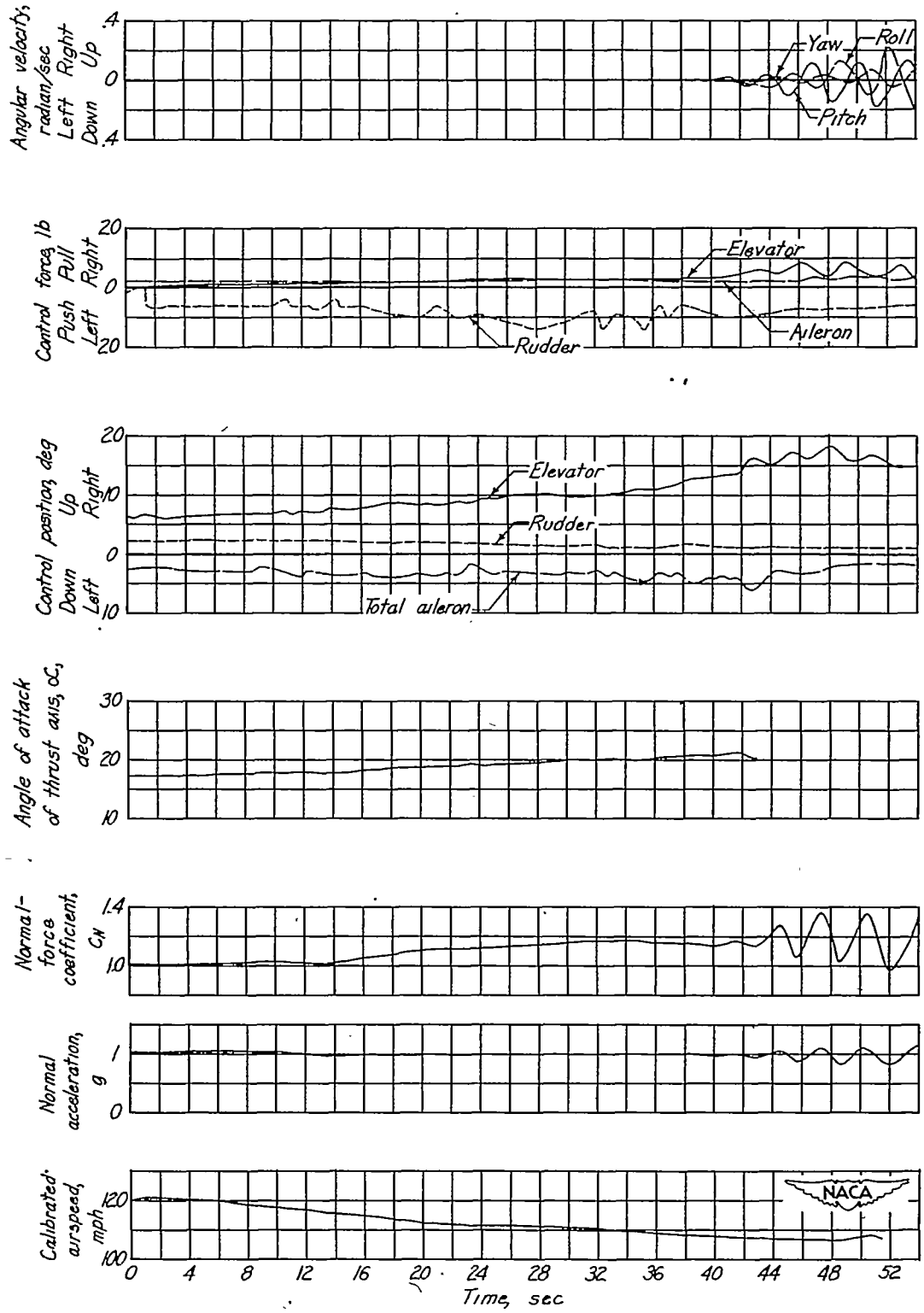

(a) Time history.

Figure 34.- Stall for test airplane with 80-percent-span slots on wing. Flaps up; nose wheel up; engine idling; center of gravity at 26.9 percent mean aerodynamic chord.

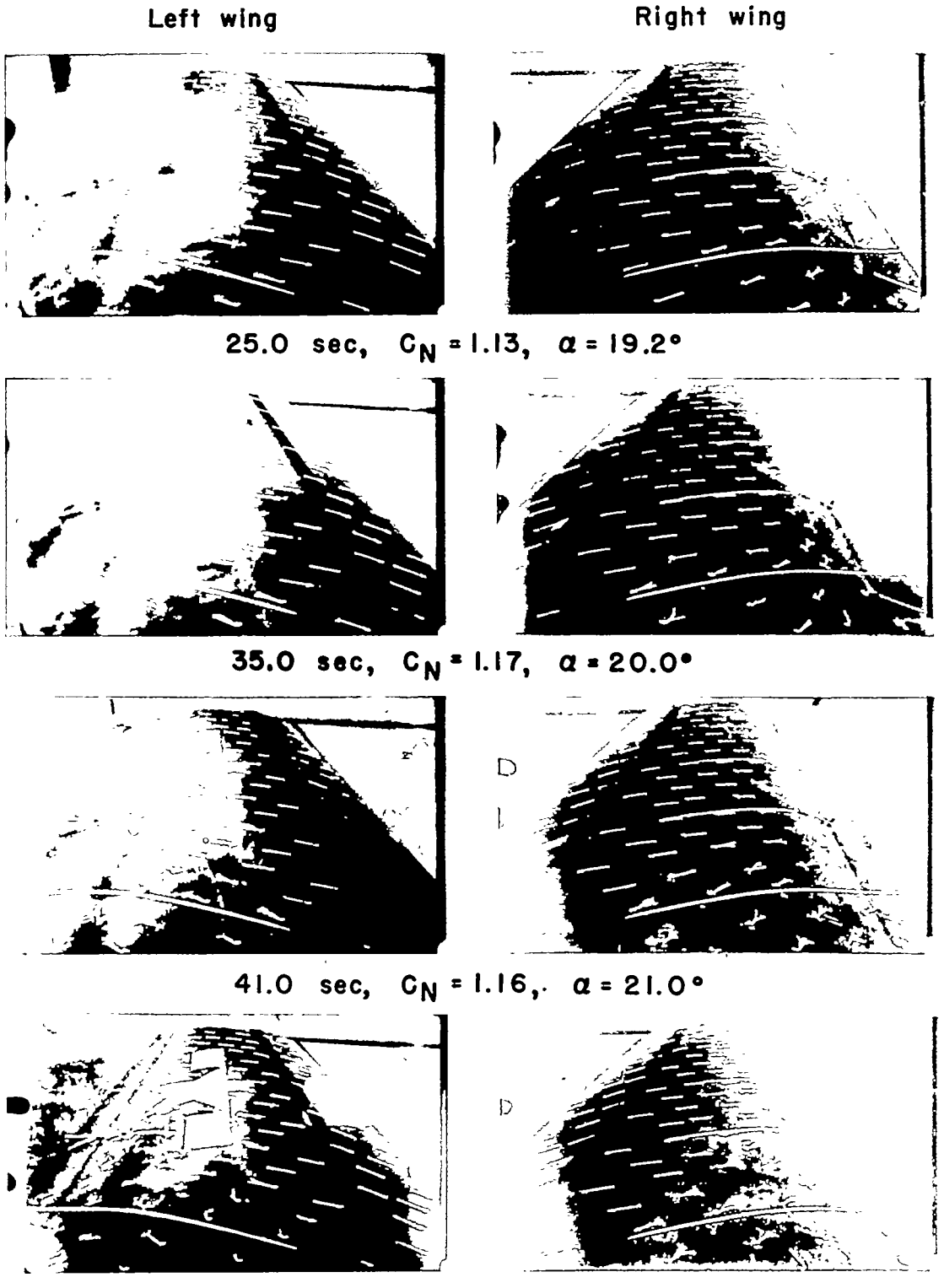

(b) Tuft pictures.

Figure 34.- Concluded.

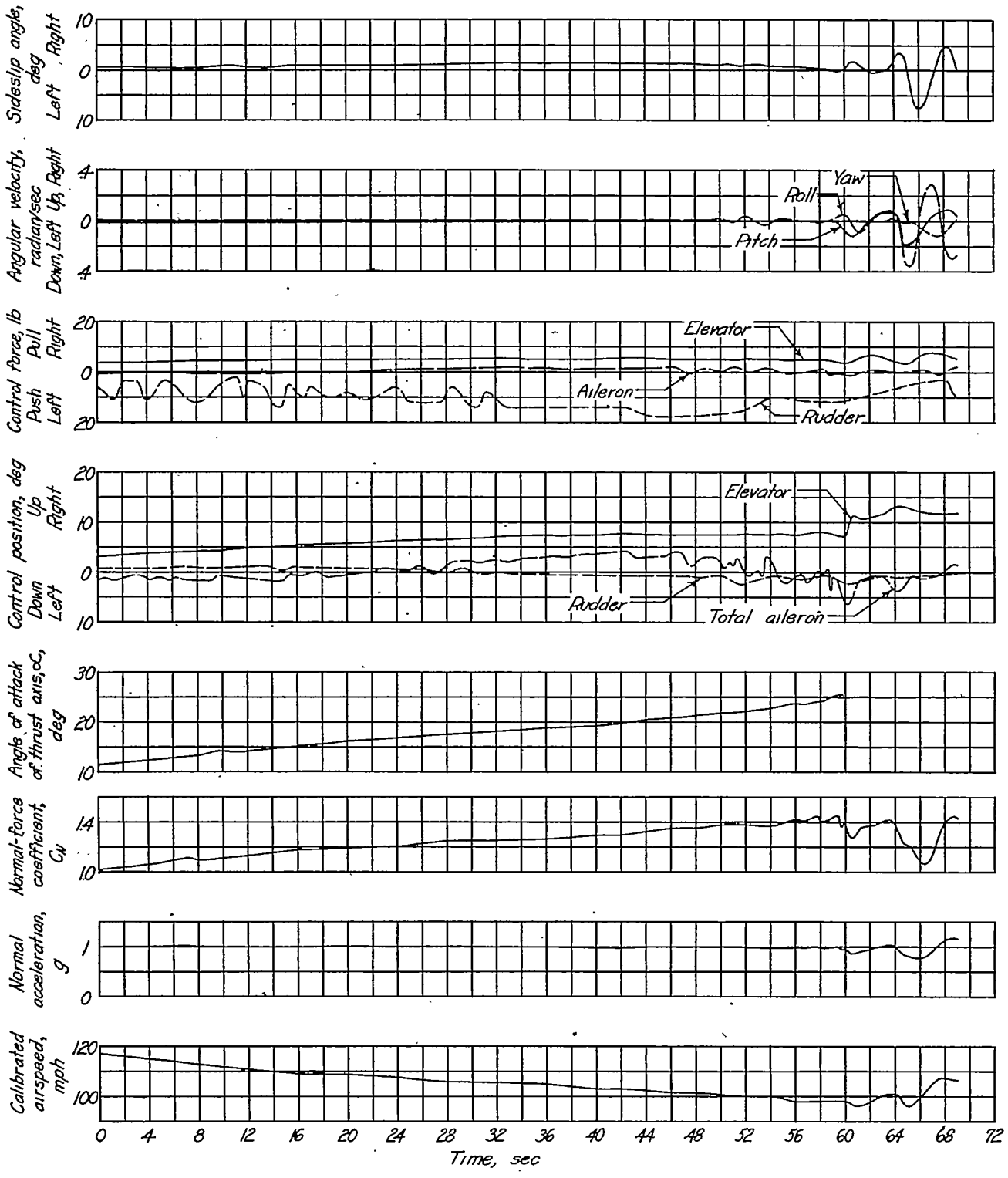

(a) Time history.

Figure 35.- Stall for test airplane with 80-percent-span slots on wing. Flaps down; nose wheel down; engine idling; center of gravity at 27.1 percent mean aerodynamic chord.

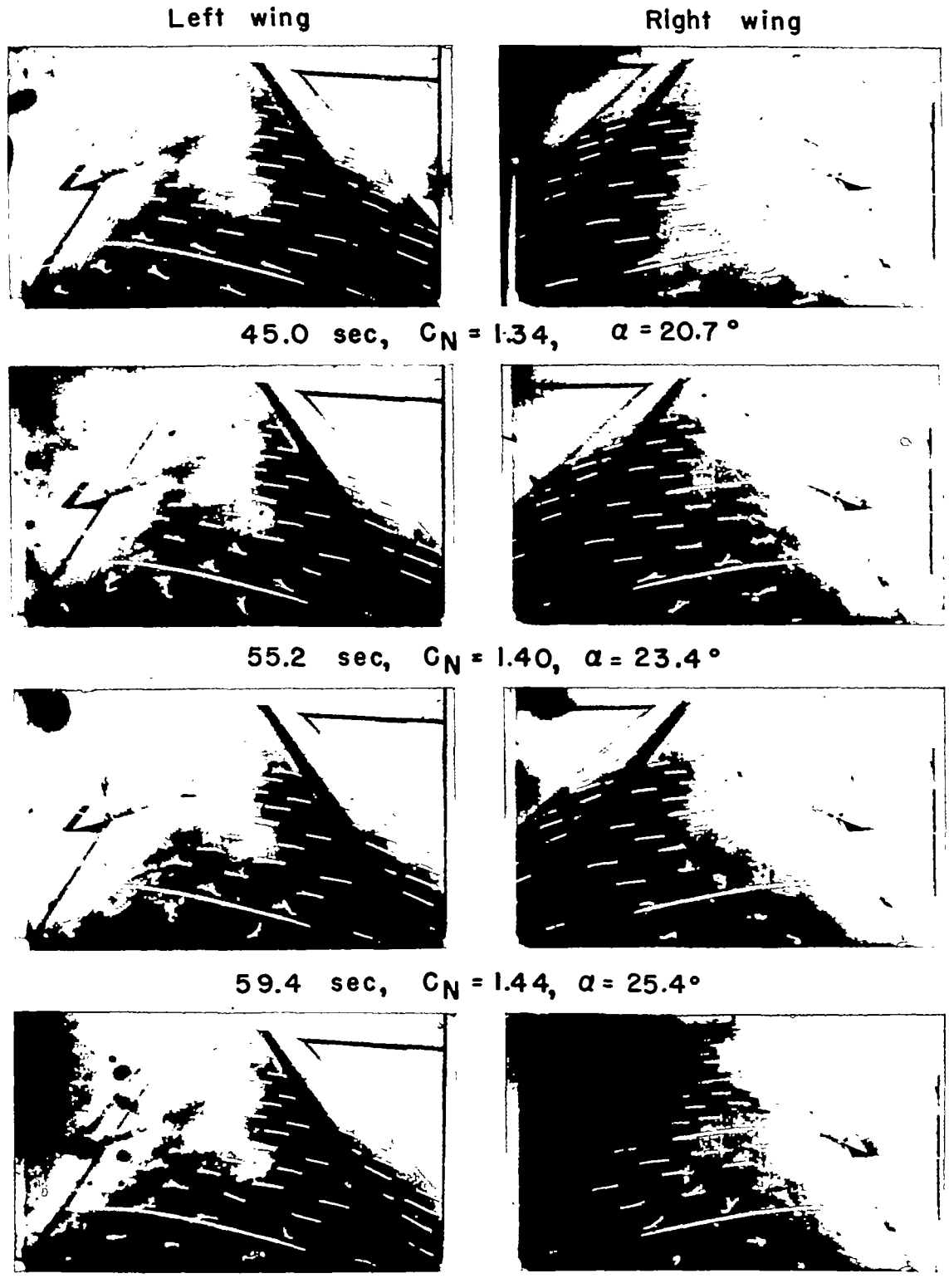

(b) Tuft pictures.

Figure 35.- Concluded.

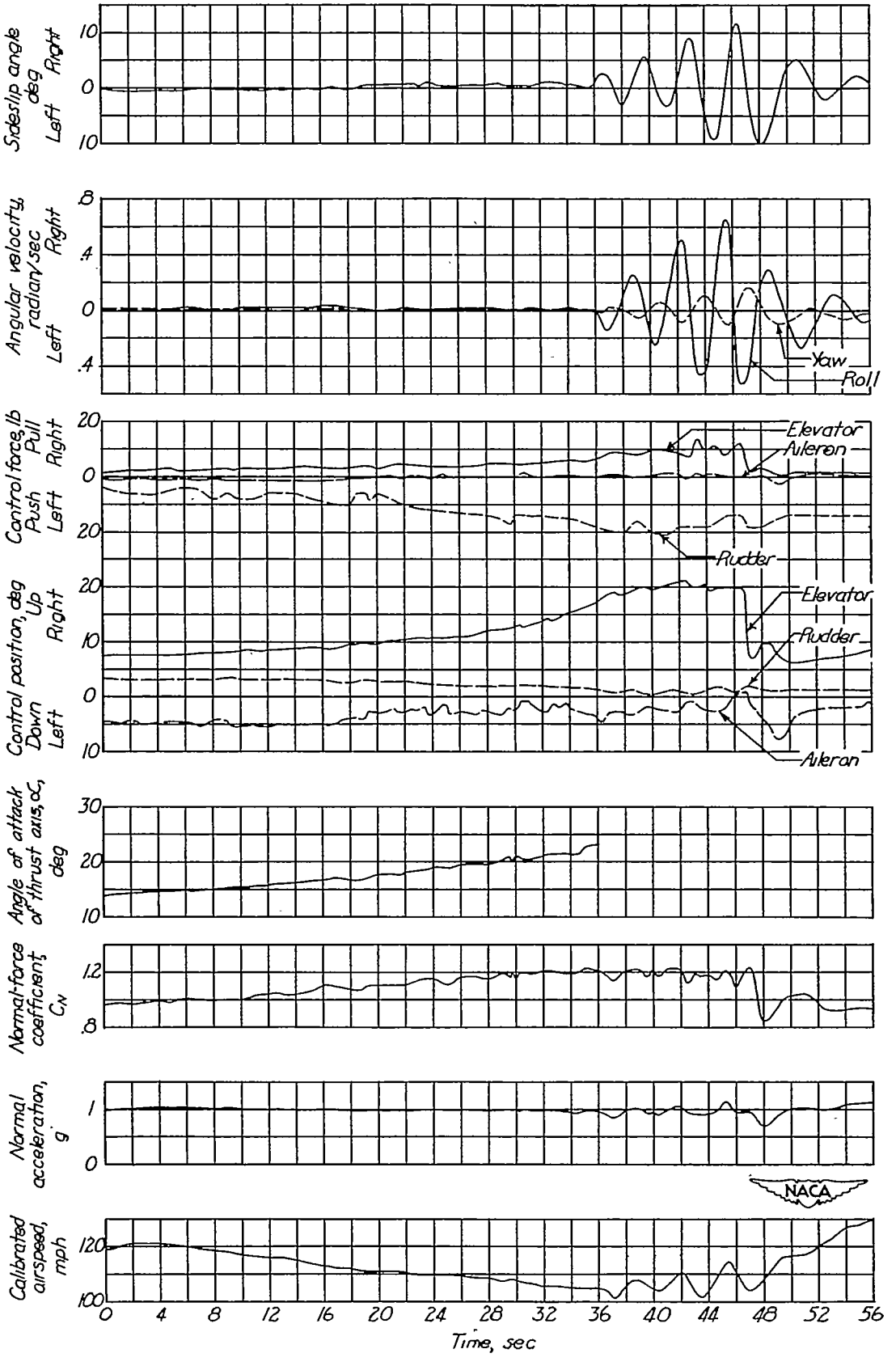

Figure 36.- Time history of stall for test airplane with 80-percent-span slots on wing. Ventral-fin extension off; flaps up; nose wheel up; engine idling; center of gravity at 27.1 percent mean aerodynamic chord.

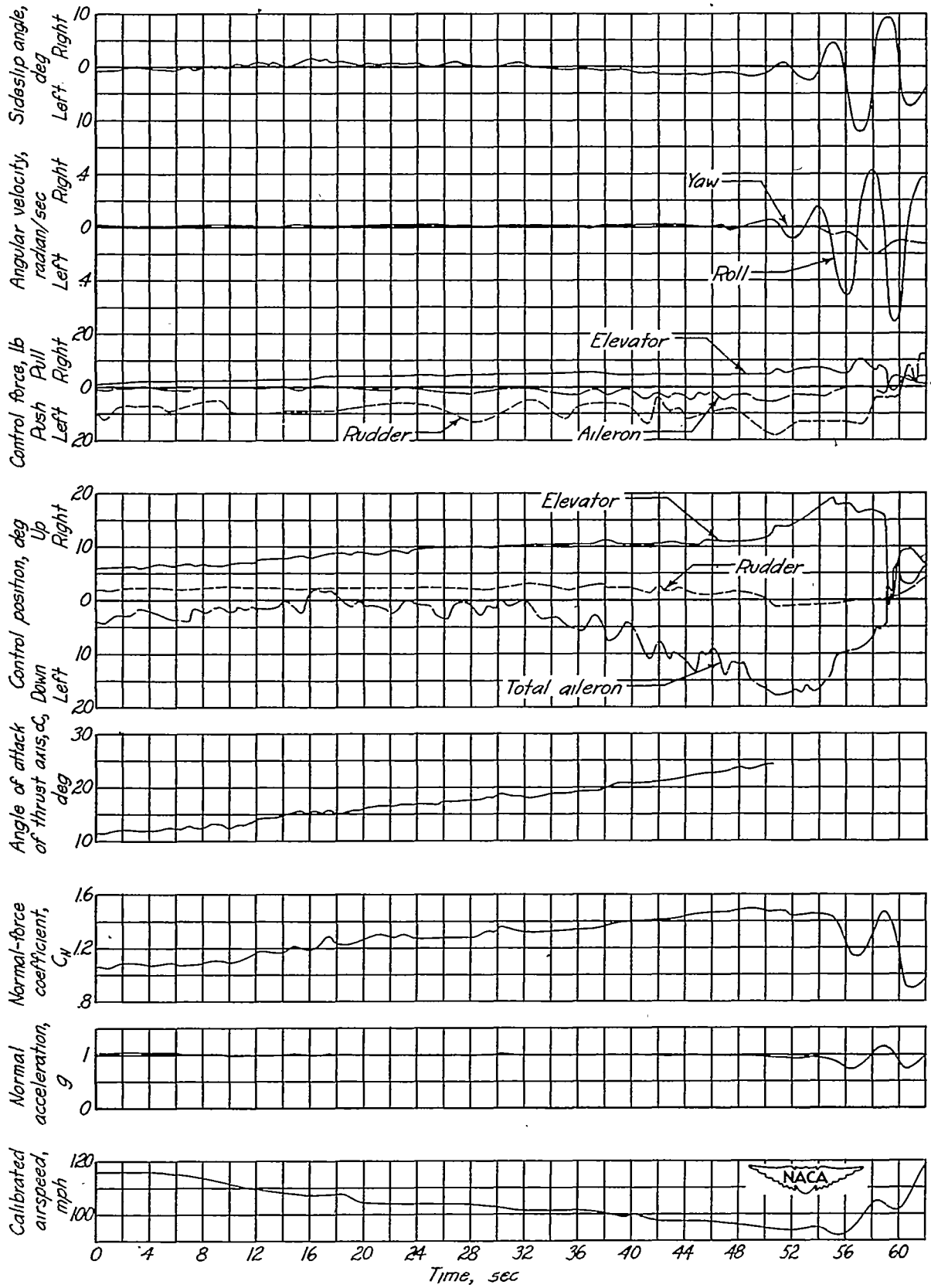

Figure 37.- Time history of stall for test airplane with 80-percent-span slots on wing. Ventral-fin extension off; flaps down; nose wheel down; engine idling; center of gravity at 27.1 percent mean aerodynamic chord.

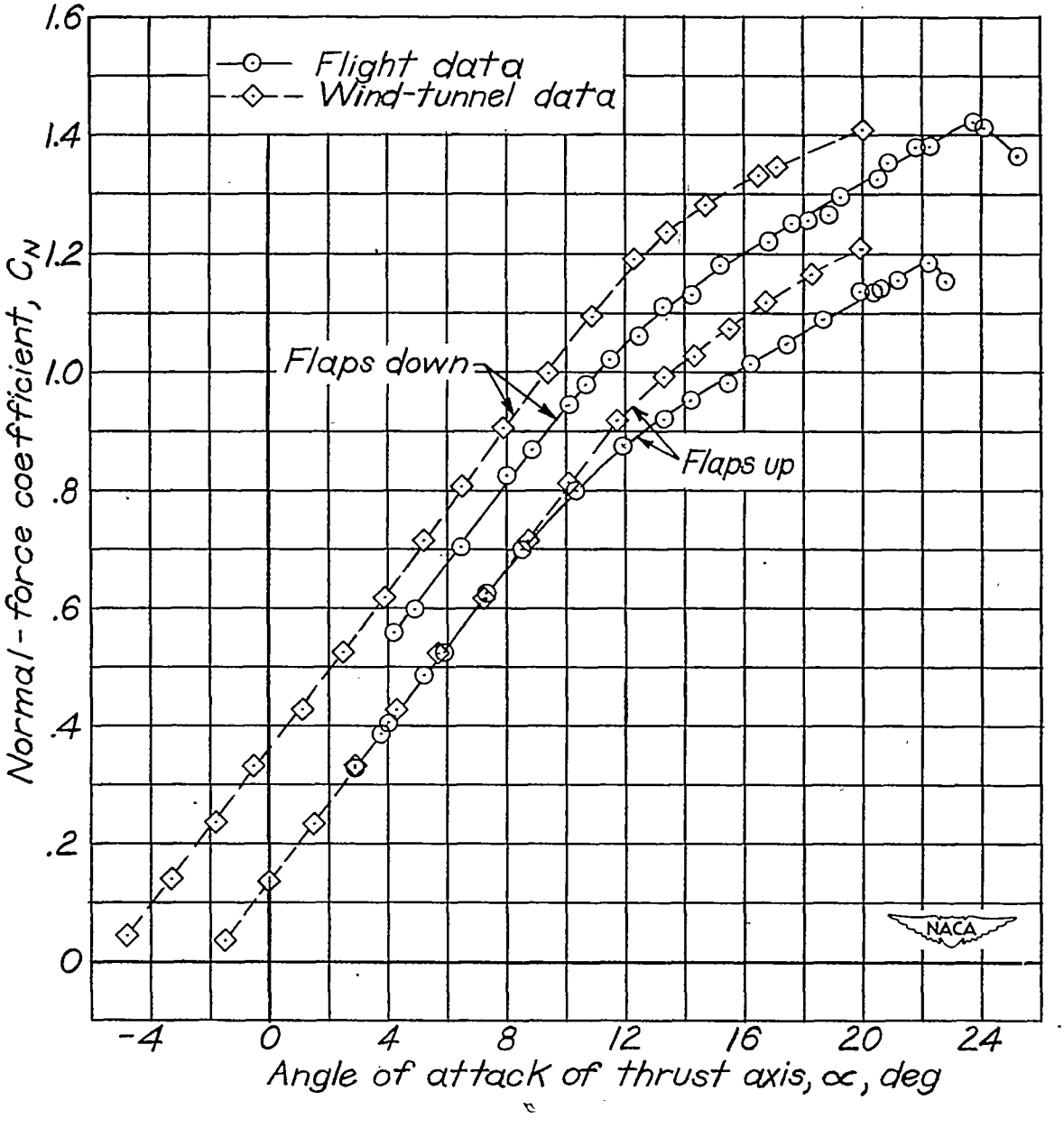

Figure 38.- Variation of normal-force coefficient with angle of attack of thrust axis for test airplane with 80-percent-span slots on wing. Engine idling.